UNIONE EUROPEA
Fondo Sociale Europeo

Ministero dell'Università e della Ricerca

PON RICERCA E INNOVAZIONE 2014-2020

RNAi-MEDIATED IMMUNOSUPPRESSION FOR THE DEVELOPMENT OF NEW INSECT CONTROL TECHNOLOGIES

Gennaro Volpe

Dottorato in Biotecnologie – XXXV ciclo

Università di Napoli Federico II

Dottorato in Biotecnologie – XXXV ciclo

Università di Napoli Federico II

RNAi-MEDIATED IMMUNOSUPPRESSION FOR THE DEVELOPMENT OF NEW INSECT CONTROL TECHNOLOGIES

Gennaro Volpe

Dottorando:	Gennaro Volpe
Relatore:	Chiar.mo Prof. Francesco Pennacchio
Coordinatore:	Chiar.mo Prof. Marco Moracci
Settore Scientifico Disciplinare:	AGR/11

INDEX

SUMMARY

The need to develop new pest management strategies which are effective and ecologically sustainable has stimulated significant research efforts on molecules of natural origin and on gene regulation strategies that mimic and/or enhance mechanisms of pest suppression by insect antagonists. This area of research can allow the exploitation of a nearly untapped source of genes and molecules with potential bioinsecticide activity. Besides the direct use of virulence factors as physiological disruptors of pest insects, it is possible to target the molecular targets of these factors and alter vital functions of pests. This latter approach is made possible by genetic tools now available, such RNA interference (RNAi), which can be used to suppress the expression of host genes targeted by virulence factors, reproducing the negative/lethal effects that the natural antagonists have on their hosts.
In this context, the present PhD thesis aims to develop (1) new solutions for insect pest control using RNAi mediated suppression of gene expression, and (2) sustainable and safe field delivery systems of dsRNA.
The first part of the thesis reports the expression analysis of the immune gene *Sl102,* that is suppressed in parasitized noctuid moth larvae, during the embryogenesis of *Spodoptera littoralis* (Lepidoptera: Noctuidae). The functional role was analyzed by RNAi and by transmission electron microscopy (TEM) observations. The very high mortality observed upon gene silencing was associated with morphological alterations associated with a general delay in the embryonic development, suggesting a possible role of this gene in tissue organization and differentiation during embryogenesis. This embryonic mortality is of particular interest from an applied point of view, since it prevents the damage caused by the larval feeding stages.
The second part concerns the study of a gene encoding a protein of the REPAT (REsponse to PAThogens) family, which is known to be involved in the response to entomopathogens infection. Here, the *Slrepat1* gene in *S. littoralis* larvae has been identified and functionally characterized. This gene is mostly expressed in the midgut, and its dsRNA-mediated silencing determines an immunosuppressed phenotype that makes larvae more susceptible to the entomopathogen *Bacillus thuringiensis*. Therefore, the combined administration of the dsRNA targeting this gene and of *B. thuringiensis* would enhances the

killing activity of the entomopathogen in an integrated pest management strategy.

The third part is focused on the development of a new delivery and protection system for dsRNA molecules, which is based on the use of chitosan polymers and humic substances for the synthesis of a nanoconjugate. The results in terms of synthesis efficiency, physicochemical characterization, and *in vivo* administration to *S.littoralis* larvae indicate that the Chi/Hum-dsRNA nanoconjugate can be a valuable and a sustainable tool for the delivery of dsRNAs.

The results of this PhD thesis pave the way towards the development of novel strategies of pest control which are not only based on direct pest suppression, but also on the enhancement of natural biocontrol agents, reinforcing the ecosystem services they provide.

RIASSUNTO

L'intensificazione delle pratiche agricole ha determinato un concomitante aumento dell'uso di pesticidi e fertilizzanti di sintesi, caratterizzati da un elevato impatto ambientale, tra i più importanti fattori della progressiva erosione della biodiversità degli agroecosistemi. Emerge, quindi, la necessità di adottare un modello integrato per la protezione delle colture (Integrated Pest Management, IPM), che consideri tutte le strategie attuabili per il controllo dei parassiti, consentendo la riduzione sia delle popolazioni di insetti infestanti, sia dell'uso di pesticidi dannosi per la salute umana e l'ambiente. Uno dei pilastri dell'IPM è il controllo biologico, che si basa sull'utilizzo di antagonisti naturali per ridurre le popolazioni di insetti dannosi. Lo studio funzionale e molecolare delle relazioni antagonistiche tra insetti dannosi e i loro antagonisti naturali rappresenta una fonte preziosa di molecole e geni coinvolti nell'induzione di rilevanti alterazioni patologiche, che possono essere riprodotte attraverso strategie di controllo ispirate da meccanismi naturali. I due gruppi di organismi maggiormente studiati in questo senso, sono gli entomopatogeni e i parassitoidi.

Tra i diversi entomopatogeni, i batteri rappresentano i più utilizzati per il controllo dei parassiti, sebbene, il loro uso massiccio ha determinato l'evoluzione di fenomeni di resistenza negli insetti bersaglio che ne minaccia l'uso sostenibile e prolungato nel tempo. In generale, la patogenesi indotta da batteri entomopatogeni è mediata dalla produzione di molteplici fattori di virulenza, come le tossine, che raggiunto l'intestino, si legano ai recettori delle cellule dell'epitelio provocando la formazione di pori non selettivi per il traffico ionico e conseguente lisi osmotica delle cellule epiteliali. Le lesioni della barriera intestinale che ne derivano consentono il passaggio di batteri nella cavità emocelica, causando una setticemia letale.

Gli imenotteri parassitoidi sono in grado di svilupparsi a carico dell'ospite parassitizzato, portandolo rapidamente a morte (idiobionti) o lasciandolo lungamente in vita (coinobionti) e interagendo finemente con esso regolandone fisiologia, sviluppo e riproduzione, al fine di consentire la sopravvivenza e la crescita della propria progenie. Fra le varie funzioni regolate, l'immunità è, ovviamente, quella che risulta più profondamente condizionata. Questo controllo è mediato da fattori di regolazione dell'ospite divisi in fattori di origine materna che includono il veleno, le proteine ovariche e, in alcuni braconoidi parassiti di larve di lepidotteri, virus simbionti, e in fattori di origine embrionale che

includono teratociti (cellule derivanti dalla membrana embrionale del parassitoide) e secrezioni larvali. Tra i fattori di origine materna ci sono i Polydnavirus (PDV), virus simbionti il cui genoma, integrato in quello del parassitoide, si replica solo in alcune cellule degli ovari (cellule del calice ovarico). Una volta iniettati nell'emocele delle larve dei lepidotteri, i virioni dei PDV infettano diversi tessuti, esprimendo geni che inducono, in particolare, soppressione della risposta immunitaria e alterazione del sistema endocrino, di fondamentale importanza per la sopravvivenza degli stadi giovanili del parassitoide. Da queste considerazioni è chiaro che lo studio dei meccanismi molecolari alla base delle interazioni ospite-parassitoide, può consentire l'identificazione di molecole e geni con un potenziale impiego per lo sviluppo di nuovi bioinsetticidi e di strategie innovative di controllo, basate sulla regolazione dell'espressione genica, ad esempio, attraverso l'uso dell'RNA interference (RNAi), per alterare l'espressione di quei geni dell'ospite che sono colpiti dai fattori di virulenza parassitari. L'RNAi è un meccanismo di modulazione dell'espressione genica, conservato negli organismi superiori, che sfrutta un RNA complementare all'RNA messaggero (mRNA target) per formare una struttura a doppio filamento (dsRNA). Il dsRNA, riconosciuto dai macchinari molecolari delle cellule, induce la degradazione del mRNA target e quindi il blocco dell'espressione genica in maniera altamente selettiva. Negli ultimi anni, l'RNAi è stato utilizzato nel controllo degli insetti dannosi, prendendo come target geni essenziali dell'ospite, con un ridotto impatto sulle specie non bersaglio. Un aspetto fondamentale per il miglioramento di questa tecnica riguarda la stabilità della molecola di double strand RNA (dsRNA) utilizzata, che risente di diversi fattori ambientali.

Lo scopo della mia tesi di dottorato consiste nello sviluppo di strategie di controllo basate sull'utilizzo della tecnica dell'RNAi per il silenziamento di geni essenziali per l'insetto bersaglio, in diversi stadi di sviluppo, isolati da studi sulle basi molecolari e funzionale delle interazioni fra insetti e loro antagonisti naturali. La mia attività di ricerca è stata indirizzata, non solo verso l'identificazione di nuovi target molecolari, ma anche verso il miglioramento dell'applicabilità in campo delle molecole di dsRNA, attraverso un sistema di rilascio ambientale basato su nanoconiugati di origine naturale. Nello specifico, il progetto si articola in tre parti: I) Il silenziamento mediato da RNAi di un gene immunitario in *Spodoptera littoralis* (Lepidoptera, Noctuidae) che ne altera lo sviluppo embrionale; II) Analisi e caratterizzazione di un gene immunitario (*Slrepat1*), un potenziale bersaglio per sviluppare nuove strategie di controllo degli insetti dannosi basate sulla tecnica RNAi; III)

Sviluppo di una nuova strategia di rilascio delle molecole dsRNA basata sulla formulazione di nanoconiugati a base di chitosano e sostanze umiche.

La prima parte della tesi riguarda lo studio funzionale del gene immunitario *Sl102* durante l'embriogenesi di *S. littoralis* e include la valutazione degli effetti fenotipici associati al suo silenziamento mediato da RNAi. Negli ultimi anni, grazie allo studio dell'interazione ospite-parassitoide, è stato isolato e caratterizzato un gene, denominato *102*, espresso negli emociti delle larve di *Heliothis virescens* (Lepidoptera, Noctuidae), che codifica per una proteina precursore delle fibrille amiloidi. Tali fibre amiloidi, favoriscono la biosintesi localizzata di melanina, a ridosso dell'oggetto non-self, evitando la diffusione sistemica di precursori tossici. Nel sistema ospite parassitoide in cui è stato isolato, la sua espressione viene fortemente ridotta in ospiti parassitizzati, che mostrano una severa compromissione della loro competenza immunitaria. L'omologo di questo gene è stato isolato e caratterizzato anche nel lepidottero nottuide *S. littoralis*, mostrando un ruolo analogo nella risposta immunitaria allo stadio larvale. Poiché questo gene risulta espresso anche durante lo stato embrionale, nelle fasi in cui le difese immunitarie non sono ancora attive si è proceduto a studiare il suo possibile ruolo durante questa fase precoce dello sviluppo. Da un'analisi del profilo temporale di espressione si desume la presenza di un picco molto evidente a 32 ore dopo l'ovideposizione. Il silenziamento di questo gene è stato effettuato prima del picco di espressione, immergendo le uova di *S. littoralis* in una soluzione di dsRNA per 120, 60, 30 e 15 minuti. Ciò ha consentito di osservare un livello di silenziamento linearmente associato al tempo di trattatmento, con la massima diminuzione dell'espressione genica ottenibile quando le uova sono immerse per 2 ore. Il silenziamento del gene *Sl102* nelle uova di *S. littoralis* ha ridotto significativamente la percentuale di schiusa, indicando un ruolo cruciale per questo gene nello sviluppo dell'embrione. Ciò è evidenziato anche dall'osservazione fenotipica degli embrioni dissezionati, in cui è visibile una chiara differenza morfologica tra il gruppo dei silenziati e quello dei controlli. Inoltre, è stata registrata un'elevata mortalità anche nelle poche larve sgusciate dalle uova sottoposte a silenziamento. Infine, il silenziamento è stato associato a un evidente ritardo nello sviluppo degli embrioni, come osservato al microscopio ottico. Nel distretto dell'intestino medio sono state osservate cellule indifferenziate e scarsa organizzazione tissutale. Le proteine del tuorlo, che forniscono la nutrizione per l'embrione in via di sviluppo, sono consistentemente presenti nel lume dell'intestino medio degli individui silenziati a 72 ore

dall'ovideposizione, mentre queste proteine sono completamente assorbite nei controlli. Questi risultati sono stati confermati anche dall'analisi ultrastrutturale TEM, che ha mostrato evidenti ritardi nello sviluppo delle cellule dell'epitelio intestinale nel gruppo dei silenziati, mentre nei gruppi di controllo le stesse cellule presentano strutture differenziate come, ad esempio, i microvilli. Infine, anche la formazione della cuticola dell'insetto, che appare meno spessa e stratificata, sembra risentire degli effetti del silenziamento del gene *Sl102*. L'elevata mortalità osservata nel gruppo dei silenziati unitamente alle osservazioni morfologiche, che hanno evidenziato un generale ritardo nello sviluppo embrionale, suggeriscono che questo gene, noto per il suo ruolo nel sistema immunitario delle larve di lepidotteri, possa avere una funzione chiave nell'organizzazione strutturale e nel differenziamento di diversi tessuti/organi durante l'embriogenesi. Ulteriori indagini funzionali saranno necessarie per meglio caratterizzare la funzione embrionale di questo gene, il cui silenziamento negli embrioni induce un elevato livello di mortalità precoce, utile a prevenire i danni inflitti dalle larve.
La seconda parte della tesi riguarda lo studio della famiglia di geni *repat* (REsponse to PAThogens), che sono stati isolati per la prima volta in larve di *S. exigua*. Sebbene il loro ruolo non sia ancora chiaro, le proteine di questa famiglia sembrano essere coinvolte in molteplici processi attivati in risposta ad entomopatogeni. Nel presente lavoro, viene studiato uno dei membri di questa famiglia di geni, *Slrepat1*, nelle larve di *S. littoralis*. È stato dimostrato che esso è espresso principalmente nell'intestino medio delle larve di quinto stadio analizzate, sebbene un'espressione basale sia evidente anche nell'intestino posteriore e nel tessuto adiposo. Il silenziamento del gene *Slrepat1* mediato da RNAi risulta stabile nelle larve trattate e le rende maggiormente suscettibili ad una dose sub letale della formulazione commerciale di *B. thuringiensis* (Xentari™), con una sopravvivenza ridotta di circa il 60% rispetto al gruppo di controllo. Questi risultati dimostrano l'ipotesi di un coinvolgimento dei membri della famiglia *repat* nelle risposte di difesa agli entomopatogeni e offrono una nuova possibilità di potenziamento dell'azione del *B. thuringiensis* attraverso il silenziamento dei membri di questa famiglia proteica.
L'ultima parte della tesi riguarda lo sviluppo di nanoconiugati, chiamati Chi/Hum-dsRNA, per il rilascio ambientale e la protezione delle molecole di dsRNA, ottenuti utilizzando polimeri di chitosano e sostanze umiche. L'approccio innovativo di questo lavoro consiste nell'uso delle sostanze umiche, ottenute dal compostaggio di residui vegetali, che sono noti per avere vari effetti benefici sulla fertilità del

suolo e sulla crescita delle piante, agendo anche come biostimolanti. Abbiamo adottato diverse condizioni sperimentali per la sintesi del nanoconiugato Chi/Hum-dsRNA, e tra quelle testate abbiamo selezionato quella che fornisce la migliore percentuale di intrappolamento (91,1%). L'analisi per DLS (dynamic light scattering) ha mostrato una misura delle dimensioni del formulato pari a 300 nm, un valore superiore alla dimensione media spesso riportata in letteratura di circa 200 nm. Le analisi FE-SEM e TEM hanno mostrato forme irregolari simili a scaglie senza una nanostruttura ben definita. Ciononostante, la struttura amorfa ottenuta ha dimensioni nanoscopiche ed elevata percentuale di intrappolamento del dsRNA. In seguito, allo scopo di ottenere informazioni sulla stabilità del nonoconiugato in diverse condizioni di pH, che includono l'elevata alcalinità dell'intestino dei lepidotteri, abbiamo valutato il rilascio e l'integrità del dsRNA in seguito ad alterazione del pH della sospensione di Chi/Hum-dsRNA. Come previsto, il rilascio di dsRNA è stato osservato per valori di pH > 7, probabilmente dovuto al fatto che il polimero di chitosano è stabile in ambiente acido. Questi risultati suggeriscono che questo formulato è efficace per il controllo dei Lepidotteri, caratterizzati da forti condizioni alcaline nell'intestino. Per verificare la stabilità del Chi/Hum-dsRNA nel tempo, abbiamo trattato con il nanoconiugato e con il dsRNA nudo due diverse superfici: capsula di Petri e foglia di pomodoro, in condizioni di laboratorio. Il risultato ha mostrato che la formulazione sintetizzata è stabile su entrambe le superfici fino a 30 giorni dopo l'applicazione. Tuttavia, lo stesso risultato è stato ottenuto con dsRNA nudo, suggerendo che in condizioni di laboratorio controllate l'utilizzo del nanoconiugato non consente una maggiore stabilità rispetto al dsRNA non coniugato. Pertanto, futuri esperimenti saranno condotti in condizioni di campo, testando sia la stabilità che l'efficacia del Chi/Hum-dsRNA. Inoltre, è stata valutata la stabilità del prodotto a 4°C e a 25°C (shelf-life), dopo 6 e 12 mesi di conservazione. In entrambi i casi nanoconiugati rimangono nella loro condizione iniziale e il dsRNA, una volta rilasciato, risulta integro. Questi risultati non sono sorprendenti, dato che in letteratura è descritto che le condizioni di conservazione a 4°C e 25°C sono le più efficienti, anche utilizzando procedure diverse. Infine, per valutare l'efficacia *in vivo* del nanoconiugato sintetizzato, abbiamo utilizzato *S. littoralis* come insetto modello e *Sl102* come gene bersaglio. È stato eseguito un saggio biologico confrontando l'efficacia del nanoconiugato con quella del dsRNA nudo mediante alimentazione. Le larve alimentate con Chi/Hum-*dsSl102* hanno mostrato alti livelli di silenziamento genico, sia a 24 che a 48 ore dopo il trattamento,

paragonabili a quelli ottenuti con il dsRNA nudo. In conclusione, abbiamo sintetizzato un nuovo tipo di nanoconiugato a base di chitosano e sostanze umiche per il rilascio e la protezione di molecole di dsRNA, con l'obiettivo di migliorare l'efficienza della loro applicazione in campo per il controllo degli insetti nocivi.
I risultati di questo lavoro di ricerca promuovono lo sviluppo di di nuove strategie di controllo che non sono solo basate sull’effetto diretto sugli insetti bersaglio, ma anche sul potenziamento dei loro antagonisti naturali, rafforzando i servizi ecosistemici da essi forniti.

1. GENERAL INTRODUCTION

1.1. Biological control

With a predicted increase in world population to 10 billion over the next years (Figure 1.1), one of the biggest challenges of the 21st-century is to maximize food production in an environmentally sustainable and cost-effective manner. To meet the world's future food security and sustainability needs, to reduce the use of chemical pesticides is a priority and an imperative for agriculture imposed by the Farm to Fork Strategy in the European Green Deal (European Commission, 2020). Indeed, reducing the use of chemical pesticides is one of the main objectives to be pursued to make the agriculture both ecologically and economically more sustainable.

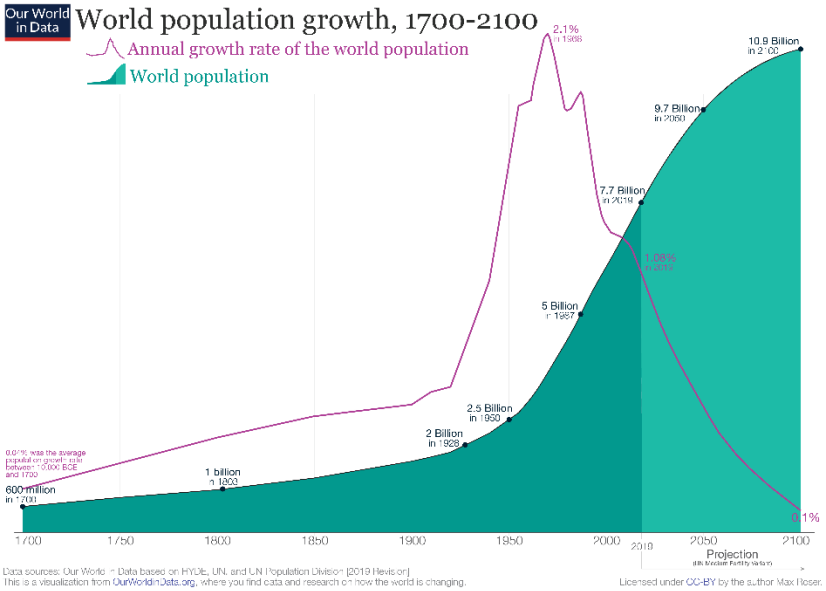

Fig. 1.1 Graph showing global human population growth from the mid-18th century to the end of the 21st century (figure from Roser, 2020; https://ourworldindata.org/world-population-growth-past-future).

However, the control of pest insects in intensive agriculture is still largely dependent on the use of synthetic agrochemicals, which have generated several problems, such as resistance, environmental contamination, toxicity for non-target organisms (including humans), and biodiversity loss (Mahmood *et al.*, 2016). A pivotal role in pesticides use reduction is played by biological control, a strategy for insect control

based on the use of parasites, predators, and pathogens (DeBach, 1964). Starting from the second half of the last century, this pest control strategy, has been increasingly adopted for plant protection against phytophagous insects (Pennacchio *et al.*, 2014) and it has successfully been improved for more than a century and still represents one of the key-aspects in the integrated pest management (IPM) (Bale *et al.*, 2008). According to the Food and Agriculture Organization of the United Nations (FAO), "Integrated Pest Management (IPM) means the careful consideration of all available pest control techniques and subsequent integration of appropriate measures that discourage the development of pest populations and keep pesticides and other interventions to levels that are economically justified and reduce or minimize risks to human health and the environment. IPM promotes the growth of a healthy crop with the least possible disruption to agro-ecosystems and encourages natural pest control mechanisms" (FAO 2020). IPM is an ecosystem-based strategy that focuses on long-term prevention of pests or their damage through a combination of techniques such as biological control, habitat manipulation, modification of cultural practices, use of resistant varieties, and the use of low-risk compounds (Baker *et al.*, 2020). Pesticides should be used as a final alternative, when all the other approaches fail, and treatments are made with the goal of removing only the target organism, when present at a level that can cause economic damage. This is a promising approach to minimize losses in crop quality and quantity caused by pests, which reduces the negative impact of pest management on human health, environment and nontarget organisms. Biological control should be a core component of sustainable IPM plans, increasingly based on the protection and use of natural enemies, such as pathogens, parasitoids, and predators, to regulate pest densities and keep them below the economic threshold (DeBach, 1964). In addition to the use of living organisms, it is possible to use nature-based substances such as plant-derived molecules (Isman 2006), semiochemicals (Bruce *et al.*, 2005; Witzgall *et al.*, 2010), protein applications (Thakur and Sohal, 2013), and RNA interference (Koch *et al.,* 2016; Zhu *et al.,* 2011). The International Biocontrol Manufacturers' Association (IBMA) promotes the broader term *bioprotection,* which includes the use of both biocontrol agents and non-living plant protection tools originated from nature (Stenberg *et al*., 2021). The growing knowledge on the functional basis of biological control allows to include in this definition also the use of molecules/genes deriving from natural antagonists, which can reproduce the lethal syndrome they induce in the target pests they use as hosts (Bale *et al.,* 2008; Pennacchio *et al.,* 2012; Mahmood *et al.,*

2016). Many bioactive molecules, that regulate insect antagonistic interactions, have been already isolated and characterized from plants and microorganisms (bacteria, fungi, and viruses), to obtain insecticides of natural origins (Kachhawa, 2017), and many untapped sources are available in nature.

Plant and microorganisms are clear examples of natural sources of molecules that regulate insect antagonistic interactions and thus can have insecticide activity. This basic concept of mimicking the natural killing mechanisms can be extended to the interaction between insects and their natural antagonists and underlies the potential of using them beyond the organism level, not only as biocontrol agents, but also as a source of molecules and genes that may have a relevant role in crop protection.

The bacterium *Bacillus thuringiensis* (*Bt*) provides the best example of a very effective natural antagonist used in spraying formulations and as a source of toxin genes expressed in transgenic plants (Romeis *et al.*, 2006), which encode proteins produced as parasporal inclusions during the sporulation process. These insecticidal toxins are extremely selective against insects and then, ideal candidates for sustainable IPM plans (Bale *et al.*, 2008). The most widely used are the δ-endotoxins, which belong to the two large multigene families *cry* and *cyt* (Palma *et al.*, 2014). The Cry toxins are active against Lepitopteran larvae, Coleoptera, Hymenoptera and Diptera. The Cyt proteins are produced by *Bt* strains active against Diptera. Genes encoding Cry toxins have been used, since 1996, to produce insect-resistant plants (Roh *et al.*, 2007). *Bt* plants are currently used in many countries and their use has led to a significant reduction in chemical pesticides applications (Toenniessen *et al.*, 2003; Brookes and Barfoot, 2005), without any scientific evidence of negative impact on non-target organisms and environment (Rukarwa *et al.*, 2014). Thanks to the studies of the interactions between this entomopathogen and some of its target insects, it is possible to characterize new genes of interest to be used for the development of new control strategies. An example is given by the *repat* (REsponse to PAThogens) gene family, characterized for the first time by Herrero *et al.* (2007) in *Spodoptera exigua* larvae. The proteins of this family are expressed in response to *Bt* infection and appear to be involved in defense mechanisms that have not yet been clarified. Understanding these mechanisms and associated gene pathways may therefore improve current pest control strategies.

Among the wealth of insect natural enemies, predators and parasitoids are by far the most abundant and used as biocontrol agents (Bale *et al.*, 2008). However, recent studies do also uncover their interesting

potential as source of molecules and genes to be used for the development of new biotechnologies for insect pest control (Pennacchio *et al.*, 2012). The molecules involved in the regulation of host physiology and its killing by parasitic wasps (Pennacchio and Strand, 2006) are ideal candidates for the development of new biological insecticides, in theory highly selective, given the stenophagy level exhibited by these beneficial insects. The identification of the genes regulating the molecular interactions between insect hosts and their natural antagonists offers the opportunity to identify new virulence factors and their cognate target receptors in the host, that can be used to develop innovative biotechnologies for insect control (Pennacchio *et al.*, 2012). These biotechnologies, based on molecules and genes that are produced and delivered by natural enemies, could fall into an expanded definition of biological control, denoted also as bioprotection, which includes not only the use of the organisms, but also of genes and molecules derived from them.

1.2. The host-parasitoids interaction as sources of new bio-inspired control strategies

Parasitoid wasps are entomophagous insects that are free-living during their adult stage, while their juveniles have a parasitic life habit and feed on all different life stages of insect hosts, showing a wide range of exploitation strategies of the living food source they colonize and regulate to their own advantage (Harvey, 2005; Pennacchio and Strand, 2006).

Parasitoids are largely represented in Hymenoptera (Quicke, 1997), although they can be found in other several orders of insects, such as Coleoptera, Diptera, Lepidoptera, Trichoptera, Neuroptera, Strepsiptera (Pennacchio and Strand, 2006). The high species diversity is almost matched by an equally wide spectrum of interactions with hosts (Godfray, 1994; Pennacchio and Strand, 2006). Parasitoids are generally classified as "idiobiont" (e.g., *Bracon hebetor*), which develop on a permanently paralyzed host, and "koinobiont" (e.g., *Aphidius ervi*), whose host continues to feed and grow after parasitization (Quicke, 1997; Askew and Shaw, 1986). Furthermore, idiobionts are mostly ectoparasitoids (external) and koinobionts are mostly endoparasitoids (internal), although rarely a parasitoid can use a combination of strategies (Heraty, 2017).

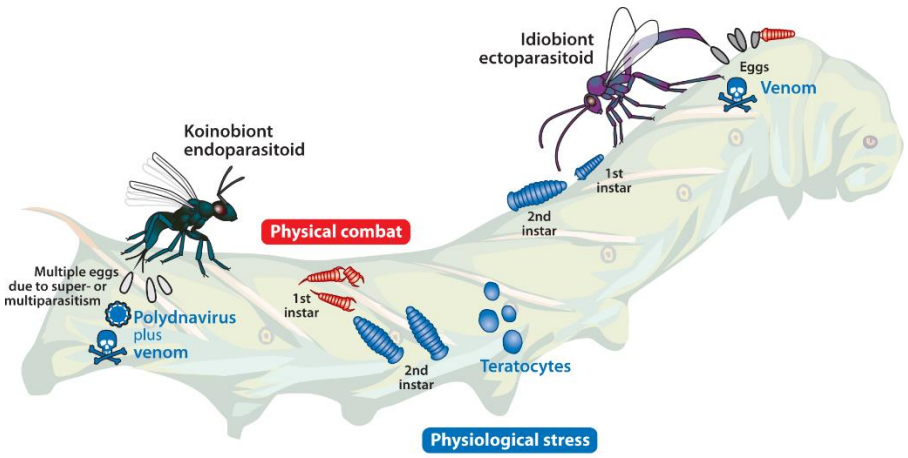

Fig. 1.2 Illustration of a caterpillar (Lepidoptera) parasitized by a solitary koinobiont endoparasitoid (left) or a solitary idiobiont ectoparasitoid (right) (figure from Harvey *et al.*, 2013).

The interactions between parasitoids and hosts are mainly controlled by regulation factors, which originate from the parasitoid adult female (maternal regulation factors) and/or from her progeny (embryonic regulation factors) (Figure 1.2).
The host regulation factors injected by the ovipositing wasp females are venom, ovarian proteins and symbiotic viruses named Polydnavirus (PDVs) (Quicke, 1997). Among these factors, the PDVs and virus-like particles described in many parasitoid wasps have a crucial role in the disruption of the lepidopteran host immunity and development (Beckage and Gelman, 2004, Beck and Strand, 2007, Strand and Burke 2013, Strand and Burke, 2015, Wang *et al.,* 2018; Shi *et al.,* 2019; Strand and Burke, 2019).

1.3. Polydnaviruses

PDVs are divided into two genera called bracovirus (BVs) and ichnovirus (IVs), which are associated with Hymenoptera belonging to Braconidae and Ichneumonidae families, respectively (Strand and Drazen, 2012; Strand and Burke, 2013).
The absence of PDVs in basal lineages of Hymenoptera strongly suggests that the association of BV with braconids and IV with ichneumonids arose independently (Huguet *et al.,* 2012), driven by strong evolutionary constraints leading to unique cases where a eukaryotic organism uses a virus to genetically manipulate the physiology of another eukaryote (Drezen *et al.,* 2003).

PDVs are obligate symbionts stably integrated into the genome of Hymenoptera parasitizing lepidopteran larvae, capable of replication only in the female ovaries and once injected (Strand and Burke, 2012, Strand and Burke 2019) infect different host cell types, without replicating (Figure 1.3).

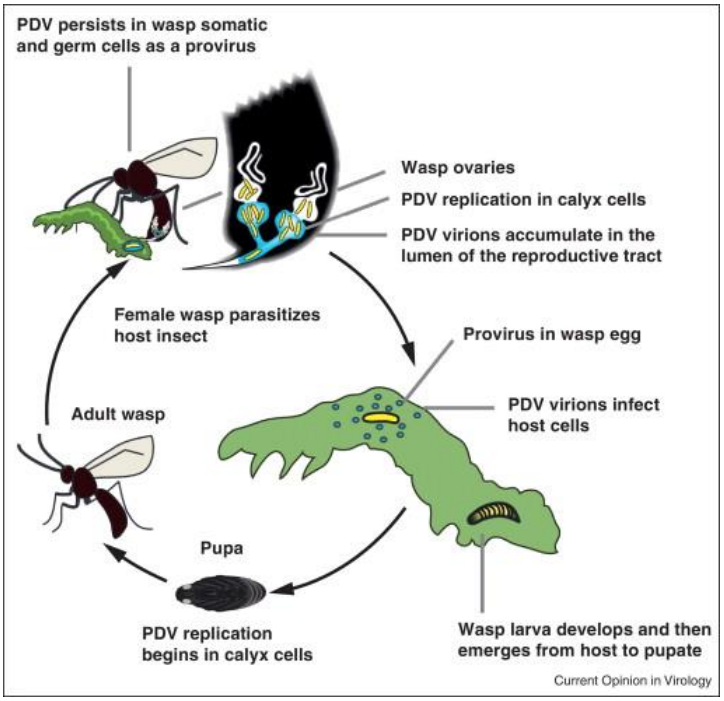

Fig. 1.3 The life cycle of parasitoid wasps and PDVs (figure from Strand and Burke, 2013).

After host cells infection the PDV express several virulence genes that result in numerous alterations, essential for the success of parasitism (Beckage and Gelman, 2004, Webb *et al.,* 2006, Strand and Burke 2019), including physiological alterations, development arrest and the suppression of the host immune response (Shelby and Webb, 1999, Strand and Burke, 2012; Gueguen *et al.,* 2013; Strand and Burke, 2015; Gauthier *et al.,* 2018; Shi *et al.,* 2019; Strand and Burke 2019).
The wealth of virulence factors required for successful parasitism target different functions in the host and makes the PDVs a natural source of potential bioinsecticides molecules (Pennacchio *et al.,* 2012). The study of the mechanism of action of these virulence factors offers the possibility not only to exploit them as new bioinsecticides but also to develop new control strategies based on the use of molecular tools (e.g., RNAi and genome editing) to target the same functions which are

disrupted in naturally parasitized hosts (Price and Gatehouse, 2008; Pennacchio *et al.,* 2012; Perkin *et al.,* 2016).

1.4. PDV-inspired pest control strategies: an example

The characterization of the virulence factors encoded by the bracovirus (*Tn*BV) associated with *Toxoneuron nigriceps* (Hymenoptera, Braconidae), an endophagous parasitoid of the tobacco budworm larvae, *Heliothis virescens* (Lepidoptera, Noctuidae), allowed the isolation of a host gene that is negatively modulated soon after oviposition This gene designated *102* plays an important role in the cellular and humoral immune response (Falabella *et al.,* 2012). *102* gene codes for a protein essential in the encapsulation process which generates a scaffold of amyloid fibrils promoting the binding of toxic melanin precursors and polymerization of melanin itself onto the target site, avoiding their harmful diffusion outside the capsule (Falabella *et al.,* 2012) that would be fatal for the insect (Lemaitre and Hoffmann, 2007, Cerenius *et al.,* 2008, 2010; Nappi *et al.,* 2009). Interestingly, *102* silencing leads to an immunosuppressed phenotype probably reproducing the syndrome observed in parasitized larvae from *T. nigriceps*. In the *H. virescens* larvae treated with *102* dsRNA a reduced level of encapsulation is observed (Falabella *et al.*, 2012).
A homolog of *102* gene was detected in *S. littoralis* (Lepidoptera, Noctuidae), named *Sl102*. This gene was highly expressed in the haemocytes (Di Lelio *et al.*, 2014) and its silencing trough RNAi induces an immunosuppressed phenotype with an enhanced sensitivity to the entomopathogen *B. thuringiensis* (Caccia *et al.*, 2020; Di lelio *et al.*, 2022).

1.5. RNAi-based pest control strategies

The discovery of RNA interference (RNAi) has significantly expanded our understanding of gene regulation, by revealing an array of related pathways in which small, ∼20- to 30-nucleotide (nt) long, noncoding RNAs and their associated proteins control the expression of genetic information (Carthew and Sontheimer, 2009; Wilson and Doudna, 2013). RNAi is a mechanism of modulation of gene expression, conserved in higher organisms, which acts in the transcriptional, post-transcriptional and translational phases (Carthew and Sontheimer, 2009; Berezikov, 2011). In the presence of complementary RNA, a messenger RNA (mRNA) forms a very stable double-stranded structure, which, recognized by other factors, determines its

degradation and therefore the blocking of gene expression (Bartel, 2009). The mechanism of action of RNAi was first demonstrated *in C. elegans* (Fire *et al.*, 1998), where double-stranded RNA (dsRNA), of exogenous or endogenous origin, was described as the trigger of whole process. The three pathways of RNAi (miRNA, siRNA, piRNA) share a common mode of action: after dsRNA processing, a ribonucleoprotein complex comprising an Argonaute family protein bound to a single-stranded ~20- to 30-nt RNA that grants silencing specificity via base-pairing interactions with the target gene transcript. In miRNA and siRNA pathways, this is known as RNA-induced silencing complex (RISC), and it drives silencing of a target mRNA via degradation and/or transcriptional repression (Figure 1.4) (Wilson and Doudna, 2013).

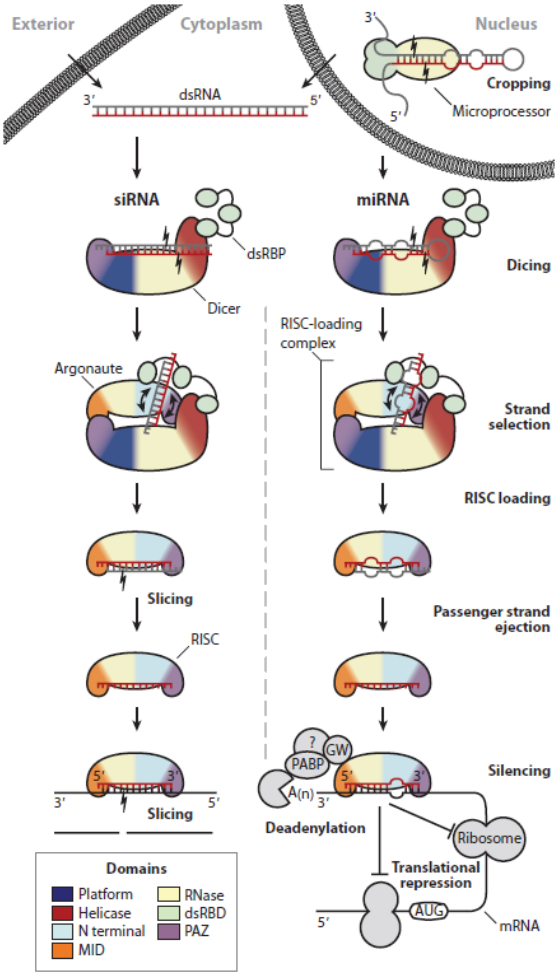

Fig. 1.4 The siRNA (*left*) and miRNA (*right*) pathways of RNA interference (figure from Wilson and Doudna, 2013).

Given its high sequence specificity, this technique has been used for functional studies of genes involved in insect development, physiology, and reproduction (Schmitt-Engel *et al.*, 2015; Ulrich *et al.*, 2015). Furthermore, in recent years, RNAi has had extensive use in the selective control of insect pests, targeting essential genes, without adversely affecting non-target species (Gordon and Waterhouse, 2007; Price and Gatehouse, 2008; Gu and Knipple, 2013). This approach can be pursued either directly, by suppressing functions in the target insect host that generate lethal phenotypes, or, indirectly, by enhancing the impact and biocontrol efficiency of natural pathogens, because of the immune disruption syndrome of the host (Washburn *et al*., 2000; Fath-Goodin *et al*., 2006). The immunosuppressed host is made more susceptible to a wide range of other pathogens including fungi, viruses, and bacteria. This offers the possibility to develop new integrated control strategies not exclusively relying on toxic molecules but aiming at achieving a sustainable manipulation of biocontrol agents.

An interesting aspect of the RNAi technique concerns the ability of dsRNA to pass intestinal barriers reaching other tissues, a mechanism called systemic (sys) RNAi (Joga *et al.*, 2016), which makes this approach very interesting for the control of insect pests. Specifically, in some insects, administration of dsRNA can result in the generation of an RNAi response throughout the entire insect's body. The systemic RNAi is robust in Coleoptera, absent in Diptera and not uniformly present in other insect orders (Joga *et al.*, 2016; Cooper *et al.*, 2019), such as in Lepidoptera, where it occurs in several noctuid species (e.g., *Helicoverpa* and *Spodoptera* spp.) (Di Lelio *et al.*, 2014; Lim *et al.*, 2016; Cooper *et al.*, 2019). To maximize the potential of RNAi for insect control it is important to understand the different dsRNA delivery methods for insecticidal applications, such as microinjection, ingestion, soaking, electroporation, and virus-mediated delivery. Another fundamental aspect for the improvement of this technique concerns the dsRNA stability, which is affected by different environmental causes such as the presence of nucleases produced by microorganisms, UV rays, chemical hydrolysis due to gut pH or to enzymes present in the hemolymph (Terenius *et al.*, 2011; Singh *et al.*, 2017). Therefore, the use of dsRNAs for insect control requires that adequate delivery strategies must be defined to reduce environmental degradation and enhance efficacy. This will be taken into consideration by developing polymer-based nanomaterials to protect dsRNA and assessing their impact on delivery efficiency. One of the most widely used polymers for the development of nanocarriers is chitosan, and its first application as

a delivery strategy for insect control was reported in mosquito (Zhang *et al.*, 2010).

1.6. Objectives

The aim of this PhD thesis is to develop novel field deliverable control strategies based on the use of RNAi for the silencing of target genes involved in the insect antagonistic associations.
This general objective is pursued with 3 experimental approaches:

I) RNAi-mediated silencing of the immune gene *Sl102* in embryos of *Spodoptera littoralis* (Lepidoptera, Noctuidae), causes morphological alterations and blocking of embryonic development (Chapter 2).

II) Analysis and characterization of a new immune target gene (*Slrepat1*) for the development of a new approach based on the enhancement of the killing activity of entomopathogens through RNAi- mediated silencing (Chapter 3).

III) Development of a new delivery strategy for dsRNA molecules, using chitosan/humic substances-based nanoconjugates (Chapter 4).

References

Askew, R. R., & Shaw, M. R. (1986). Parasitoid communities: their size, structure and development. In *[" Waage, J and Greathead, D (eds), Insect Parasitoids, 13th Symposium of Royal Entomological Society of London"]*. Academic Press, London: now Elsevier.

Bale, J. S., Van Lenteren, J. C., & Bigler, F. (2008). Biological control and sustainable food production. *Philosophical Transactions of the Royal Society B: Biological Sciences*, *363*(1492), 761-776.

Baker, B. P., Green, T. A., & Loker, A. J. (2020). Biological control and integrated pest management in organic and conventional systems. *Biological Control*, *140*, 104095.

Bartel, D. P. (2009). MicroRNAs: target recognition and regulatory functions. *cell*, *136*(2), 215-233.

Beck, M. H., & Strand, M. R. (2007). A novel polydnavirus protein inhibits the insect prophenoloxidase activation

pathway. *Proceedings of the National Academy of Sciences*, *104*(49), 19267-19272.

Beckage, N. E., & Gelman, D. B. (2004). Wasp parasitoid disruption of host development: implications for new biologically based strategies for insect control. *Annual review of entomology*, *49*, 299.

Berezikov, E. (2011). Evolution of microRNA diversity and regulation in animals. *Nature Reviews Genetics*, *12*(12), 846-860.

Brookes, G., & Barfoot, P. (2005). GM crops: the global economic and environmental impact--the first nine years 1996-2004.

Bruce, T. J., Wadhams, L. J., & Woodcock, C. M. (2005). Insect host location: a volatile situation. *Trends in plant science*, *10*(6), 269-274.

Caccia, S., Astarita, F., Barra, E., Di Lelio, I., Varricchio, P., & Pennacchio, F. (2020). Enhancement of *Bacillus thuringiensis* toxicity by feeding *Spodoptera littoralis* larvae with bacteria expressing immune suppressive dsRNA. *Journal of Pest Science*, *93*(1), 303-314.

Carthew, R. W., & Sontheimer, E. J. (2009). Origins and mechanisms of miRNAs and siRNAs. *Cell*, *136*(4), 642-655.

Cerenius, L., Lee, B. L., & Söderhäll, K. (2008). The proPO-system: pros and cons for its role in invertebrate immunity. *Trends in immunology*, *29*(6), 263-271.

Cerenius, L., Kawabata, S. I., Lee, B. L., Nonaka, M., & Söderhäll, K. (2010). Proteolytic cascades and their involvement in invertebrate immunity. *Trends in biochemical sciences*, *35*(10), 575-583.

Cooper, A. M., Silver, K., Zhang, J., Park, Y., & Zhu, K. Y. (2019). Molecular mechanisms influencing efficiency of RNA interference in insects. *Pest management science*, *75*(1), 18-28.

DeBach, P. (1964). Biological control of insect pests and weeds. *Biological control of insect pests and weeds.*

Di Lelio, I., Varricchio, P., Di Prisco, G., Marinelli, A., Lasco, V., Caccia, S., ... & Pennacchio, F. (2014). Functional analysis of an immune gene of Spodoptera littoralis by RNAi. *Journal of insect physiology*, *64*, 90-97.

Di Lelio, I., Barra, E., Coppola, M., Corrado, G., Rao, R., & Caccia, S. (2022). Transgenic plants expressing immunosuppressive dsRNA improve entomopathogen efficacy against Spodoptera littoralis larvae. *Journal of Pest Science*, *95*(3), 1413-1428.

Drezen, J. M., Provost, B., Espagne, E., Cattolico, L., Dupuy, C., Poirie, M., ... & Huguet, E. (2003). Polydnavirus genome: integrated vs. free virus. *Journal of Insect Physiology*, *49*(5), 407-417.

European Comission. Communication from the Commission to the European Parliament, the Council, the European Economic and Social Committee and the Committee of the Regions: A Farm to Fork Strategy for a Fair, Healthy and Environmentally Friendly Food System COM/2020/381 Final (European Comission, 2020).

Falabella, P., Riviello, L., Pascale, M., Di Lelio, I., Tettamanti, G., Grimaldi, A., ... & Pennacchio, F. (2012). Functional amyloids in insect immune response. *Insect biochemistry and molecular biology*, *42*(3), 203-211.

Fath-Goodin, A., Kroemer, J., Martin, S., Reeves, K., & Webb, B. A. (2006). Polydnavirus genes that enhance the baculovirus expression vector system. *Advances in virus research*, *68*, 75-90.

Fire, A., Xu, S., Montgomery, M. K., Kostas, S. A., Driver, S. E., & Mello, C. C. (1998). Potent and specific genetic interference by double-stranded RNA in Caenorhabditis elegans. *nature*, *391*(6669), 806-811.

Gauthier, J., Drezen, J. M., & Herniou, E. A. (2018). The recurrent domestication of viruses: major evolutionary transitions in parasitic wasps. *Parasitology*, *145*(6), 713-723.

Godfray, H. C. J., & Godfray, H. C. J. (1994). *Parasitoids: behavioral and evolutionary ecology* (Vol. 67). Princeton University Press.

Gordon, K. H., & Waterhouse, P. M. (2007). RNAi for insect-proof plants. *Nature biotechnology*, *25*(11), 1231-1232.

Gueguen, G., Kalamarz, M. E., Ramroop, J., Uribe, J., & Govind, S. (2013). Polydnaviral ankyrin proteins aid parasitic wasp survival by coordinate and selective inhibition of hematopoietic and immune NF-kappa B signaling in insect hosts. *PLoS pathogens*, *9*(8), e1003580.

Gu, L., & Knipple, D. C. (2013). Recent advances in RNA interference research in insects: Implications for future insect pest management strategies. *Crop Protection*, *45*, 36-40.

Harvey, J. A. (2005). Factors affecting the evolution of development strategies in parasitoid wasps: the importance of functional constraints and incorporating complexity. *Entomologia experimentalis et applicata*, *117*(1), 1-13.

Harvey, J. A., Poelman, E. H., & Tanaka, T. (2013). Intrinsic inter-and intraspecific competition in parasitoid wasps. *Annual review of entomology*, *58*, 333-351.

Heraty, J. (2017). Parasitoid biodiversity and insect pest management. *Insect biodiversity: science and society*, 603-625.

Herrero, S., Ansems, M., Van Oers, M. M., Vlak, J. M., Bakker, P. L., & de Maagd, R. A. (2007). REPAT, a new family of proteins induced by bacterial toxins and baculovirus infection in *Spodoptera exigua*. Insect biochemistry and molecular biology, 37(11), 1109-1118.

Huguet, E., Serbielle, C., & Moreau, S. J. (2012). Evolution and origin of polydnavirus virulence genes. In *Parasitoid viruses* (pp. 63-78). Academic Press.

Isman, M. B. (2006). Botanical insecticides, deterrents, and repellents in modern agriculture and an increasingly regulated world. *Annu. Rev. Entomol.*, *51*, 45-66.

Joga, M. R., Zotti, M. J., Smagghe, G., & Christiaens, O. (2016). RNAi efficiency, systemic properties, and novel delivery methods for pest insect control: what we know so far. *Frontiers in physiology*, *7*, 553.

Kachhawa, D. (2017). Microorganisms as a biopesticides. *J Entomol Zool Stud*, *5*(3), 468-473.

Koch, A., Biedenkopf, D., Furch, A., Weber, L., Rossbach, O., Abdellatef, E., ... & Kogel, K. H. (2016). An RNAi-based control of *Fusarium graminearum* infections through spraying of long dsRNAs involves a plant passage and is controlled by the fungal silencing machinery. *PLoS pathogens*, *12*(10), e1005901.

Lemaitre, B., & Hoffmann, J. (2007). The host defense of *Drosophila melanogaster*. *Annual review of immunology*, *25*(ARTICLE), 697-743.

Lim, Z. X., Robinson, K. E., Jain, R. G., Chandra, G. S., Asokan, R., Asgari, S., & Mitter, N. (2016). Diet-delivered RNAi in *Helicoverpa armigera*–Progresses and challenges. *Journal of Insect Physiology*, *85*, 86-93.

Mahmood, I., Imadi, S. R., Shazadi, K., Gul, A., & Hakeem, K. R. (2016). Effects of pesticides on environment. In *Plant, soil and microbes* (pp. 253-269). Springer, Cham.

Nappi, A., Poirie, M., & Carton, Y. (2009). The role of melanization and cytotoxic by-products in the cellular immune responses of

Drosophila against parasitic wasps. *Advances in parasitology*, *70*, 99-121.
Palma, L., Muñoz, D., Berry, C., Murillo, J., & Caballero, P. (2014). *Bacillus thuringiensis* toxins: an overview of their biocidal activity. *Toxins*, *6*(12), 3296-3325.
Pennacchio, F., & Strand, M. R. (2006). Evolution of developmental strategies in parasitic Hymenoptera. *Annu. Rev. Entomol.*, *51*, 233-258.
Pennacchio, F., Giordana, B., & Rao, R. (2012). Applications of parasitoid virus and venom research in agriculture. In *Parasitoid Viruses* (pp. 269-283). Academic Press.
Pennacchio, F., Caccia, S., & Digilio, M. C. (2014). Host regulation and nutritional exploitation by parasitic wasps. *Current Opinion in Insect Science*, *6*, 74-79.
Perkin, L. C., Adrianos, S. L., & Oppert, B. (2016). Gene disruption technologies have the potential to transform stored product insect pest control. *Insects*, *7*(3), 46.
Price, D. R., & Gatehouse, J. A. (2008). RNAi-mediated crop protection against insects. *Trends in biotechnology*, *26*(7), 393-400.
Quicke, D. L. (1997). *Parasitic wasps*. Chapman & Hall Ltd.
Roh, J. Y., Choi, J. Y., Li, M. S., Jin, B. R., & Je, Y. H. (2007). *Bacillus thuringiensis* as a specific, safe, and effective tool for insect pest control. *Journal of microbiology and biotechnology*, *17*(4), 547-559.
Romeis, J., Meissle, M., & Bigler, F. (2006). Transgenic crops expressing *Bacillus thuringiensis* toxins and biological control. *Nature biotechnology*, *24*(1), 63-71.
Roser, M. (2020). Two centuries of rapid global population growth will come to an end. Our World in Data.
Rukarwa, R. J., Mukasa, S. B., Odongo, B., Ssemakula, G., & Ghislain, M. (2014). Identification of relevant non-target organisms exposed to weevil resistant *Bt* sweetpotato in Uganda. *3 Biotech*, *4*(3), 217-226.
Schmitt-Engel, C., Schultheis, D., Schwirz, J., Ströhlein, N., Troelenberg, N., Majumdar, U., ... & Bucher, G. (2015). The iBeetle large-scale RNAi screen reveals gene functions for insect development and physiology. *Nature communications*, *6*(1), 1-10.
Shelby, K. S., & Webb, B. A. (1999). Polydnavirus-mediated suppression of insect immunity. *Journal of Insect Physiology*, *45*(5), 507-514.

Shi, M., Wang, Z., Ye, X., Xie, H., Li, F., Hu, X., ... & Chen, X. (2019). The genomes of two parasitic wasps that parasitize the diamondback moth. *BMC genomics*, *20*(1), 1-13.

Singh, I. K., Singh, S., Mogilicherla, K., Shukla, J. N., & Palli, S. R. (2017). Comparative analysis of double-stranded RNA degradation and processing in insects. *Scientific reports*, *7*(1), 1-12.

Stenberg, J. A., Sundh, I., Becher, P. G., Björkman, C., Dubey, M., Egan, P. A., ... & Viketoft, M. (2021). When is it biological control? A framework of definitions, mechanisms, and classifications. *Journal of Pest Science*, *94*(3), 665-676.

Strand, M. R., & Burke, G. R. (2012). Polydnaviruses as symbionts and gene delivery systems. *PLoS pathogens*, *8*(7), e1002757.

Strand, M. R., & Burke, G. R. (2013). Polydnavirus-wasp associations: evolution, genome organization, and function. *Current opinion in virology*, *3*(5), 587-594.

Strand MR and Burke GR (2015). "Polydnaviruses: from discovery to current insights." *Virology* 479: 393-402.

Strand, M. R., & Burke, G. R. (2019). Polydnaviruses: evolution and function. *Current Issues in Molecular Biology*, *34*(1), 163-182.

Strand, M. R., & Drezen, J. M. (2012). Family polydnaviridae. *Virus taxonomy: ninth report of the international committee on taxonomy of viruses. Amsterdam: Elsevier*, 237-248.

Terenius, O., Papanicolaou, A., Garbutt, J. S., Eleftherianos, I., Huvenne, H., Kanginakudru, S., ... & Smagghe, G. (2011). RNA interference in Lepidoptera: an overview of successful and unsuccessful studies and implications for experimental design. *Journal of insect physiology*, *57*(2), 231-245.

Thakur, M., & Sohal, B. S. (2013). Role of elicitors in inducing resistance in plants against pathogen infection: a review. *International Scholarly Research Notices*, *2013*.

Toenniessen, G. H., O'Toole, J. C., & DeVries, J. (2003). Advances in plant biotechnology and its adoption in developing countries. *Current opinion in plant biology*, *6*(2), 191-198.

Ulrich, J., Dao, V. A., Majumdar, U., Schmitt-Engel, C., Schwirz, J., Schultheis, D., ... & Bucher, G. (2015). Large scale RNAi screen in *Tribolium* reveals novel target genes for pest control and the proteasome as prime target. *BMC genomics*, *16*(1), 1-9.

Wang, Z. Z., Ye, X. Q., Shi, M., Li, F., Wang, Z. H., Zhou, Y. N., ... & Chen, X. X. (2018). Parasitic insect-derived miRNAs modulate host development. *Nature communications*, *9*(1), 1-9.

Washburn, J. O., Haas-Stapleton, E. J., Tan, F. F., Beckage, N. E., & Volkman, L. E. (2000). Co-infection of *Manduca sexta* larvae with polydnavirus from *Cotesia congregata* increases susceptibility to fatal infection by *Autographa californica* M nucleopolyhedrovirus. *Journal of Insect Physiology*, *46*(2), 179-190.

Webb, B. A., Strand, M. R., Dickey, S. E., Beck, M. H., Hilgarth, R. S., Barney, W. E., ... & Witherell, R. A. (2006). Polydnavirus genomes reflect their dual roles as mutualists and pathogens. *Virology*, *347*(1), 160-174.

Wilson, R. C., & Doudna, J. A. (2013). Molecular mechanisms of RNA interference. *Annual review of biophysics*, *42*, 217-239.

Witzgall, P., Kirsch, P., & Cork, A. (2010). Sex pheromones and their impact on pest management. *Journal of chemical ecology*, *36*(1), 80-100.

Zhang, X., Zhang, J., & Zhu, K. Y. (2010). Chitosan/double-stranded RNA nanoparticle-mediated RNA interference to silence chitin synthase genes through larval feeding in the African malaria mosquito (*Anopheles gambiae*). *Insect molecular biology*, *19*(5), 683-693.

Zhu, F., Xu, J., Palli, R., Ferguson, J., & Palli, S. R. (2011). Ingested RNA interference for managing the populations of the Colorado potato beetle, *Leptinotarsa decemlineata*. *Pest management science*, *67*(2), 175-182.

2. RNAi-mediated silencing of the immune gene *Sl102* in embryos of *Spodoptera littoralis* (Lepidoptera, Noctuidae), causes morphological alterations and blocking of embryonic development

2.1. INTRODUCTION

Lepidoptera are among the most harmful pests in agriculture causing important damages to a wide range of crops (Hill, 1987). Considering their ability to develop resistance to different insecticides, including *Bacillus thuringiensis* (*Bt*) toxins (Matten *et al.*, 2008), the development of new sustainable control strategies using cutting-edge techniques against these insects is of fundamental importance. The study of the molecular interaction between pest insects and their Hymenoptera parasitoids is an important and unexplored source of gene and molecules to be implemented in control strategies (Pennacchio *et al.*, 2012). Indeed, virulence factors encoded by the wasp or by associated symbiotic viruses in the family polydnaviridae can disrupt vital functions, influencing, among others, the neuroendocrine balance, and the immune barriers (Pennacchio and Strand, 2006). The suppression of the immune defense is under strong selection pressure, since if it fails the parasitoid's progeny dies (Pennacchio and Strand, 2006). Therefore, this aspect has received considerable attention, leading to the identification of several parasitoid-derived factors and their cognate targets in the host (Pennacchio and Strand, 2006). Among these latter, a novel immune gene, named *102*, was identified, and found to be highly expressed in the haemocytes, producing a protein which gives rise to functional amyloids mediating immune response in *Heliothis virescens* (Lepidoptera, Noctuidae) larvae (Falabella *et al.*, 2012). A homologue gene has also been found in the related noctuid moth species *Spodoptera littoralis* (Di Lelio *et al.*, 2014). In both species, these amyloids, by coating the non-self-intruders in the haemocoel, provide the structural scaffold that mediates a strictly localized polymerization of melanin on the surface of the invader to be suppressed. Indeed, the RNAi-mediated silencing of *Sl102* gene generates an immunosuppressed phenotype, unable to encapsulate and melanize non-self-objects, enhancing susceptibility to the entomopathogens (Di Lelio *et al.*, 2014; Caccia *et al.*, 2020; Di lelio *et al.*, 2022).

The fibrillar/tubular material present in the cisternae of the rough endoplasmic reticulum of *H. virescens* haemocytes originates from P102, as supported by immunogold detection experiments, further confirmed by overexpression of the *102* gene in insect cells (Falabella *et al.*, 2012). It is interesting to note that several literature reports indicate that consistent amounts of secreted tubular material, contained in large mature vesicles, which also accumulates in immune capsules, significantly contribute to the formation of the basal lamina (Akai and Sato, 1973; Beaulaton, 1968; Sass *et al.*, 1994; Wigglesworth, 1973). Immunodetection studies, which demonstrate the presence of shared molecular epitopes in the basal lamina and haemocytes, have further reinforced these ultrastructural evidence (Nardi and Miklasz, 1989; Sass *et al.*, 1994). Therefore, it is reasonable to speculate that Sl102 protein, in addition to its role in insect immune response, could have an impact on development due to its putative function on the formation of the basal lamina lining the haemocoel and all internal organs of insects, as already proposed for P102 by Falabella *et al.* (2012). Therefore, the disruption of *Sl102* gene expression can potentially affect both immunity and development. Here we investigated the hypothesis that *Sl102* gene has a role in the formation of epithelial basal membranes during the embryonic development. Indeed, if so, the disruption of the fast growth at the embryo stage would likely generate more pronounced phenotypic changes. Therefore, we developed a successful RNAi-based protocol to silence *Sl102* gene during the embryogenesis of *S. littoralis*, performed by eggs immersion in a solution containing dsRNA targeting this gene, and characterized the major ultrastructural changes associated with the very high mortality rate induced by gene silencing. The possibility to suppress *S. littoralis* embryogenesis offers an interesting opportunity of precocious killing of this pest, totally preventing any damage, but adequate delivery strategies will have to be defined to pursue this objective.

2.2. MATERIALS AND METHODS

2.2.1. *S. littoralis* rearing and collection of eggs

S. littoralis is permanently lab-reared at the Department of Agricultural Sciences and derives from a population collected on flower crops in Agro-Pontino (Latina, Italy). The larvae were reared on an artificial diet (41.4 g/l wheat germ, 59.2 g/l brewer's yeast, 165 g/l corn meal, 5.9 g/l ascorbic acid, 1.53 g/l benzoic acid, 1.8 g/l methyl-4-hydroxybenzoate,

and 29.6 g/l agar), as previously described in Di Lelio *et al.*, (2014), at 25 ± 1°C, 70 ± 5% RH, and photoperiod of 16:8 hours light/dark until pupation. The pupae were collected in a plastic box (40 × 30 × 20) closed with a paper sheet until the adult's emergence. The moths (male and female) were collected, soon after emergence, in a cylindric glass jar with the internal perimeter totally covered with two paper sheets, fed with water/honey solution (50%), and allowed to mate for 16 hours at the rearing condition described above. The jar was closed with a paper sheet. The female moth laid the eggs in mass (usually of 100-600 eggs/mass) on the paper sheet, which was collected and replaced. The freshly laid eggs, collected from the same mass, cleaned from the maternal scales, singly separated, and selected with a brush, were then used for the experiments reported above.

2.2.2. *Sl102* gene expression during embryogenesis

A time course analysis was carried out to evaluate the expression level of *Sl102* gene during embryogenesis. Highly synchronized egg mass, laid in a time interval of 30 minutes, were used. Nine time points were investigated 8, 16, 24, 32, 40, 48, 56, 64, 72 hours after oviposition. Briefly 9 pools of 20 eggs, for each time points, were collected from the same mass with a brush in a 1.5 mL Eppendorf tube. Each pool of eggs was processed for total RNA extraction as described below. The obtained RNA samples were used to assess the absolute number of gene transcripts during the embryonic development through an absolute quantitative Real Time PCR (qRT-PCR).

2.2.3. Total RNA extraction

Total RNA was extracted from *S. littoralis* eggs using Invitrogen™ TRIzol™ Reagent (Thermo Fisher Scientific) and stored at -80°C according to the manufacturer's instructions. The concentration and purity of total RNA were determined by measuring the 260/280 nm absorbance ratio with a Varioskan Flash (Thermo Fisher Scientific).

2.2.4. Production of standards for absolute qRT-PCR

Total RNA extracted from *S. littoralis* eggs was subjected to retro-transcription (Ambion® RETROscript® Kit, Thermo Fisher Scientific) and then, used for PCR amplification of *Sl102* gene, with specific primers RT-*Sl102*-Fwd/Rev (Table 2.1). PCR products were ligated into

the pCR4-TOPO TA Vector (Thermo Fisher Scientific) (Figure 2.1), that was introduced into chemically competent One Shot® TOP10 *E. coli* cells and, plated on LB agar. Plasmids from colonies grown overnight were extracted (GRS Plasmid Purification Kit – Mini, Grisp Research Solutions) and sequenced. The plasmid copy number was quantified by spectrophotometry using a Varioskan Flash (Thermo Fisher Scientific), and calculation of the gene copy number was performed according to the molar mass derived from the plasmid and amplicon sequences (Paulin *et al.*, 2009).

Table 2.1 Primer pairs used for qRT-PCR analysis and *in vitro* dsRNA production. Underlying nucleotides indicate the T7 promoter.

Oligos	Sequence 5' – 3'	Amplicon size (bp)	Tm (°C)
RT-*SlActin*-Fwd	CCGTCTTCCCATCCATCGT	66	60
RT-*SlActin*-Rev	CCTTCTGACCCATACCAACCA		
RT-*Sl102*-Fwd	GGCGGTGTCGTCGATTAT	111	60
RT-*Sl102*-Rev	ATTGAACATTTCCTCGCTC		
EST-*Sl102*-Fwd	TACATCCAAGTAAATTTGCAAGGC	580	62
EST-*Sl102*-Rev	TGCCCACGAACATCGTCACCTC		
T7-*Sl102*-Fwd	TAATACGACTCACTATAGGGAGAAAC CTCCTGAGCGTGCCTGA	514	65
T7-*Sl102*-Rev	TAATACGACTCACTATAGGGAGAGGA GTGCTGCTTCAGAATCAT		
T7 Fwd/Rev	TAATACGACTCACTATAGGGAGA	720	60

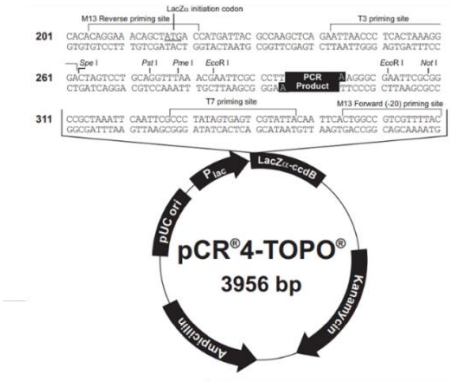

Fig. 2.1 Invitrogen pCR4-TOPO TA Vector for the direct ligation of *Taq*-amplified PCR products.

2.2.5. qRT-PCR absolute quantification of *Sl102* gene during embryonic development

An absolute quantification of the *Sl102* gene expression during embryonic development was achieved using a standard curve constructed by amplifying known amounts of target DNA. The quantification was performed by qRT-PCR, using Applied Biosystems™ SYBR™ Green master mix (Thermo Fisher Scientific). The quantity of transcripts in the samples was determined by relating the obtained Ct values to an established standard calibration curve (Figure 2.2), according to the absolute quantification method (Rutledge and Côté, 2003). The standard curve for *Sl102* transcripts was established by plotting the logarithm of 8 10-fold dilutions of a starting solution containing 10 ng/µl (number of copies: about 3*10^9) of PCR®4 TOPO vector (Figure 2.2) with insert (RT-PCR fragment of *Sl102*) against the corresponding Ct values. The PCR efficiency was calculated based on the slope and the coefficient of correlation (R^2) of the standard curve, according to the following formula: $E = 10^{(-1/slope)} - 1$. Primers RT-*Sl102*-Fwd and RT-*Sl102*-Rev were used for this experiment (Table 2.1).

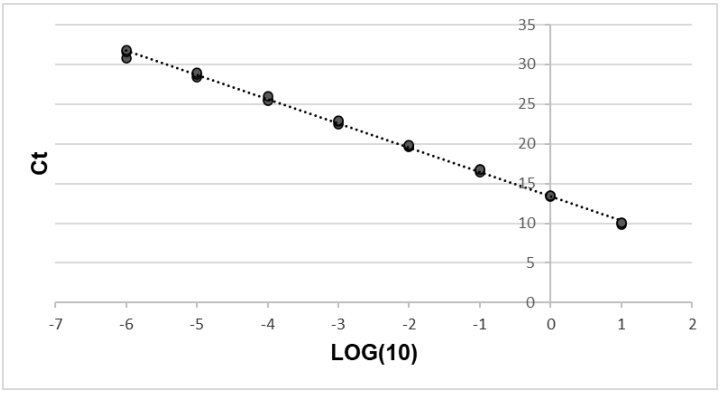

Fig. 2.2 Standard calibration curve of *Sl102* RT-PCR fragment. PCR efficiency is E = 112,676%; slope = - 3,0514; intercept = 13,408; coefficient of correlation R^2 = 0,9981.

2.2.6. *In vitro* synthesis of *Sl102* dsRNA

Total RNA was extracted from *S. littoralis* eggs using Invitrogen™ TRIzol™ Reagent (Thermo Fisher Scientific) according to the manufacturer's instructions, retro-transcribed with the Applied

Biosystems™ High-Capacity cDNA Reverse Transcription Kit (Thermo Fisher Scientific), and a 580 bp long *Sl102* cDNA fragment was obtained by PCR, using primers EST-*Sl102*-Fwd and EST-*Sl102*-Rev (Table 2.1). This cDNA fragment was used as template for a nested PCR reaction, performed with primers containing at their 5' ends the T7 polymerase promoter sequence, T7-*Sl102*-Fwd and T7-*Sl102*-Rev (Table 2.1). The resulting PCR product was used as a template for an *in vitro* synthesis of *Sl102* dsRNA (*dsSl102*) using the MEGAscript® RNAi Kit (Thermo Fisher Scientific), according to the manufacturer's instructions. Synthesized dsRNA (514 bp long) was quantified by measuring its absorbance at 260 nm with a Varioskan Flash Multimode Reader (Thermo Fisher Scientific), and purity was evaluated by assessing 260/280 nm absorbance ratios. The quantified dsRNA molecules were visualized on 1% agarose gel to evaluate their integrity. A *GFP* dsRNA (*dsGFP*), used in control experiments, was similarly produced starting from the cloning vector pcDNA® 3.1/CT-GFP TOPO® (Thermo Fisher Scientific) (Figure 2.3), which was used as template for a PCR reaction, performed with a T7 primer (Table 2.1). The resulting PCR product served as template to synthesize a dsRNA (720 bp long), as described above.

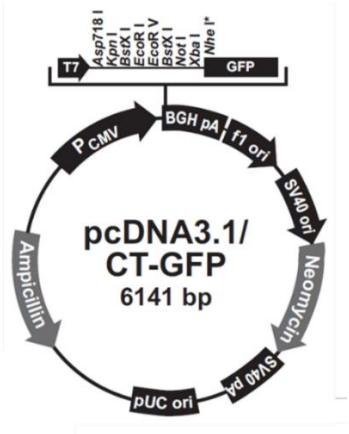

Fig. 2.3 pcDNA™3.1/CT-GFP-TOPO® vector cloning containing the green fluorescent protein (GFP) sequence.

2.2.7. *Sl102* gene silencing by eggs soaking

The silencing efficiency of the *Sl102* gene was tested on eggs collected over a 16 hours' time interval (overnight). Briefly, 8 pools of 100 eggs each were collected from the same mass, as described above, and placed in a 1.5 mL Eppendorf tube. The experimental eggs were

soaked at room temperature in 50 µL of a PBS 1 × solution (phosphate buffered saline 1 ×; 137 mM NaCl, 2.7 mM KCl, 10 mM Na2HPO4, 1.8 mM KH2PO4; pH 7.4) containing 250 ng/µL of *dsSl102* or *dsGFP* (as control). For each experimental condition, after 15, 30, 60 and 120 minutes, the eggs were washed with 1 × PBS (2 times), checked under the stereomicroscope for integrity, and placed, using a paint brush, in a Petri dish which was maintained under the conditions reported above. After 48 hours, for each experimental time, 10 eggs were collected in an Eppendorf tube (1.5 mL), using a paint brush, for total RNA extraction in Trizol reagent, as described above. The RNA was stored at -80 °C until qRT-PCR which was carried out, using the 2-ΔΔCT method (Livak and Schmittgen, 2001; Pfaffl, 2001), as described in Di Lelio *et al.*, 2014, using *Sl102* gene-specific primers and *SlActin* gene-specific primers (Table 2.1). The phenotypic alterations induced by *Sl102* gene silencing were characterized on *S. littoralis* eggs soaked for 120 minutes in 50 µL of *dsSl102* solution, which induced the highest level of gene silencing, and *dsGFP* solution. The eggs were treated as described above and the experiment was replicated 12 times. For each experiment a group of 10 eggs were collected and processed for total RNA extraction and qRT-PCR as described above, 10 eggs were processed for optical and transmission electron microscopy, and the remaining were allowed to develop in the Petri dishes at the rearing conditions described above. The eggs were daily observed until hatching. For each experimental group the newborn larvae were placed in 4-wells plastic rearing trays (RT32W, Frontier Agricultural Sciences, Pitman, NJ, United States), with a piece of artificial diet, closed with perforated plastic lids (RTCV4, Frontier Agricultural Sciences), and daily checked for survival.

2.2.8. Optical and Transmission Electron Microscopy

The silenced and the control eggs, obtained as described above, 72 hours post dsRNA treatment, were dissected in 10 µL 2% glutaraldehyde in 0.1 M sodium cacodylate buffer (pH 7.4), the obtained embryos were fixed with 2% glutaraldehyde in 0.1 M sodium cacodylate buffer (pH 7.4) for 2 h and then washed three times (5 min each) with the same buffer. Specimens were postfixed with 1% osmium tetroxide in cacodylate buffer for 2 h at room temperature and, after standard dehydration in ethanol, they were embedded in Epon-Araldite 812 mixture (Sigma-Aldrich, Milan, Italy). Sections were obtained with Reichert Ultracut S ultramicrotome (Leica, Wien, Austria). Semithin sections (0.75-µm-thick) were stained with crystal violet and basic

fuchsin, analysed with Nikon Eclipse Ni light microscope (Nikon, Tokyo, Japan), and images were obtained with DS-5 M-L1 digital camera system (Nikon). Ultrathin sections (70-nm-thick) were collected on copper grids, stained with uranyl acetate and lead citrate, and analysed with JEOL-1010 TEM (Jeol, Tokyo, Japan) equipped with Morada digital camera (Olympus, Tokyo, Japan) - Centro Grandi Attrezzature, University of Insubria.

2.2.9. Statistical analysis

Time course analysis was analyzed by using the one-way ANOVA and Tukey's multiple comparisons test. The *Sl102* gene expression in egg soaking experiments were analyzed by using the unpaired Student's *t test*. The percentage of hatching eggs was analyzed by using the Fisher's exact test (*Chi-square* test), while the survival rate of newborn larvae was analyzed by using the Log-rank (Mantel-Cox) test. Normality of all data was checked by using the D'Agostino-Pearson test and/or Kolmogorov-Smirnov test. All the data were analyzed using GraphPad Prism (version 6.0).

2.3. RESULTS

2.3.1. Expression profile of *Sl102* gene during embryogenesis

The qRT-PCR analysis revealed that the *Sl102* gene is expressed during the entire embryonic development in *S. littoralis* (Figure 2.4). Starting from the basal expression at 8 hours (number of copies: about 750) after oviposition, a sharp peak was observed at 32 hours (number of copies: about 2*10^4) (One-Way ANOVA, $P < 0.0001$). Then, a drastic decrease to basal levels of expression was recorded at 40 hours (number of copies: about 820). Subsequently, a gradual increase occurred, which culminated at 64-72 hours (number of copies: about 1*10^4), just before hatching.

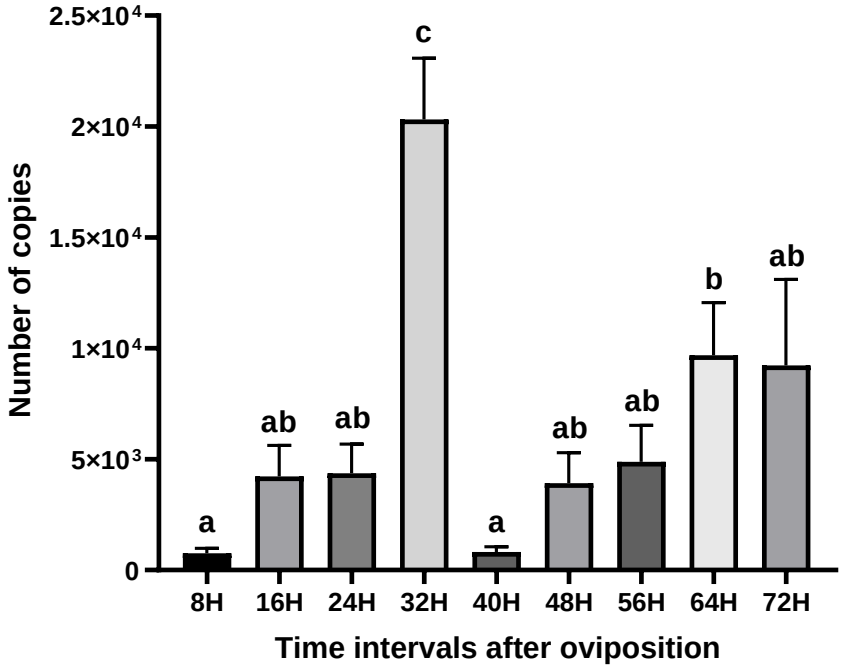

Fig. 2.4 Absolute quantification of *Sl102* gene expression during embryogenesis. The values reported are the mean ± standard error. Mean values denoted with different letters are significantly different (One-Way ANOVA, $F_{(8,95)} = 9{,}71$, $P < 0.0001$).

2.3.2. Impact of gene silencing on egg survival and development

The gene silencing experiment was carried out at different times of soaking (15, 30, 60 and 120 minutes) in a *dsSl102* solution, using *dsGFP* as control. The transcription level of the target gene resulted, for all experimental times considered, significantly lower in *dsSl102* treated eggs (Fold-change: 15-minutes 0.73; 30-minutes 0.61; 60-minutes 0.5; 120-minutes 0.05) compared to controls (Fold-change 1) (Student's t test, $P < 0.0001$). The level of gene silencing increased over time reaching its maximum after 2 hours of soaking (Fig. 2.5). Therefore, this soaking time interval was used to characterize the phenotypic alterations induced by gene silencing by evaluating the survival of both eggs and hatching larvae, along with morphological and ultrastructural alterations.

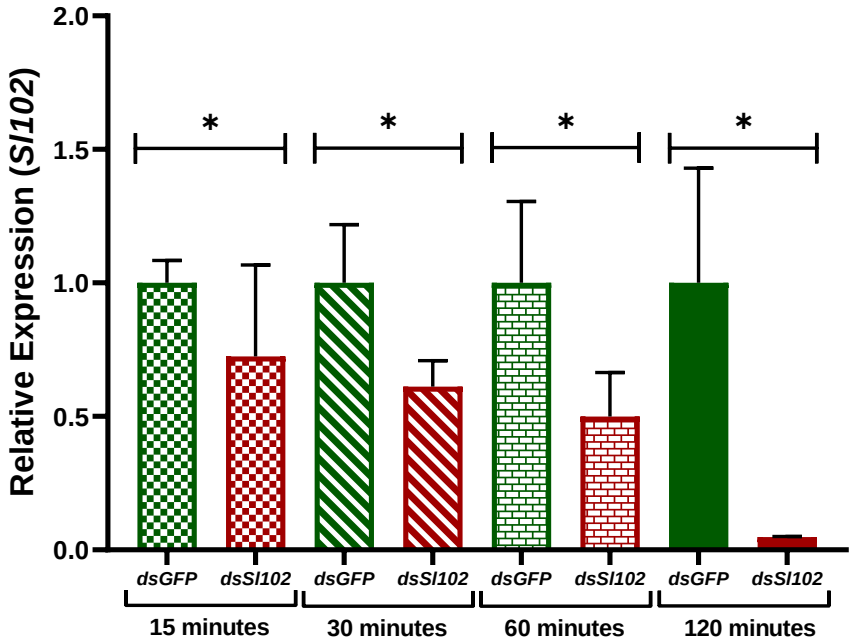

Fig. 2.5 Transcript levels of *Sl102* gene in *S. littoralis* eggs soaked in a dsRNA solution (250 ng/µL). In green, the relative expression of the gene in eggs soaked in *dsGFP*, in red those soaked in *dsSl102*, for different time intervals. The values reported are the mean ± standard error (Student's *t* test: (15 minutes) *t*-test: t = 2.429, df = 23, *P* = 0.0234; (30 minutes) *t*-test: t = 6.249, df = 19, *P* < 0.0001; (60 minutes) *t*-test: t = 6.373, df = 24, *P* < 0.0001; (120 minutes) *t*-test: t = 28.96, df = 22, *P* < 0.0001).

The gene silencing analysis confirmed a strong reduction of *Sl102* gene expression in eggs soaked in *dsSl102* solution (Fold-change 0.04) compared to controls (Fold-change 1) (Student's t test, *P* < 0.0001) (Figure 2.6 A). The silenced eggs treated suffered a very high embryonic mortality and only 5.58% hatched, compared to a hatching rate of 84.21% recorded for the control eggs (Fisher's exact test, *P* < 0.0001) (Figure 2.6 C). The observed reduction of the survival rate was associated, at a first observation with the stereomicroscope, with the presence of only partially formed larvae inside the silenced eggs, compared to the normally developed control larvae (Figure 2.6 B). Silenced larvae gave rise only to 43 new-born larvae, while for controls a 10-fold higher hatching rate was observed (450 larvae). Moreover, the larvae hatched from the silenced eggs showed a survival rate by far much lower than controls (Log-rank (Mantel-Cox) test, *P* < 0.0001) (Figure 2.6 D).

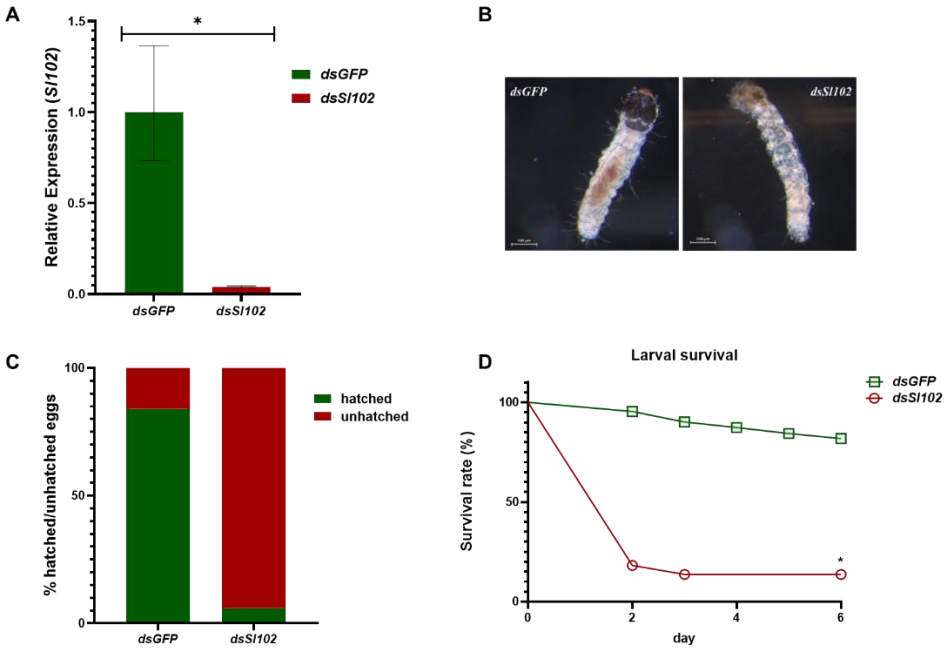

Fig. 2.6 (A) Transcript levels of *Sl102* gene in *S. littoralis* eggs soaked in a dsRNA solution. In green, the relative expression of the gene in eggs soaked in *dsGFP*, in red those soaked in *dsSl102*. The values reported are the mean ± standard error (Student's *t* test: t = 24.97, df = 14, $P < 0.0001$). **(B)** Stereomicroscope observations of larvae treated with *dsSl102* and *dsGFP* (controls). **(C)** Percentage of hatched/unhatched eggs after treatments (Fisher's exact test: $P < 0.0001$). **(D)** Survival rate of new-born larvae after eggs soaking treatment (Log-rank (Mantel-Cox) test: Chi square = 133; df = 1; $P < 0.0001$).

2.3.3. Light and electron microscopy observations

Figure 2.7 shows a comparison of the silenced and control 72 hours old embryos. Optical microscopy demonstrated a developmental delay in *dsSl102* embryos (Figure 2.7 B), as clearly evidenced in the midgut, where the undifferentiated morphology of midgut cells, in addition to the presence of yolk granules in the lumen, could be attributed to a delay in the development of this organ (Figure 2.7 B). This evidence was confirmed by the ultrastructural analysis of this organ. Goblet cells were not completely differentiated in *dsSl102* embryos (Figure 2.7 D). In detail, above the big basal nucleus that was visible in both samples, the goblet cavity was just at the beginning of its formation in *dsSl102* embryos, while in *dsGFP* embryos it was completely differentiated and covered by microvilli (Figure 2.7 C). The apical membrane of columnar cells was also affected by *Sl102* gene silencing. In fact, differently from columnar cells of *dsGFP* embryos, in which a well-developed brush

border was clearly visible (Figure 2.7 E), no microvilli were observed in the apical membrane of these cells in *dsSl102* embryos (Figure 2.7 F). Finally, *Sl102* gene silencing also affected the stratification and thickness of the cuticle. Although the electron-dense envelope of the epicuticle was visible in both samples (Figure 2.7 G, H), a higher thickness of the cuticle (due to the presence of a developed procuticle) in control embryos (Figure 2.7 G) (average thickness: 1 µm (n=4)) compared to *dsSl102* embryos (Figure 2.7 H) (average thickness: 0.12 µm (n=4)) was detected.

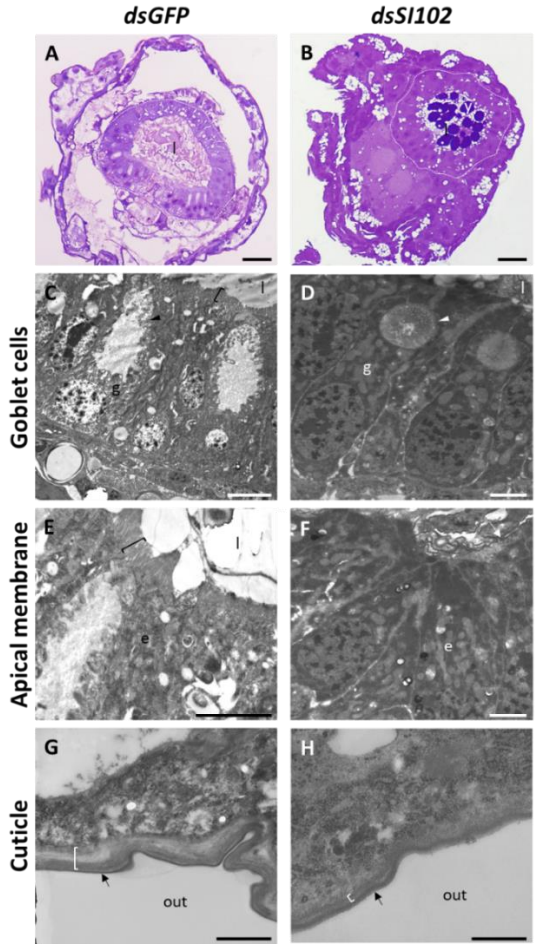

Fig. 2.7 Morphological analysis of *dsGFP* and *dsSl102* embryos. (A, B) optical microscopy; (C-H) TEM. arrowhead: goblet cavity; black arrow: envelope of the epicuticle; black square bracket: microvilli; dotted line: midgut; e: epithelium; g: goblet cell; l: lumen; out: outer environment; white arrow: apical membrane; white square bracket: procuticle; y: yolk granule. Bars: 10 µm (A, B), 5 µm (C, E), 2 µm (D, F, G), 500 nm (H).

2.4. DISCUSSION

In the recent years, thanks to the study of host-parasitoid interaction, a gene, called *102*, expressed in the hemocytes of *Heliothis virescens* larvae was isolated and characterized (Falabella *et al.*, 2012). This gene encodes a precursor protein of amyloid fibrils, which mediates the addition of melanin and therefore the encapsulation mechanism against foreign intruders (Falabella *et al.*, 2012). The homolog of this immune gene was also isolated and characterized, through an RNAi approach, in *S. littoralis* larvae (Di Lelio *et al.*, 2014), showing an analogous role in larval immune response. The indirect evidence that haemocytes are involved not only in the immune response but also in the basal lamina formation, by releasing consistent amounts of secreted tubular material, which also accumulates in the immune capsules (Akai and Sato, 1973; Beaulaton, 1968; Wigglesworth, 1973, Nardi and Miklasz, 1989; Sass *et al.*, 1994), lead us to investigate trough RNAi strategy, the role of the *Sl102* in embryonic development. Our results further expand the understanding of the *Sl102* gene function during embryonic development of *S. littoralis*, assessing the phenotypic effects associated with its silencing mediated by RNAi. The time-course analysis showed that *Sl102* is expressed during all the embryonic development stage, from oviposition to hatching, suggesting a possible functional role during later stages of embryogenesis. Indeed, a peak of maximum expression has been observed around 32 hours after oviposition, suggesting that *Sl102* may exert its function in the following hours, corresponding to an advanced stage of organogenesis. Gene silencing can be obtained by soaking *S. littoralis* eggs in a dsRNA solution for 120, 60, 30, and 15 minutes. However, the highest decrease in gene expression was obtained when the eggs were soaked for 2 hours, while at shorter time intervals the silencing level resulted gradually lower. This data demonstrated that the entry of molecules such as dsRNA, through the egg chorion, occurs in a time-dependent manner with the same dose applied (250 ng/µL). This result can be explained by looking at the structure of the insect egg chorion. The chorion is a complex structure that protects the developing embryo in a hostile environment, allowing gas exchange and preventing desiccation. The specialized regions that facilitate gas exchange between the embryo and the environment are called aeropyles, while micropyles, located at the anterior end of the egg, form a channel which allows the sperm entrance for fertilization (Spradling, 1993; Raikhel, 2005). Another specialized structure is the operculum, which is the chorion region through which the larva will exit (Spradling, 1993;

Raikhel, 2005). Therefore, dsRNA molecules may enter in the egg through one of the structures/openings described above, to overcome the almost completely impermeable protective layer, requiring a certain amount of time to being in contact with the embryo tissues, where gene silencing occurs. The *Sl102* gene silencing in the egg resulted in a high percentage reduction of the hatching rate, suggesting that *Sl102* has a crucial role in the development of the embryo itself, also evidenced by the phenotypic observation of embryos after dissection, in which a clear morphological difference between silenced and controls is evident. The *Sl102* silenced embryos lack head and cuticle sclerotization, a process which starts during the last stage of embryonic development in lepidopteran larvae (Abidalla and Battaglia 2018). Even the new-born larvae of the group of silenced eggs showed a high mortality. The optical microscope observations pointed out an evident delay in the development of the silenced embryos. In the midgut district undifferentiated cells and a poor tissue organization was observed. Yolk proteins, that provides the nutrition for the developing embryo (Correia *et al.*, 2013) are consistently present in the midgut lumen of silenced individuals at 72 hours after oviposition, while these proteins are completely absorbed in the controls. These findings were also confirmed by TEM ultrastructural analysis. Goblet cells appear to be still undifferentiated in the silenced group, where a cavity is observed above a not well-defined nucleus, whereas in the control groups a vesicle is present at the apical level, that is in continuity with the microvilli: a clear signal of differentiation as evidenced in *Manduca* embryos (Hakim *et al.*, 1988). The apical membrane of the columnar cells in the silenced group is also undifferentiated, as the absence of microvilli suggests. In contrast, the control group shows the brush border membrane, which is a clear signal of differentiation of midgut epithelial cells (Kadiri and Louvet, 1982). Also, insect cuticle, which appears to be less thick and stratified, seems to be affected by *Sl102* gene silencing. This is probably due to the different development of the procuticle, which in the control group is structurally similar the one described in *Drosophila* by Moussian *et al.* (2010). These results demonstrate that the *Sl102* gene could play a fundamental, but still unclear, role in the embryonic development of *S. littoralis*. The high mortality observed in the silenced group together with the morphological observations, which highlighted a general delay in the embryonic development, suggest that this gene, which is known for its role in the immune system of lepidopteran larvae, may have a key function in the structural organization and differentiation of different tissues/organs during embryogenesis. These findings appear to corroborate the hypothesis made by Falabella *et al.* (2012)

concerning the role of haemocytes in the formation of the basal laminae by generated by fragments of the protein encoded by *Sl102*. Although these data provide convincing evidence in support of this hypothesis, further functional investigation will be necessary to better characterize the embryonic function of this gene. Finally, the use of RNAi, which regulates the expression of this gene, appears to be promising for the development of control strategies targeting the early stages of development, although further research efforts are necessary to develop more effective and applicable delivery strategies in the environment.

References

Abidalla, M., & Battaglia, D. (2018). Observations of embryonic changes in middle and late stages of the greater wax moth, *Galleria mellonella* (Lepidoptera: Pyralidae). Advances in Entomology, 6(03), 189.

Akai, H., & Sato, S. (1973). Ultrastructure of the larval hemocytes of the silkworm, *Bombyx mori* L.(Lepidoptera: Bombycidae). International Journal of Insect Morphology and Embryology, 2(3), 207-231.

Beaulaton, J., (1968). Etudé ultrastructural et cytochemique des glandes prothoraciques de vers a soil aux quatrieme and cinquieme ages larvaires. I. La tunica propria et ses relations avec le fibres conjoctives et les hemocytes. J. Ultrastruct. Res. 23, 474e498.

Caccia, S., Astarita, F., Barra, E., Di Lelio, I., Varricchio, P., & Pennacchio, F. (2020). Enhancement of *Bacillus thuringiensis* toxicity by feeding *Spodoptera littoralis* larvae with bacteria expressing immune suppressive dsRNA. *Journal of Pest Science*, *93*(1), 303-314.

Correia, A. A., Wanderley–Teixeira, V., Teixeira, Á. A., Oliveira, J. V., Gonçalves, G. G., Cavalcanti, M. G., ... & Alves, L. C. (2013). Microscopic analysis of *Spodoptera frugiperda* (Lepidoptera: Noctuidae) embryonic development before and after treatment with azadirachtin, lufenuron, and deltamethrin. *Journal of Economic Entomology*, *106*(2), 747-755.

Di Lelio, I., Varricchio, P., Di Prisco, G., Marinelli, A., Lasco, V., Caccia, S., ... & Pennacchio, F. (2014). Functional analysis of an immune gene of *Spodoptera littoralis* by RNAi. *Journal of insect physiology*, *64*, 90-97.

Di Lelio, I., Barra, E., Coppola, M., Corrado, G., Rao, R., & Caccia, S. (2022). Transgenic plants expressing immunosuppressive dsRNA improve entomopathogen efficacy against *Spodoptera littoralis* larvae. *Journal of Pest Science*, *95*(3), 1413-1428.

Falabella, P., Riviello, L., Pascale, M., Di Lelio, I., Tettamanti, G., Grimaldi, A., ... & Pennacchio, F. (2012). Functional amyloids in insect immune response. *Insect biochemistry and molecular biology*, *42*(3), 203-211.

Hakim, R. S., Baldwin, K. M., & Bayer, P. E. (1988). Cell differentiation in the embryonic midgut of the tobacco hornworm, *Manduca sexta*. Tissue and Cell, 20(1), 51-62.

Hill, D. S. (1987). *Agricultural insect pests of temperate regions and their control*. CUP Archive.

Kadiri, Z., & Louvet, J. P. (1982). Ultrastructural study of midgut embryonic cytodifferentiation in the phasmid *Clitumnus extradentatus* Br. Journal of morphology, 172(3), 323-334.

Livak, K. J., & Schmittgen, T. D. (2001). Analysis of relative gene expression data using real-time quantitative PCR and the 2−ΔΔCT method. *methods*, *25*(4), 402-408.

Matten, S. R., Head, G. P., & Quemada, H. D. (2008). How governmental regulation can help or hinder the integration of *Bt* crops within IPM programs. In Integration of insect-resistant genetically modified crops within IPM programs (pp. 27-39). Springer, Dordrecht.

Moussian, B. (2010). Recent advances in understanding mechanisms of insect cuticle differentiation. Insect biochemistry and molecular biology, 40(5), 363-375.

Nardi, J. B., & Miklasz, S. D. (1989). Hemocytes contribute to both the formation and breakdown of the basal lamina in developing wings of *Manduca sexta*. Tissue and Cell, 21(4), 559-567.

Paulin, M. M., Novinscak, A., St-Arnaud, M., Goyer, C., DeCoste, N. J., Privé, J. P., ... & Filion, M. (2009). Transcriptional activity of antifungal metabolite-encoding genes phlD and hcnBC in Pseudomonas spp. using qRT-PCR. *FEMS microbiology ecology*, *68*(2), 212-222.

Pennacchio**,** F., & Strand, M. R. (2006). Evolution of developmental strategies in parasitic Hymenoptera. *Annu. Rev. Entomol.*, *51*, 233-258.

Pennacchio, F., Giordana, B., & Rao, R. (2012). Applications of parasitoid virus and venom research in agriculture. In *Parasitoid Viruses* (pp. 269-283). Academic Press.

Pfaffl, M. W. (2001). A new mathematical model for relative quantification in real-time RT–PCR. Nucleic acids research, 29(9), e45-e45.

Raikhel, A. S. (2005). 1.3 Vitellogenesis and Post-Vitellogenic Maturation of the Insect Ovarian Follicle.

Rutledge, R. G., & Cote, C. (2003). Mathematics of quantitative kinetic PCR and the application of standard curves. *Nucleic acids research*, *31*(16), e93-e93.

Sass, M., Kiss, A., & Locke, M. (1994). Integument and hemocyte peptides. Journal of insect physiology, 40(5), 407-421.

Spradling, A. (1993). Developmental genetics of oogenesis. *The development of Drosophila melanogaster*.

Wigglesworth, V. B. (1973). Haemocytes and basement membrane formation in Rhodnius. Journal of Insect Physiology, 19(4), 831-844.

3. Analysis and characterization of a new immune target gene (*Slrepat1*) for the development of a new approach based on the enhancement of the killing activity of entomopathogens through RNAi-mediated silencing

3.1. INTRODUCTION

The insect gut represents the major contact interface with external microorganisms which were ingested along with food, especially during the larval stage, when the insect spends much of its time feeding. Insects have developed unique intestinal defenses against invasion by foreign microorganisms, including physical defenses and immune responses. The physical defenses of the insect gut consist mainly of the peritrophic matrix (PM) and mucus layer, which are the first barriers to pathogens (Zeng *et al.*, 2022). Moreover, several signaling molecules produced by pathogens activate a range of immune responses, controlled by molecular pathways such as Toll, Imd, and JAK/STAT (Wang and Ligoxygakis, 2006; Cherry and Silverman, 2006). The Imd and JAK/STAT signaling pathways produce antimicrobial peptides (AMPs) (Cheng *et al.*, 2006; Zhang *et al.*, 2014), Duox enzymes reactive oxygen species (ROS) (Bouchon *et al.*, 2009), while the melanization response produces a range of bactericidal substances (Rivkin *et al.*, 2006; Blissard, 1996). Many studies for the characterization of the genes involved in the activation of immune responses have been carried out using several non-pathogenic and pathogenic bacteria, including *Bacillus thuringiensis*. The pathological effect of this bacterium is mediated by crystal proteins (Cry), produced during sporulation, which are pore-forming toxins that bind specific receptors in the microvilli of the gut epithelium (de Maagd *et al.*, 2001), generating tissue lesion and a consequent haemocoelic septicemia (Caccia *et al.*, 2016). From the study of the interaction between this bacterium and *Spodoptera exigua*, Herrero *et al.* (2007) identified a novel family of midgut proteins that are expressed in response to pathogens, called REPAT, (REsponse to PAThogens). Members of this gene family are up regulated after feeding *S. exigua* larvae with different *Bt* toxins as well as in response to baculovirus. Moreover, a reduction of virulence following overexpression of REPAT1 was observed after infection with baculovirus, suggesting a possible role of this family in responses against pathogens. The *repat* genes encode small proteins

with a molecular weight of about 15 kDa and their expression is mainly restricted to midgut cells (Herrero *et al.*, 2007; Hernandez-Rodriguez *et al.*, 2009). The first four isolated family members (REPAT1 to 4) are up-regulated in response to Cry1Ca and Cry1A toxins and baculovirus (Herrero *et al.*, 2007), while three other members (REPAT5 to 7) were isolated in populations of *S. exigua* resistant to *Bt* (Hernandez-Martinez *et al.*, 2010). Following a yeast two-hybrid experiment, the protein REPAT8 which interacts with REPAT1 was also isolated (Navarro-Cerrillo *et al.*, 2012). Subsequently, the analysis of the transcriptome of *S. exigua* larvae (Navarro-Cerrillo *et al.*, 2013) led to the identification of other REPAT-related proteins, revealing the existence of at least 46 *repat* genes. This family has been divided into two main groups: αREPAT present only in *Spodoptera* spp and closely related species, and βREPAT also present in distant species and in other insect orders (Diptera). Among the REPAT homologs in other species, only MBF2 proteins have been characterized and appear to be involved in developmental processes as co-transcriptional activators (Liu *et al.*, 2000). Moreover, MBF2-R, a homologous protein of MBF2, is up regulated upon exposure to different types of bacteria (Tanaka *et al.*, 2010). Based on these findings, together with the fact that REPAT1-REPAT8 proteins are translocated in the cell nucleus (Navarro-Cerrillo *et al.*, 2012), it is possible that REPAT proteins may act as transcriptional activators. However, given the large number of members in this family, REPAT proteins may be involved in multiple processes associated with insect midgut physiology. A recent study identified *repat* genes also in *Spodoptera frugiperda*, predicting their function and their cellular localization using bioinformatic tools (Machado *et al.*, 2016). This study pointed out that some members of this family are expressed in fat body, hemocytes and are included in functional categories related to protein transport and binding, energy metabolism, cell envelope and repair of cellular damage. Finally, Hrithik *et al.* (2021) investigated the role of REPAT33 in mediating humoral and cellular immune responses of *S. exigua*. This member of the REPAT family is a secretory protein possessing a multiprotein-bridging factor 2 (MBF2) domain, suggesting that REPAT33 may have a function of co-activator of some transcription factors (TFs) that induce specific immune genes. Its expression occurs in various tissues such as gut, epidermis, hemocytes and fat body, and is controlled by eicosanoids, known as mediators of both cellular and humoral immune responses in insects (Liu *et al.*, 2000). The in-depth study of this protein family, with members controlling several important physiological processes related to immune response, could provide new mechanistic insights that may guide the development of new pest

control strategies. The aim of the present work is to increase our knowledge about this gene family by identifying *repat* genes also in *Spodoptera littoralis* (Lepidoptera, Noctuidae), that is one of the most dangerous pests in agriculture (Hill, 1987). Here we have focused our research efforts on the molecular and functional characterization of the *Slrepat1* gene, using RNAi to negatively modulate its expression, which allowed to discover an important role in immunity. Indeed, silenced moth larvae exposed to sublethal doses of a commercially available *Bt*-based biopesticides (Xentari™) showed an enhanced mortality. These results pave the way towards the development of new pest control strategies aiming at enhancing the killing activity of biocontrol agents.

3.2. MATERIALS AND METHODS

3.2.1. Insect rearing

Spodoptera littoralis larvae were reared as described above (see section 2.2.1.). 5 new molted 5th instar larvae were selected, to collect, in separate Eppendorf tube (1.5 mL), different tissues: midgut, hindgut, fat body, hemocytes, and carcass. Bleeding of larvae anesthetized on ice was carried out by cutting an abdominal proleg to isolate haemocytes as previously described (Di Lelio *et al.*, 2014). Then, the larva was lengthwise dissected to isolate the internal tissues to be used for RNA extraction. Total RNA extraction was carried out using TRIzol® reagent (Thermo Fisher Scientific), according to manufacturer's instructions.

3.2.2. Analysis of the new target gene *Slrepat1* in *S. littoralis* larvae

S. littoralis repat1 gene sequence (Accession Number. JQ660356.1), found in the public database National Center for Biotechnology Information (NCBI, https://www.ncbi.nlm.nih.gov/), was used to design two pairs of oligos on the Primer3 Input online tool (https://primer3.ut.ee/) (Table 3.1). The first pair of oligos (RT-*Slrepat1*-Fwd/Rev) was designed to be used in qRT PCR experiments, while the second pair of oligos (T7-*Slrepat1*-Fwd/Rev) was designed to synthesize dsRNA targeting *Slrepat1* gene (*dsSlrepat1*), to be used in RNAi gene silencing experiments.

Table 3.1 Primer pairs used for qRT-PCR analysis and *in vitro* dsRNA production. Underlying nucleotides indicate the T7 promoter.

Oligos	Sequence 5' – 3'	Amplicon size (bp)	Tm (°C)
RT-*SlActin*-Fwd	CCGTCTTCCCATCCATCGT	66	60
RT-*SlActin*-Rev	CCTTCTGACCCATACCAACCA		
RT-*SlRepat1*-Fwd	AGTTAGTTAGGATGAGGAGCTTCA	101	60
RT-*SlRepat1*-Rev	GGTGACCATCTCCTCTTCGC		
T7-*SlRepat1*-Fwd	TAATACGACTCACTATAGGGAGA CGAGCGAAGAGGAGATGGTC	522	65
T7-*SlRepat1*-Rev	TAATACGACTCACTATAGGGAGA AACCCGACTCAAGTGGTAGC		

The total RNA, extracted from *S. littoralis* midgut and carcass was converted into cDNA, using High-Capacity cDNA Reverse Transcription Kit (Thermo Fisher Scientific) according to the manufacturer's protocol. The obtained template was used to perform the semiquantitative PCR with DreamTaq Green PCR Master Mix (2X) (Thermo Fisher Scientific) according to the manufacturer's protocol, by using both the pairs of oligos (RT-*Slrepat1*-Fwd/Rev; T7-*Slrepat1*-Fwd/Rev) (Table 3.1). The obtained template was visualized on 1% agarose gel electrophoresis, to verify if the amplified sequence had the expected size (see amplicon size in Table 3.1).

3.2.3. Cloning and sequencing of amplified products

Amplified PCR products were purified by using the GRS PCR & Gel Band Purification Kit (GRISP Research Solutions, Porto, Portugal) according to the manufacturer's protocol. Then, the resulting purified products were cloned using the TOPO® TA Cloning® Kit (Thermo Fisher Scientific) according to the manufacturer's protocol, to obtain PCR4-vectors (Figure 2.2) containing the target sequences of interest to be analyzed. The obtained plasmids (pT7-*Slrepat1* and pRT-*Slrepat1*) were finally sequenced by using the Sanger method, single sequencing (Eurofins Genomics, Germany). The obtained pT7-*Slrepat1* sequence was aligned with the published *Slrepat1* sequence (Accession Number: JQ660356.1) by using MuscleWS alignment (Jalview 2.11.2.5 software).

3.2.4. *Slrepat1* gene expression profile in *S. littoralis* larvae

The cDNA obtained as described above, from the different 5th instar *S. littoralis* larvae tissues (midgut, hindgut, fat body and hemocytes), was used to perform a semiquantitative PCR with DreamTaq Green PCR Master Mix (2X) according to the manufacturer's protocol, using the pair oligos RT-*Slrepat1*-Fwd/Rev and RT-*SlActin*-Fwd/Rev (Table 3.1).

3.2.5. *In vitro* synthesis of *Slrepat1* dsRNA

The obtained T7-flanking purified PCR product (522 bp) was used as a template to synthesize dsRNA directed against *Slrepat1* gene (*dsSlrepat1*), using the MEGAscript® RNAi kit (Thermo Fisher Scientific), according to the manufacturer's instructions. *A dsGFP* used in control experiments, was similarly produced as above (see section 2.2.6.). The obtained dsRNA solutions were quantified by measuring its absorbance at 260 nm with a Varioskan Flash Multimode Reader (Thermo Fisher Scientific), and purity was evaluated by assessing 260/280 nm absorbance ratios. dsRNA was run on 1% agarose gels to check its integrity. The obtained dsRNA was stored in the elution solution at -20°C, at concentration of 200 ng/µL.

3.2.6. *Slrepat1* gene silencing by oral administration

To assess the efficiency of gene silencing, 5th instar *S. littoralis* larvae were treated with *dsSlrepat1* and *dsGFP*, as previously described (Di Lelio *et al.*, 2014; Caccia *et al.*, 2016). Briefly, 16 newly molted *S. littoralis* 5th instar larvae were anaesthetized on ice and 1 µL of *dsSlrepat1* (or *dsGFP* for control larvae) solution, was directly poured into the larva foregut lumen by means of a Hamilton Microliter syringe (1701RNR 10 µL, gauge 26 s, length 55 mm, needle3). This treatment was repeated 3 times, at 24 hours intervals, during which the larvae returned to normal growth conditions on artificial diet (see section 2.2.1.). The midgut of treated larvae was collected 24 and 48 hours after the last administration for total RNA extraction, as described above, to evaluate the silencing efficiency through qRT-PCR experiments. The experiment was replicated twice.

3.2.7. qRT-PCR analysis

Differential relative expression of *Slrepat1* was assessed by means of qRT-PCR, using the primer pairs RT-*Slrepat1*-Fwd/Rev and RT-*SlActin*-Fwd/Rev reported in Table 3.1, to check gene silencing efficiency. One-step qRT-PCR using the SYBR Green PCR Kit (Applied Biosystems) and 1 µL containing 200 ng of total RNA extracted as described above was performed according to the manufacturer's instructions. Relative gene expression data were analyzed using the $2^{-\Delta\Delta CT}$ method (Livak and Schmittgen 2001; Pfaffl, 2001). For validation of the ΔΔCt method the difference between the Ct value of *Slrepat1* and the Ct value of *SlActin* transcripts [ΔCt = Ct (*Slrepat1*) - Ct (*SlActin*)] was plotted versus the log of two-fold serial dilutions (400, 200, 100, 50, and 25 ng) of the extracted RNA. The plot of log total RNA input versus ΔCt displayed a slope lower than 0.1 (slope = -3.171; R^2 = 0.9972) indicating that the efficiencies of the 2 amplicons were approximately equal.

3.2.8. *Slrepat1* gene functional analysis

To assess if *Slrepat1* gene was involved in *S. littoralis* larvae response against the entomopathogen *Bacillus thuringiensis (Bt)* (as reported for *S. exigua* by Herrero *et al.*, 2007) a bioassay was performed using Xentari™ (Valent BioSciences), a bioinsecticide based on *Bt* subsp. aizawai, containing several Cry toxins (Cry1Aa, Cry1Ab, Cry1Ca, Cry1 Da and Cry2Ab). Preliminary trials were performed to identify sublethal *Bt* doses (i.e., with no or very low effect on mortality and only moderately affecting the speed of larval development), which was 12 µg/cm^2 for 5th instar larvae. The use of this *Bt* dose allowed the assessment of any increase in the mortality rate caused by the *Slrepat1* gene silencing induced by RNAi. Briefly, 14 synchronous 5th instar larvae were silenced by oral administration of *dsSlrepat1* (and *dsGFP* as control) as described in the previous paragraph. Four hours after the administration of the last dsRNA dose, the experimental larvae were fed with a small piece of artificial diet with the upper surface (1 cm^2) uniformly overlaid with the sublethal dose of Xentari™. The treatment with Xentari™ was repeated 3 times, at 24h interval, and, since Xentari™ was suspended in distilled water (ddH_2O), the control consisted of pieces of diet overlaid with ddH_2O. Mortality was daily recorded for 8 days. This experiment was repeated 2 times.

3.2.9. Statistical analysis

The *Slrepat1* gene expression in the larval midgut was analyzed by using the unpaired Student's *t test*. The survival curves of silenced and control larvae after *Bt* treatment were compared using the Log-rank (Mantel-Cox) test. Normality of all data was checked by using the Kolmogorov-Smirnov test. All the data were analyzed using GraphPad Prism (version 6.0).

3.3. RESULTS

3.3.1. Molecular characterization of the *Slrepat1* gene

Slrepat1 gene fragment was successfully amplified using the retrotranscribed total RNA isolated form *S. littoralis* larvae midgut as template. Nonspecific bands were observed after PCR amplification with the cDNA obtained from the carcass (Figure 3.3). The PCR products obtained from larval midgut samples, separated on a 1% agarose gel, have the expected size (T7 amplicon size: 522 bp; RT amplicon size: 101 bp) (Figure 3.3).

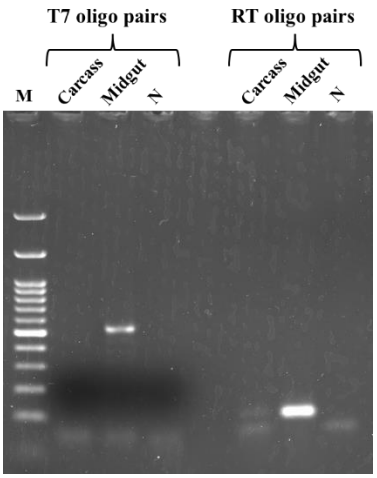

Fig. 3.3 PCR on obtained cDNA from midgut and carcass of *S.littoralis* larvae. From the first to the last lane: marker ExcelBand™ 100 bp+3K DNA Ladder; carcass cDNA, midgut cDNA, negative control for the T7 oligos; carcass cDNA, midgut cDNA, negative control for the RT oligos.

Sequencing of cloned *Slrepat1* showed 98.02% identity (2 gaps, 7 mismatches of which 4 for degenerate nucleotides) (Figure 3.4) with the predicted *Slrepat1* sequence (Accession number: JQ660356.1).

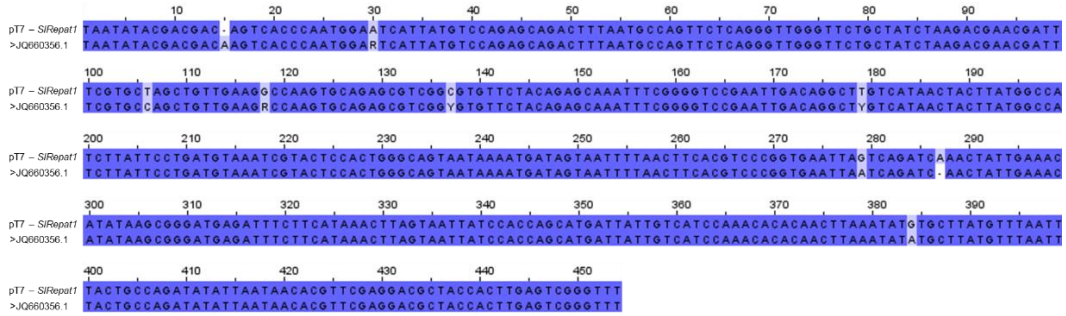

Fig. 3.4 MuscleWS alignment between pT7-*Slrepat1* sequence and predicted *Slrepat1* sequence on NCBI.

3.3.2. Semiquantitative expression of the *Slrepat1* gene

Semiquantitative PCR showed that the *Slrepat1* gene is more expressed in the midgut, even if it is also consistently expressed in the fat body. In hindgut and hemocytes only faint bands were observed (Figure 3.5), likely deriving from sample contamination.

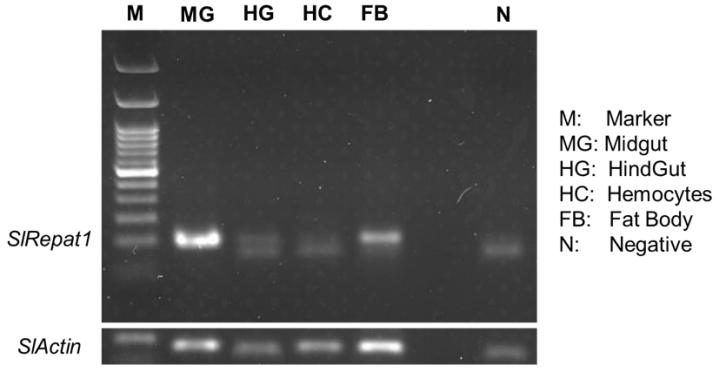

Fig. 3.5 PCR on cDNA from different tissues of *S. littoralis* larvae. From the first to the last lane: marker ExcelBand™ 100 bp+3K DNA Ladder; larval midgut cDNA, larval hindgut cDNA, larval hemocytes cDNA, larval fat body cDNA, negative for the RT oligos of *Slrepat1* and *SlActin* (as a positive control) genes.

3.3.3. Gene silencing efficiency of *Slrepat1*

Agarose gel demonstrated that the produced dsRNA molecules (*dsSlrepat1* and *dsGFP*) are intact and of the expected size (522 bp for *dsSlrepat1* and 720 bp for *dsGFP*), therefore usable for gene silencing experiments (Figure 3.6 A). Both 24 (Fold-change 0.101) and 48 (Fold-change 0.128) hours after dsRNA administration the target gene resulted significantly downregulated in *dsSlrepat1* treated larvae compared to controls (Fold-change 1) (Student's *t*-test, $P < 0.005$) (Figure 3.6 B). Gene silencing levels are nearly equal between 24 and 48 hours after treatment.

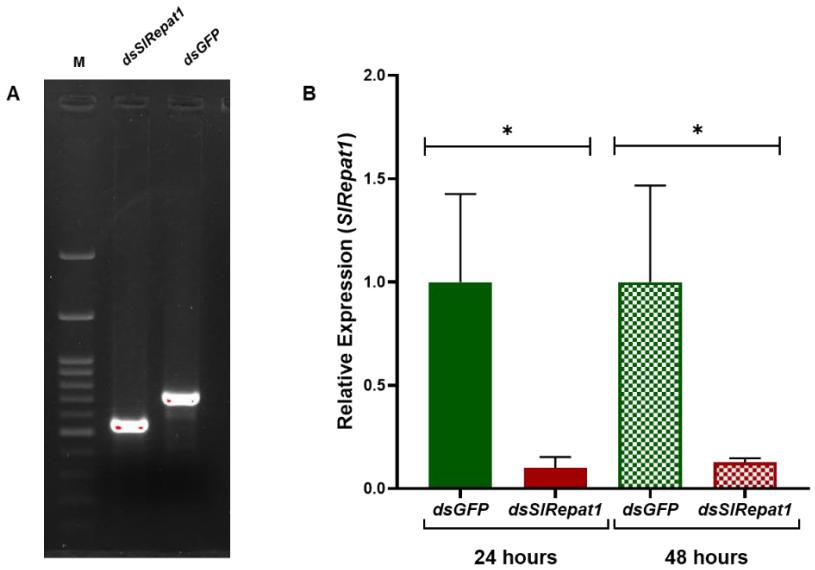

Fig. 3.6 (A) *In vitro* synthesis of dsRNA for *Slrepat1* and *GFP* (control) genes. 1% agarose gel: in the first lane the Marker ExcelBand 100 bp + 3K DNA Ladder; in the second lane the *dsSlrepat1*; in the third lane the *dsGFP* (control). **(B)** Relative expression of *Slrepat1* gene in the midgut of *S. littoralis* larvae. In green, the relative expression of the gene in larvae treated with *dsGFP* solution, in red larvae treated with *dsSlrepat1*. The values reported are the mean ± standard error (Student's *t*-test, 24h: t = 4.181, df = 8, $P < 0.005$; 48h: t = 5.017, df = 8, $P < 0.005$).

3.3.4. Survival rate of silenced larvae after Xentari™ treatment

The susceptibility of *S. littoralis* larvae treated with *dsSlrepat1* to a sublethal dose of the commercial formulation of *B. thuringiensis* (Xentari™) was significantly increased compared to controls. The

silenced larvae showed a strong reduction of the survival rate (about 60% less) starting from the day 4. No mortality was recorded for *dsGFP* treated larvae, which received ddH_2O or the Xentari™ sublethal dose, and for the silenced control group larvae which received only ddH_2O (log-rank (Mantel-Cox) test, $P < 0.0001$) (Figure 3.7 A). The qRT-PCR experiment confirmed that statistically significant silencing occurred in the *dsSlrepat1* group (Fold-change 0.41) compared to controls (Fold-change 1) (*dsGFP*) (Student's *t* test, $P < 0.005$) (Figure 3.7 B).

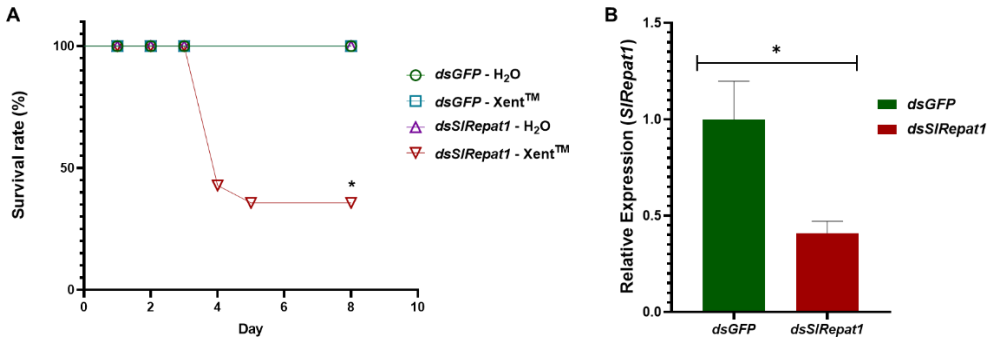

Fig. 3.7 (A) Bioassay with *S. littoralis* 5th instar larvae exposed to dsRNA before *Bt* treatment. Survival was monitored until day 8 (log-rank Mantel-Cox test: $\chi 2 = 33.32$, df = 3, $P < 0.0001$). **(B)** Relative expression of *Slrepat1* gene in the midgut of *S.littoralis* larvae 24 hours after the last dsRNA administration. In green, the relative expression of the gene in larvae treated with *dsGFP* dsRNA solution, in red larvae treated with *dsSlrepat1* dsRNA. The values reported are the mean ± standard error (Student's *t* test: t = 3.922, df = 8, $P < 0.005$).

3.4. DISCUSSION

The *repat* (REsponse to PAThogens) genes were first isolated by Herrero *et al.* (2007) in *S. exigua* larvae exposed to the Cry1Ca toxin of *B. thuringiensis*. Although their role is still unclear, proteins of this family appear to be involved in multiple processes activated in response to entomopathogens. In the present work, we studied one of the members of this gene family, *Slrepat1*, in *S. littoralis* larvae. The nucleotide sequence amplified and cloned in this study was confirmed as a member of the previously described *repat* gene family, since its high identity score of 98.02% (2 gaps, 7 mismatches of which 4 for degenerate nucleotides) and it is mainly expressed in the gut of *S. littoralis* larvae, as described for *S. exigua* by Herrero *et al.* (2007). In previous studies it has been shown that some of the proteins of this family, such as REPAT1, participate in immune responses during

midgut infection by entomopathogens (Herrero *et al.*, 2007; Hernandez-Rodriguez *et al.*, 2012; Navarro-Cerrillo *et al.*, 2012, 2013). In the present work, we demonstrated that *Slrepat1* is mainly expressed in the midgut of the analyzed 5th instar larvae of *S. littoralis*, although a basal expression is also evident in the hindgut, according to what described by Herrero *et al.* (2007) in *S. exigua* larvae, and in the fat body, suggesting that in *S. littoralis* larvae this gene has a similar expression pattern compared to that previously observed. After selecting the nucleotide sequence for synthesis of *dsSlrepat1*, it was performed sequence alignment with the other genes of the same family. The only gene that shows consistent similarity is *Slrepat3* (Query cover: 62%; percent identity 78.45%). The possibility that *Slrepat3* gene is partially silenced after *dsSlrepat1* treatment, and whether any silencing has an additive effect on the observed phenotypes will be demonstrated in future studies. *Slrepat1* RNAi mediated silencing through dsRNA administration showed a consistent and stable downregulation of the target gene in the treated larvae. The *Slrepat1* silenced larvae showing an enhanced susceptibility to a sublethal dose of a commercial formulation of *B. thuringiensis* (Xentari^{TM}) with a survival reduced of about 60% compared to control group. This finding corroborates the hypothesis made by Herrero *et al.* (2007) regarding the possibility that members of the REPAT family are involved in defense responses to entomopathogens. Moreover, it provides additional support and new opportunities to develop control strategies based on the enhancement of the impact of biocontrol agents. As recent studies have shown (Caccia *et al.*, 2020; Di Lelio *et al.*, 2022), the modulation of the immune competences of a target pest can enhance the insecticidal activity of an entomopathogen such as *B. thuringiensis*. A fundamental problem with the use of *Bt*-based bioinsecticides is that prolonged administration in the field can lead to the emergence of resistance and a decline in efficacy on mature larvae (Peralta and Palma, 2017; Cory, 2017). Therefore, to mitigate this problem, it is important to develop methods that can affect the insect's immune system, which can counteract the pathogenic effects induced by *Bt*. Therefore, this gene, along with other immune genes, can concur in the definition of a control strategy based on multiple gene silencing, with possible synergistic effects in terms of insect immunosuppression and susceptibility to natural antagonists. In conclusion, *Slrepat1* gene in *S. littoralis* larvae plays a functional role in line with that observed for the other members of this gene family, which has an important role entomopathogens control. Therefore, it can be used as a target for indirect killing strategies based on the exploitation

of the insect natural antagonists, broadening the tools available and the potential of this approach.

References

Blissard, G. W. (1996). Baculovirus-insect cell interactions. *Insect Cell Culture: Fundamental and Applied Aspects*, 73-93.

Buchon, N., Broderick, N.A., Poidevin, M., Pradervand, S. and Lemaitre, B. (2009) *Drosophila* intestinal response to bacterial infection: activation of host defense and stem cell proliferation. Cell Host Microbe 5: 200–211.

Caccia, S., Astarita, F., Barra, E., Di Lelio, I., Varricchio, P., & Pennacchio, F. (2020). Enhancement of *Bacillus thuringiensis* toxicity by feeding *Spodoptera littoralis* larvae with bacteria expressing immune suppressive dsRNA. *Journal of Pest Science*, *93*(1), 303-314.

Caccia, S., Di Lelio, I., La Storia, A., Marinelli, A., Varricchio, P., Franzetti, E., ... & Pennacchio, F. (2016). Midgut microbiota and host immunocompetence underlie *Bacillus thuringiensis* killing mechanism. *Proceedings of the National Academy of Sciences*, *113*(34), 9486-9491.

Cheng, T., Zhao, P., Liu, C., Xu, P., Gao, Z., Xia, Q., & Xiang, Z. (2006). Structures, regulatory regions, and inductive expression patterns of antimicrobial peptide genes in the silkworm *Bombyx mori*. *Genomics*, *87*(3), 356-365.

Cherry, S. and Silverman, N. (2006). Host-pathogen interactions in *Drosophila*: new tricks from an old friend. Nat Immunol 7: 911–917.

Cory, J. S. (2017). Evolution of host resistance to insect pathogens. *Current opinion in insect science*, *21*, 54-59.

De Maagd, R. A., Bravo, A., & Crickmore, N. (2001). How *Bacillus thuringiensis* has evolved specific toxins to colonize the insect world. *TRENDS in Genetics*, *17*(4), 193-199.

Di Lelio, I., Barra, E., Coppola, M., Corrado, G., Rao, R., & Caccia, S. (2022). Transgenic plants expressing immunosuppressive dsRNA improve entomopathogen efficacy against *Spodoptera littoralis* larvae. *Journal of Pest Science*, *95*(3), 1413-1428.

Hernandez-Martinez, P., Navarro-Cerrillo, G., Caccia, S., de Maagd, R. A., Moar, W. J., Ferre, J., ... & Herrero, S. (2010). Constitutive activation of the midgut response to *Bacillus thuringiensis* in *Bt*-resistant *Spodoptera exigua*. *PLoS One*, *5*(9), e12795.

Hernández-Rodríguez, C. S., Ferré, J., & Herrero, S. (2009). Genomic structure and promoter analysis of pathogen-induced *Repat* genes from *Spodoptera exigua*. Insect molecular biology, 18(1), 77-85.

Herrero, S., Ansems, M., Van Oers, M. M., Vlak, J. M., Bakker, P. L., & de Maagd, R. A. (2007). REPAT, a new family of proteins induced by bacterial toxins and baculovirus infection in *Spodoptera exigua*. Insect biochemistry and molecular biology, 37(11), 1109-1118.

Hill, D. S. (1987). *Agricultural insect pests of temperate regions and their control*. CUP Archive.

Hrithik, M. T. H., Vatanparast, M., Ahmed, S., & Kim, Y. (2021). *Repat33* acts as a downstream component of eicosanoid signaling pathway mediating immune responses of *Spodoptera exigua*, a Lepidopteran insect. Insects, 12(5), 449.

Liu, Q. X., Ueda, H., & Hirose, S. (2000). MBF2 is a tissue-and stage-specific coactivator that is regulated at the step of nuclear transport in the silkworm *Bombyx mori*. Developmental Biology, 225(2), 437-446.

Livak, K. J., & Schmittgen, T. D. (2001). Analysis of relative gene expression data using real-time quantitative PCR and the 2−ΔΔCT method. *methods*, *25*(4), 402-408.

Machado, V., Serrano, J., & Galián, J. (2016). Identification and characterization of pathogen-response genes (*repat*) in *Spodoptera frugiperda* (Lepidoptera: Noctuidae). Folia Biologica (Kraków), 64(1), 23-29.

Navarro-Cerrillo, G., Ferré, J., de Maagd, R. A., & Herrero, S. (2012). Functional interactions between members of the REPAT family of insect pathogen-induced proteins. Insect molecular biology, 21(3), 335-342.

Navarro-Cerrillo, G., Hernández-Martínez, P., Vogel, H., Ferré, J., & Herrero, S. (2013). A new gene superfamily of pathogen-response (*repat*) genes in Lepidoptera: Classification and expression analysis. Comparative Biochemistry and Physiology Part B: Biochemistry and Molecular Biology, 164(1), 10-17.

Peralta, C., & Palma, L. (2017). Is the insect world overcoming the efficacy of *Bacillus thuringiensis*? *Toxins*, *9*(1), 39.

Pfaffl, M. W. (2001). A new mathematical model for relative quantification in real-time RT–PCR. Nucleic acids research, 29(9), e45-e45.

Rivkin, H., Kroemer, J. A., Bronshtein, A., Belausov, E., Webb, B. A., & Chejanovsky, N. (2006). Response of immunocompetent and immunosuppressed *Spodoptera littoralis* larvae to baculovirus infection. *Journal of General Virology*, *87*(8), 2217-2225.

Tanaka, H., Suzuki, N., Nakajima, Y., Sato, M., Sagisaka, A., Fujita, K., ... & Yamakawa, M. (2010). Expression profiling of novel bacteria-induced genes from the silkworm, *Bombyx mori*. *Archives of Insect Biochemistry and Physiology: Published in Collaboration with the Entomological Society of America*, *73*(3), 148-162.

Wang, L. and Ligoxygakis, P. (2006). Pathogen recognition and signaling in the *Drosophila* innate immune response. Immunobiology 211: 251–261.

Zeng, T., Jaffar, S., Xu, Y., & Qi, Y. (2022). The Intestinal Immune Defense System in Insects. *International Journal of Molecular Sciences*, *23*(23), 15132.

Zhang, C. R., Zhang, S., Xia, J., Li, F. F., Xia, W. Q., Liu, S. S., & Wang, X. W. (2014). The immune strategy and stress response of the Mediterranean species of the *Bemisia tabaci* complex to an orally delivered bacterial pathogen. *Plos one*, *9*(4), e94477.

4. Development of a new delivery strategy for dsRNA molecules, using chitosan/humic substances-based nanoconjugates

4.1. INTRODUCTION

Besides its well-recognized importance in reverse genetics studies, RNA interference (RNAi) technique represents a powerful tool for developing sustainable pest control strategies, given its target species specificity allowing a high degree of selectivity (Menezes *et al.*, 2022). The RNAi mechanism, conserved among higher organisms, can be initiated by exogenously applied or endogenously expressed double-stranded RNAs (dsRNA) in many species (Kim *et al.*, 2015; Jain *et al.*, 2020). RNAi-mediated post-transcriptional gene silencing is triggered by the processing of a dsRNA precursor into short single stranded RNA effector molecules, among which the most studied is siRNA (small-interfering RNA) (Schuster *et al.*, 2019). Briefly, upon processing of the dsRNA molecule, the produced siRNA strand identifies matching mRNA in a sequence dependent manner, resulting in a suppression of translation or mRNA degradation (You *et al.*, 2020). In pest control framework, RNAi efficacy is highly dependent on the target species, the target gene and its function, the site of expression of the target gene, and dsRNA delivery system (Huvenne and Smagghe, 2010; Terenius *et al.*, 2011). Recently, one of the most studied aspects of RNAi concerns the stability of dsRNA in different environments (Pantchev *et al.*, 2021). Indeed, the success of RNAi as a pest control technique in the field depends mainly on the dsRNA stability, which is affected by several biotic and abiotic aspects: its short half-life, degradation by nucleases produced by microorganisms, degradation due to UV rays, chemical hydrolysis mediated by the insect gut pH or by the enzymes present in the hemolymph, and its uptake by insect cells (Terenius *et al.*, 2011; Singh *et al.*, 2017). In this scenario, developing a suitable dsRNA delivery system, which could also protect it from environmental degradation, could facilitate RNAi applications in insect pest control. The use of carriers conjugated to dsRNA molecules can increase their stability and improve cellular and/or tissue internalization, without altering its ability to silence the target gene. These carriers can be molecules of natural or synthetic origin and can include viral particles, lipids, metals, sugars, peptides, proteins, and polymers (De Schutter *et al.*, 2021). Among these, the most studied carriers are those based on peptides and polymers (Vogel *et al.*, 2019; Christiaens *et al.*, 2020). The

use of nanoconjugates or polymer-based nanomaterials, for the delivery and protection of bioactive molecules, has been increased in recent years. One of the most studied polymers for the synthesis of nanoconjugates is chitosan (Howard *et al.*, 2006), which is a non-toxic and biodegradable polymer obtained by deacetylation of chitin, a naturally occurring and the second most abundant biopolymer after cellulose (Dass and Choong, 2008; Mujtaba *et al.*, 2019). Chitosan-based nanomaterials have been actively used in different forms including nanoparticles, microbeads, microfibers for several applications in agriculture (Sathiyabama and Parthasarathy, 2016). Chitosan can be combined with other biomaterials or active compounds to synthesize nanocomposites with enhanced characteristics to overcome problems such as hydrophilicity, weak mechanical properties, low gas permeability, low encapsulation efficiency, along with enhancing the bioavailability and biological properties. Active compounds of plant extracts or essential or non-essential oils can be used in combination with the chitosan polymers for enhancing the biological properties of chitosan (Yu *et al.*, 2021). In the present study, we report the development of a new delivery and protection system for dsRNA molecules obtained by the synthesis of chitosan-based nanoconjugates and humic substances, which are macromolecules derived from the degradation of products of plant residues and soil microorganisms (Gerke, 2018). Humic substances are known for their beneficial effects on plant growth, soil fertility, Fe acquisition by plants, nutrient uptake, and modification of the plant metabolism (Pinton *et al.*, 1999; Varanini and Pinton, 1995; Nardi *et al.*, 2002). As described above, adequate delivery strategies can contribute to the reduction of environmental degradation and to the enhancement of RNAi efficacy (Christiaens *et al.*, 2020). Recently, it was shown that it is possible to induce RNAi-mediated silencing of the immune gene *Sl102* in *Spodoptera littoralis* larvae (Lepidoptera: Noctuidae) by different application strategies (Di Lelio *et al.*, 2014, 2019; Caccia *et al.*, 2020). Here, we have shown that Chi/Hum-*dsSl102* nanoconjugates can efficiently entrap and shield the dsRNA molecules that are only released at specific pH conditions, such as those found in the gut of lepidopteran insects (Wieczorek *et al.*, 2009). Administration of the nanoconjugates caused silencing of the *Sl102* gene in *S. littoralis* larvae, suggesting that Chi/Hum-*dsSl102* may be useful for formulating new dsRNA-based biopesticides.

4.2. MATERIALS AND METHODS

4.2.1. Synthesis of chitosan-humic nanoconjugates

Chitosan/Humic substances - dsRNA nanoconjugates (Chi/Hum - dsRNA) were obtained by mixing chitosan polymer, dsRNA targeting *Sl102* (naked *dsSl102*) (synthetized *in vitro* as described in 2.2.6. section) and humic substances (HS), obtained by mixing coffee peels with corn straw and pruning shavings at 70/30 w/w (Figure 4.1).

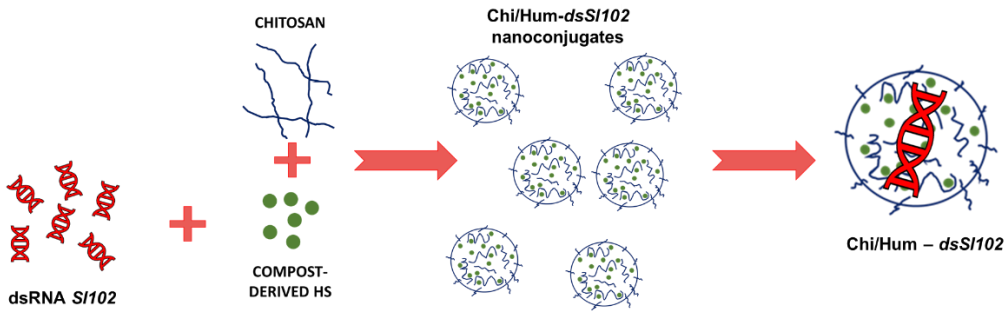

Fig. 4.1 Scheme of the synthesis protocol of the nanoconjugates based on chitosan (irregular blue line)/humic substances (green spots)/dsRNA molecules (red double strand RNA molecules).

First, chitosan and HS were dissolved in 0.5% acetic acid and ddH_2O, respectively, at the desired concentrations (see Table 4.1). Then, the pH of the HS solution was raised up to 9.0 with KOH 0.1 N. In the first reaction (A) condition, two different amounts of dsRNA (Sample 1 = 0.5 µg; Sample 2 = 1 µg) were added to a 0.4% chitosan solution, and then added to HS 0.25%. The second condition (B) was instead carried out by adding two different amounts of dsRNA solution (Sample 1 = 0.5 µg; Sample 2 = 1 µg), first to 0.25% HS solution, and then this mixture was added to 0.1% chitosan solution. As a final third reaction (C) condition, two different amounts of dsRNA solution (Sample 1 = 0.5 µg; Sample 2 = 1 µg) were first added to 0,25% HS solution, and thereafter added to 0.1% chitosan solution. For each condition, empty nanoconjugates (i.e., with no dsRNA) were synthetized as a control. The different conditions are reported in the Table 4.1 reported below.

Tab. 4.1 Different conditions used for Chi/Hum – dsRNA synthesis.

	A	B	C
Sample 1	0.5 µg dsRNA (40 µL) + 200 µL chitosan 0.4% + 100 µL HS 0.25%	0.5 µg dsRNA (100 µL) + 100 µL HS 0.25% + 500 µL chitosan 0.1%	0.5 µg dsRNA (40 µl) + 160 µl HS 0.25% + 500 µL chitosan 0.1%
Sample 2	1 µg dsRNA (40 µl) + 200 µL chitosan 0.4% + 100 µl HS 0.25%	1 µg dsRNA (100 µl) + 100 µl HS 0.25% + 500 µL chitosan 0.1%	1 µg dsRNA (40 µl) + 160 µl HS 0.25% + 500 µL chitosan 0.1%

All the mixtures were then heated at 55 °C for 1 minute at 100 rpm in a termoblock, vortexed for 30 seconds and incubated for 15 minutes in the dark. Then, the samples were centrifuged at 13,000 x g for 10 minutes and the supernatants were collected in a new Eppendorf tube (1.5 mL), while the pellets were added with 200 µL ddH_2O and resuspended by sonication (130-Watt, 20 kHz, 20 seconds ON, Amp1 95%). Both the supernatant and resuspended pellets were analyzed by electrophoresis on 1% agarose gel, to observe the possible presence of non-entrapped dsRNA. To assess the presence of dsRNA within nanoconjugates, Chi/Hum - dsRNAs were treated with 3% SDS and bicarbonate buffer (pH 9), a condition which determine the breakup of the nanoconjugates and the release of content (Yang *et al.*, 2015). Furthermore, using the Image Lab software (Bio-Rad), the amount of entrapped dsRNA was assessed by measuring the band intensities on the agarose gels. Then, the entrapment efficiency for each condition was measured using this equation:

$$entrapment\ efficiency = \frac{entrapped\ dsRNA}{total\ dsRNA} \times 100$$

Since the condition A (A1 and A2) resulted to best fit for dsRNA entrapment (see results in section 4.3.1.), all experiments described below were realized using nanoconjugates produced with this method.

4.2.2. Dynamic Light Scattering analysis

Size and zeta potential were calculated by determining the electrophoretic mobility of the nanoconjugates dispersions and then by applying the Stokes-Einstein and Henry equations. The following parameters were assumed in the calculations: Media viscosity = 0.8872 cP, dielectric constant = 78.5, temperature = 25 ◦ C. The measurements were performed using Zetasizer Nano ZS (4.0 mW He-Ne laser, 632.8 nm, Malvern Instruments, UK) while the respective calculations were performed using Zetasizer software version 7.11. The measurements were done in triplicates at 25° C and the average size and zeta potential were recorded.

4.2.3. Scanning Electron and Transmission Electron Microscopy of nanoconjugate

The morphology of the produced nanoconjugates were investigated by both field emission scanning electron microscopy (FE-SEM) and transmission electron microscopy (TEM). FE-SEM (FEI Nova NanoSEM450) was carried out by drying the samples and depositing them onto a glass slide. They were then coated with a thin layer (5-7 nm) of gold-palladium alloy and the images were acquired at an accelerating voltage of 5 kV by collecting secondary electrons (SE) with an ETD or TLD detector. The TEM was performed by using a FEI Tecnai G2 S-twin apparatus operating at 200 kV (LaB6 source) equipped with 4K Eagle camera. A drop (5 µL) of aqueous suspensions of the various nanoconjugate was placed on one side of the carbon coated copper grid (200 mesh) which were allowed to air-dry before imaging.

4.2.4. Stability and Adherence of Chi/Hum − dsRNA nanoconjugates

A time course analysis was performed to test the stability on tomato plants and on Petri dishes. For each condition 8 red spots (of one centimeter in diameter and circled with a pen) of 35 µl of Chi/Hum - *dsSl102* containing approximately 150 ng of dsRNA were applied on tomato leaves and Petri dishes (Figure 4.2). As control, 8 blue spots of 35 µl of naked *dsSl102* were applied as above. The plants and the Petri dishes were maintained at 25 °C ± 1°C, 70 ± 5% RH, and photoperiod of 16:8 h light/dark. After different time intervals (0, 1, 2, 5, 9, 14, 21,

and 30 days), the nanoconjugates and controls were recovered from leaf and Petri dish surfaces by washing with 35 µl of ddH_2O, then stored at -20 ° C until analysis. The collected samples were then analyzed on the 1% agarose gel, both before and after treatment with SDS 3% and bicarbonate buffer (pH 9).

Fig. 4.2 Tomato leaves and Petri dishes overlaid with naked dsRNA and Chi/Hum – dsRNA nanoconjugates. The spots circled with a pen are used to rediscover the previously applied solution. In red the spots for Chi/Hum-dsRNA and in blue the spots for naked dsRNA.

4.2.5. Shelf-life

To evaluate stability over time, the nanoconjugates were stored for 6 and 12 months at 4 and/or 25 °C. For each temperature, 7 different storage conditions were tested:
a) Dried pellet (at +4°C)
b) Dried pellet (at +25°C)
c) Pellet resuspended in 500 µL of ddH_2O (at +4°C)
d) Pellet resuspended in 500 µL of ddH_2O (at +25°C)
e) Pellet resuspended in 500 µL of acetate buffer (at +25°C)
f) Pellet resuspended in 500 µL of ddH_2O, and sonicated (as described above) (at +4°C)
g) Pellet resuspended in 500 µL of ddH_2O, and sonicated (as described above) (at +25°C)

After storage, the pellets were treated as reported above and analyzed on 1% agarose gel.

4.2.6. Stability at different pH conditions

The fate of the ingested Chi/Hum − dsRNA nanoconjugates would be subject to conditions encountered in the lepidopteran insect foregut, midgut, and hindgut that range from pH 9 to 11 (Wieczorek *et al.*, 2009). The Chi/Hum – *dsSl102* nanoconjugates were resuspended in solutions with an increasing pH (5, 7, 9, and 11) and analyzed on 1% agarose gel, using as control the naked *dsSl102* and nanoconjugates resuspended in ddH_2O.

4.2.7. Chi/Hum – dsRNA nanoconjugates bioassay

To assess the efficiency of the dsRNA labeled with chitosan/humic substances complex, *S. littoralis* larvae were fed on tomato leaf disks treated with Chi/Hum – dsRNA. Briefly, tomato leaf portions were uniformly overlaid with 35 µL of a suspension of a Chi/Hum – *dsSl102* (or Chi/Hum - *dsGFP* as control) containing a total of 150 ng of dsRNA. As an additional control, naked *dsSl102* and naked *dsGFP* (control), containing 150 ng of dsRNA, were used.

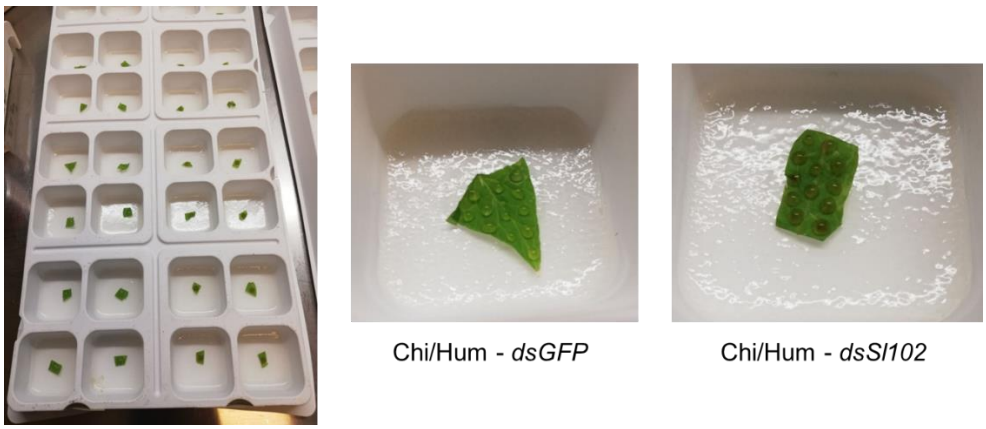

Fig. 4.3 Bioassay tray wells with a piece of tomato leaf overlaid with nanoconjugates or naked dsRNA. A larva is placed in each well.

A group of 16 newly molted 5th instar larvae (obtained as described above, section 2.2.1.), for each condition, were isolated in multi-well plastic trays, fed with the treated tomato leaves, and maintained under

rearing conditions (Figure 4.3). Fresh treated leaves were offered to larvae for 3 consecutive days (450 ng of dsRNA per larva). The experimental larvae were processed, 24 and 48 hours after the last dsRNA administration, for RNA extraction from hemocytes by using Trizol reagent, as described above (section 3.2.1.). Silencing efficiency was evaluated through qRT-PCR experiments, conducted using the $2^{-\Delta\Delta C_T}$ method (Livak and Schmittgen 2001; Pfaffl, 2001) as described above (section 2.2.7.).

4.2.8. Statistical analysis

The *Sl102* gene expression in the treated larvae was analyzed using the unpaired Student's t test. Normality of all data was checked by using the Kolmogorov-Smirnov test. All data were analyzed using GraphPad Prism (version 6.0).

4.3. RESULTS

4.3.1. Chi/Hum – dsRNA nanoconjugates analysis

The presence of non-entrapped dsRNA in the supernatant obtained from each synthesis condition was preliminary assessed. While a band of 514 bp referable to the positive control (*dsSl102*) is clearly visible on the agarose gel, no bands are visible in the supernatant of each condition, therefore indirectly supporting a high rate of entrapment (Figure 4.4).

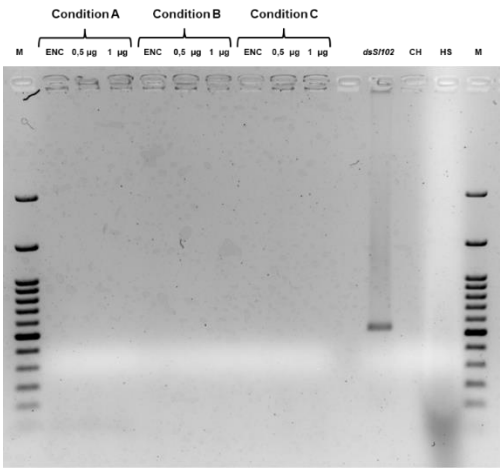

Fig. 4.4 Agarose gel electrophoresis of supernatants of the three experimental conditions considered. From the first to the last lane: Marker ExcelBand 100 bp + 3Kb DNA Ladder (M); empty nanoconjugates (ENC) and samples of Chi/Hum – dsRNA nanoconjugates with 0.5 and 1 µg of entrapped dsRNA for each condition; *dsSl102* (positive control); chitosan (CHI); humic substances (HS); marker (M).

After the treatment with 3% SDS and bicarbonate buffer pH 9, the nanoconjugates released the dsRNA, which was clearly visible on the agarose gel as bands resolving to the approximate size of the positive control (*dsSl102*). The synthesis conditions A) and C) showed an encapsulation efficiency of 91.1% and 88.1% respectively (Figure 4.5 A and C). While no bands were observed for the synthesis condition B), with an entrapment efficiency not measurable (Figure 4.5 B).

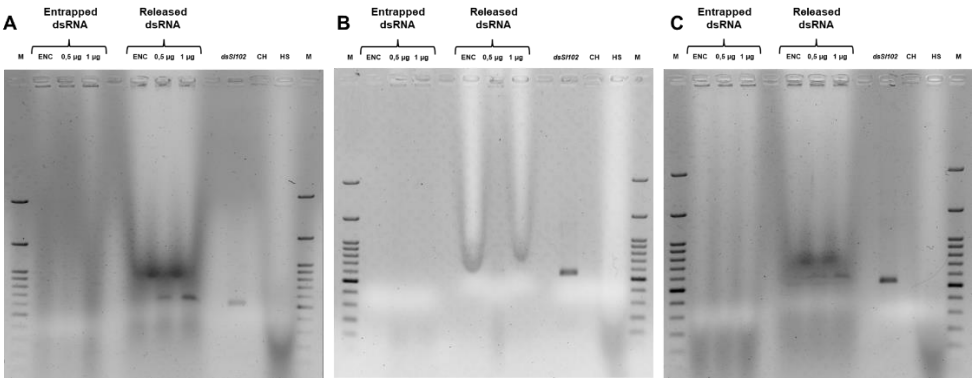

Fig. 4.5 Agarose gel electrophoresis of nanoconjugates for the three experimental conditions, **A**, **B** and **C**. From the first to the last lane: Marker ExcelBand 100 bp + 3Kb DNA Ladder (M); empty nanoconjugates (ENC) and samples of Chi/Hum – dsRNA nanoconjugates with 0.5 and 1 µg of entrapped dsRNA (both before and after treatment with SDS 3% and bicarbonate buffer pH 9); *dsSl102* (positive control); chitosan (CHI); humic substances (HS); marker (M).

4.3.2. Light scattering analysis of Chi/Hum – dsRNA nanoconjugates

The obtained nanoconjugates showed a homogeneous size distribution, with a z-average equal to 300 nm (Figure 4.6). Also, the z-potential was + 23.5 mV. This data suggested an unequal charge distribution of chitosan and HS within the obtained nanoconjugates, with chitosan being predominantly located at the outer layer of the structure.

	z-average (nm)	PDI	Zeta potential (mV)
Chi/Hum-dsRNA nanoconjugates	300	0.16	+23.5

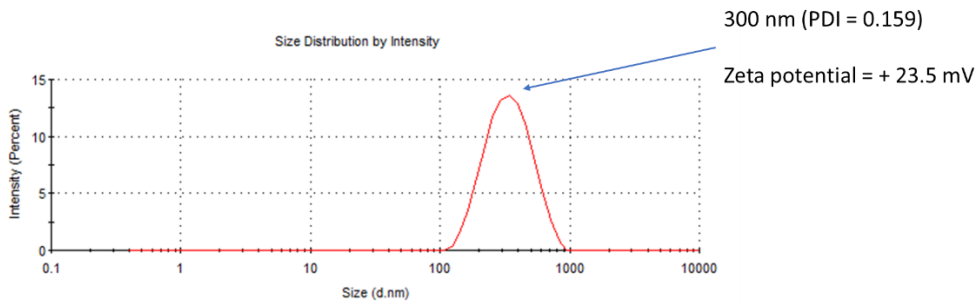

Fig. 4.6 Dynamic Light Scattering diagram. On the Y-axe is reported the Intensity (percent). On X-axe is reported the size (d.nm).

4.3.3. SEM and TEM observations

The morphology of the obtained products was analysed by both FE-SEM and TEM. According to the FE-SEM micrographs, irregular, flake-like blocks without a well-defined nanostructure were noted for the nanoconjugate (Figure 4.7). Additionally, TEM micrographs confirmed the occurrence of clusters without a well-defined nanometric shape (Figure 4.8). Taken together, SEM- and TEM-derived data pointed out that the reaction of chitosan with HS from composted coffee husks did not result in the formation of a proper nanomaterial with a spherical conformation.

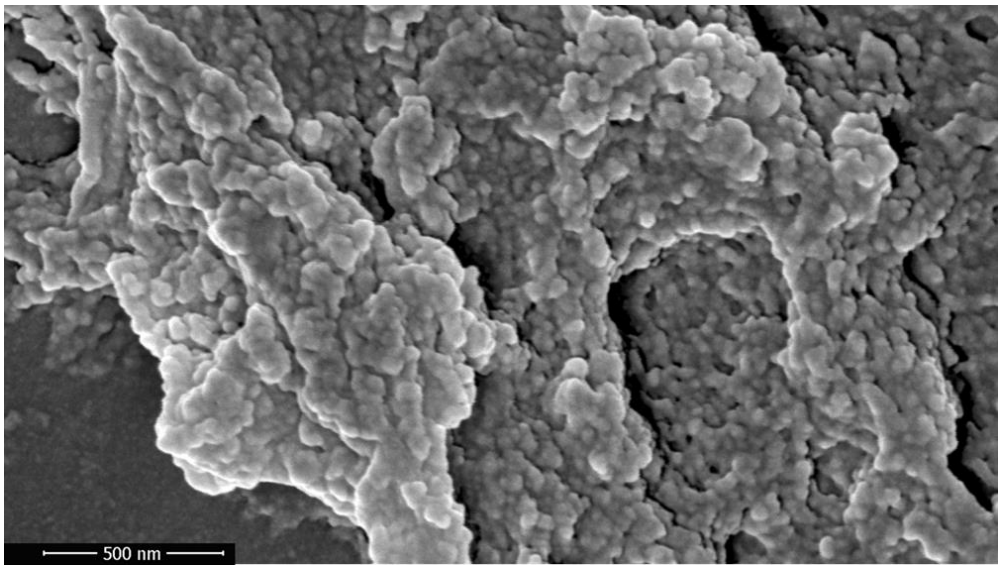

Fig. 4.7 Scanning Electron Microscopy (SEM) micrographs of nanoconjugates entrapping dsRNA obtained by chitosan and humic substances from composted coffee husks.

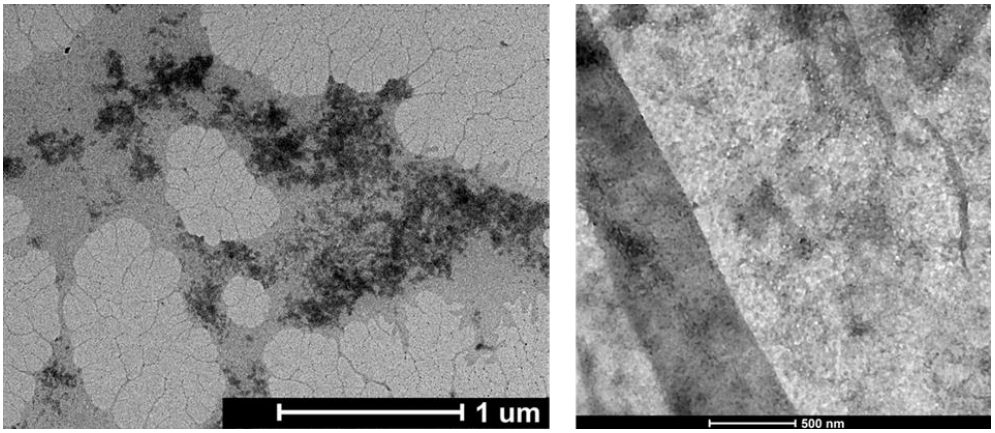

Fig. 4.8 Transmission Electron Microscopy (TEM) micrographs of nanoconjugates entrapping dsRNA obtained by chitosan and humic substances from composted coffee husks.

4.3.4. Stability analysis of nanoconjugates

The nanoconjugates used for the time course analyses, before the experiment, were analysed on agarose gel to verify the presence of the dsRNA, as in the previous section (4.3.1.). As shown in Figure 4.9, no dsRNA was found in the supernatants and in the untreated pellets, while after treatment the dsRNA was efficiently released in the solution,

indicating the nanoconjugates used in the experiment reported below contained the dsRNA.

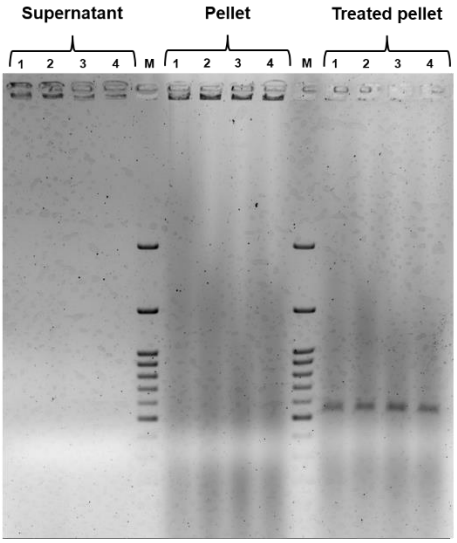

Fig. 4.9 Electrophoresis of nanoconjugates used for the stability test. 1, 2, 3 and 4 are different nanoconjugates samples used. Treated pellet refers to 3% SDS and bicarbonate buffer (pH 9) treatment (releasing of dsRNA).

After 30 days, the dsRNA was still entrapped into the nanoconjugates on both tomato leaf and Petri dish surfaces (Figure 4.10). The same result can be found for naked dsRNA, which under the controlled lab conditions showed no sign of degradation (Figure 4.11).

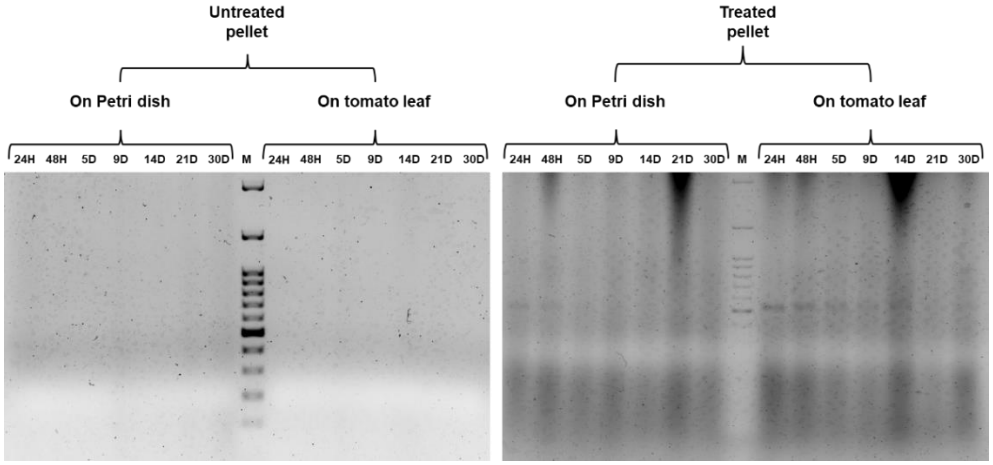

Fig. 4.10 Agarose gel analysis of nanoconjugates applied on both Petri dishes and tomato leaf surfaces. Treated pellets were dissolved in 3% SDS and bicarbonate

buffer (pH 9), releasing the entrapped dsRNA). The samples were collected after 24 hours, 48 hours, 5 days, 9 days, 14 days, 21 days, and 30 days.

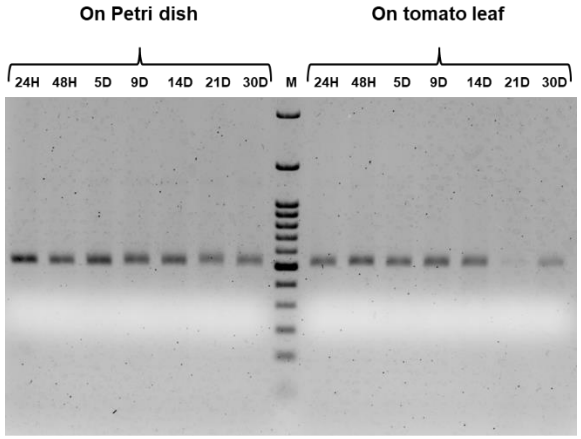

Fig. 4.11 Agarose gel analysis of naked dsRNA applied on both Petri dishes and tomato leaf surfaces. The samples were collected after 24 hours, 48 hours, 5 days, 9 days, 14 days, 21 days, and 30 days.

4.3.5. Shelf-life analysis of Chi/Hum – dsRNA nanoconjugates

The Shelf-life experiment demonstrated that the Chi/Hum - dsRNA nanoconjugate remains stable under the storage conditions considered. Released dsRNA was intact both after 6 and 12 months after the synthesis (Figure 4.12 A and B). Furthermore, after 12 months, condition g) seems to show a more intense band than the others (Figure 4.12 B).

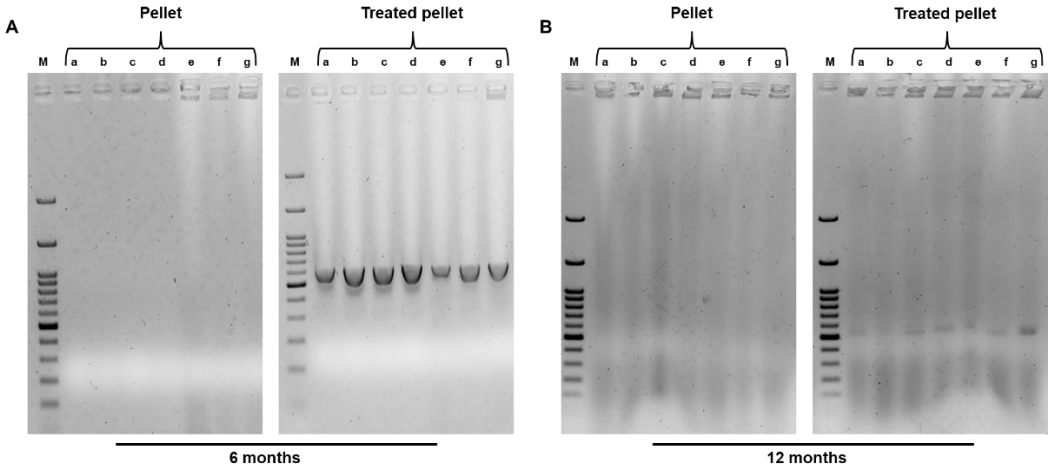

Fig. 4.12 Agarose gel analysis of nanoconjugates stored for 6 **(A)** and 12 **(B)** months. Storage conditions considered: a) Dried pellet (at +4°C); b) Dried pellet (at +25°C); c) Pellet resuspended in 500 µL of ddH_2O (at +4°C); d) Pellet resuspended in 500 µL of ddH_2O (at +25°C); e) Pellet resuspended in 500 µL of acetate buffer (at +25°C); f) Pellet resuspended in 500 µL of ddH_2O, and sonicated (at +4°C); g) Pellet resuspended in 500 µL of ddH_2O, and sonicated (at +25°C). Treated pellet refers to 3% SDS and bicarbonate buffer (pH 9) treatment (releasing of dsRNA).

4.3.6. Content release after pH changes

To assess Chi/Hum - dsRNA stability under different pH conditions, including those reported in the lepidopteran gut, the nanoconjugates complex was exposed to different pH (5, 7, 9, and 11) and analyzed by gel electrophoresis (Figure 4.13). No release of dsRNA was observed at pH 5, likely due to tight binding of the dsRNA molecules to the nanoconjugates. At the pH ranging from 7 to 11 the dsRNA was efficiently released, as demonstrated by the presence of bands on the electrophoresis gel, that resolve to the approximate size of the *dsSl102* band (positive control) (Figure 4.13).

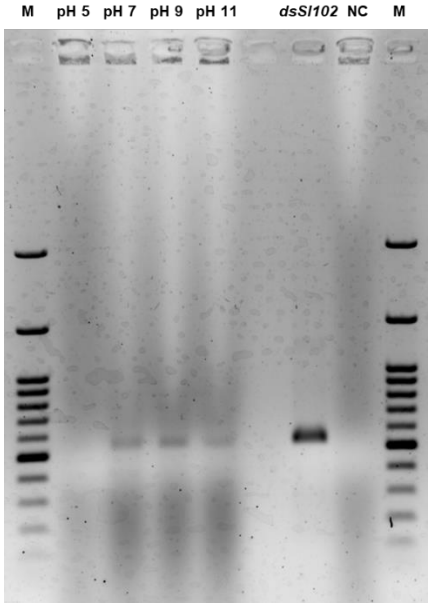

Fig. 4.13 Agarose gel analysis of nanoconjugates resuspended in solutions at different pH values. *dsSl102* is the positive control; nanoconjugates (NC) is the negative control.

4.3.7. Gene silencing efficiency of Chi/Hum – *dsSl102* nanoconjugates on *S. littoralis* larvae

The 5th instar larvae fed with tomato leaves overlaid with Chi/Hum – *dsSl102* nanoconjugates (or Chi/Hum – *dsGFP* nanoconjugates as control) and naked *dsSl102* (or naked *dsGFP* as control) were processed 24 and 48 hours after the last administration for RNA extraction, to measure the relative expression of the target gene by qRT-PCR. At 24 hours *Sl102* gene expression resulted significantly reduced in larvae fed with Chi/Hum – *dsSl102* nanoconjugates (Fold-change 0.05) compared to control larvae (Fold-change 1) (Student's *t*-test, $P < 0.0001$), as similarly observed in larvae fed with naked *dsSl102* (Fold-change 0.1) (Student's *t*-test, $P < 0.0001$) (Figure 4.14 A). Furthermore, the silencing level remained significant at 48 hours after the last administration of dsRNA, under both experimental conditions (Fold-change: Chi/Hum-*dsSl102* 0.06; *dsSl102* 0.1) compared to controls (Fold-change 1) (Student's *t*-test, $P < 0.0001$) (Figure 4.14 B).

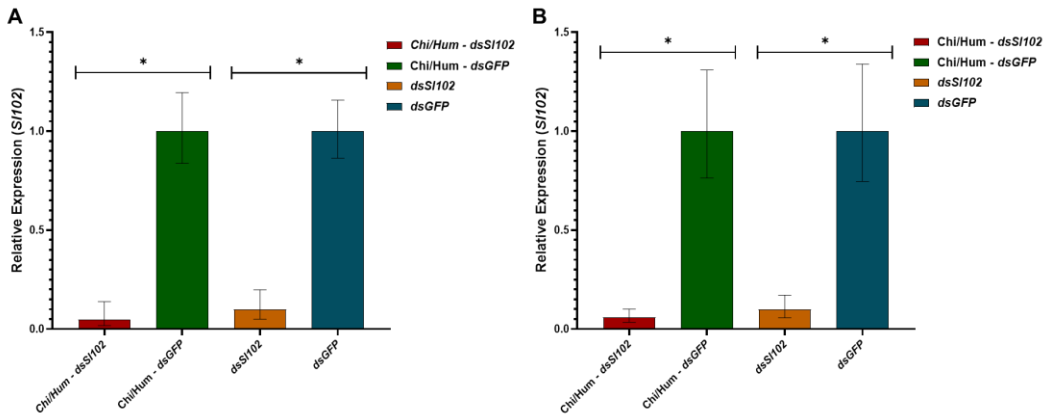

Fig. 4.14 Relative expression of *Sl102* gene after 24 hours **(A)** and 48 hours **(B)** by the treatment. In red, the relative expression of the gene in larvae treated with Chi/Hum-*dsSl102* solution; in green larvae treated with Chi/Hum-*dsGFP*; in orange larvae treated with naked *dsSl102*; in blue larvae treated with naked *dsGFP.* The values reported are the mean ± standard error (Student's *t*-test, 24h: t = 8.037, df = 14, $P < 0.0001$; t = 8.6, df = 15, $P < 0.0001$; 48h: t = 10.54, df = 8, $P < 0.0001$; t = 8.292, df = 8, $P < 0.0001$).

4.4. DISCUSSION

In this work we focused on the development of nanoconjugates incorporating a dsRNA directed against the *Sl102* gene, which is

involved in the immune response of *S. littoralis* larvae (Di Lelio *et al.*, 2014, 2019; Caccia *et al.*, 2016, 2020). We have developed a new delivery and protection system for dsRNA molecules which involves the use of the chitosan polymer (cationic crosslinker) and the humic substances (anionic crosslinker) for the synthesis of a nanoconjugate. The use of chitosan polymer to produce nanomaterials has been widespread for decades, and the first application of this polymer as a dsRNA delivery system for insect control was reported in mosquito *Anopheles gambiae* (Zhang *et al.*, 2010). The innovative approach of this work is the use of the humic substances, obtained from the composting of plant residues, which are known to have various beneficial effects on soil fertility as well as on plant growth, acting as bio stimulants by improving nutrient absorption, and metabolism (Nardi *et al.*, 2021). Taken together, the two components used for the synthesis of the nanoconjugates have a dual task: the delivery and protection of the dsRNA molecules, and the bio-stimulation of the treated plants. We have adopted different experimental conditions for the synthesis of the Chi/Hum-dsRNA nanoconjugate, to obtain the formulation with the highest percentage of dsRNA entrapment. Both the analysis of the agarose gel of the supernatant (synthesis waste) and of the nanoconjugates obtained demonstrated that condition A (see section 4.3.1.) provides the best entrapment percentage (91.1%), even higher than that seen in a recent work by Dhandapani *et al.* (2019), who used chitosan cross-linked to sodium tripolyphosphate (TPP), obtaining an entrapment rate of 80%. This could be due to the chitosan concentrations used, as reported in the literature that increasing chitosan can lead to lower trapping efficiency (Vandenberg *et al.*, 2001; Papadimitriou *et al.*, 2012). The analysis for DLS (dynamic light scattering) was performed only for the nanoconjugate with the best entrapment efficiency, showing a homogeneous size distribution, with a z-average equal to 300 nm. Thus, the mean structure size is about 300 nm, which is higher than the average size often reported (about 200 nm) (Zhang *et al.*, 2010; Kumar *et al.*, 2016; Dhandapani *et al.*, 2019). This could be due to the different ratios between the various components or to the presence of humic substances, which are mixtures of macromolecules and salts that can have a negative effect on the optical properties of the sample (da Costa Cunha *et al.*, 2014). FE-SEM and TEM analysis showed an irregular, flake-like blocks without a well-defined nanostructure. Although chitosan-based nanomaterials with spherical nanoscopic structures are reported (Dhandapani *et al.*, 2019), there are many examples of chitosan-based nanomaterials presenting amorphous and aggregating shapes (Mudo

et al., 2022) as well as for nanomaterials based on humic substances or other biopolymers (da Costa Cunha *et al.*, 2014; Lichtenberg *et al.*, 2020). The amorphous structure obtained, which could also explain the larger dimensions obtained with the DLS analysis, however, has nanoscopic dimensions and high dsRNA entrapment percentage, suggesting its possible use as a nanoconjugate. The release of dsRNA could be due to the alkaline environment of the lepidopteran gut (pH 8-11) (Wieczorek *et al.*, 2009), as chitosan is less stable at high pH (pH > 7), as seen in our tests, where we used a pH 9 bicarbonate buffer to determine dsRNA release. Indeed, we assessed whether increasing pH of the Chi/Hum-dsRNA nanoconjugate suspension could determine the release of the dsRNA. As expected, dsRNA release was observed for pH values > 7, a result that confirms what was already described (Dhandapani *et al.*, 2019). These results suggests that the synthesized nanoconjugate is effective for the control of lepidopteran pests, characterized by strong alkaline conditions in the gut. However, the transition of dsRNA from the laboratory to field environment needs to be optimized to improve its stability in the environment (Yang *et al.*, 2022), which is a key factor that affects the application of RNA biopesticides (Martinez *et al.*, 2021). For this reason, we conducted an experiment of stability for Chi/Hum-dsRNA nanoconjugate and naked dsRNA on two different surfaces, Petri dish and tomato leaf, under laboratory conditions. The result showed that the synthesized formulation is stable on both surfaces up to 30 days after application. However, the same result was obtained with naked dsRNA, suggesting that controlled laboratory conditions (see section 4.2.4.) allows a greater stability. Therefore, future experiments will be conducted testing the stability of the dsRNA nanoconjugate (and naked dsRNA as control) both in response to degradation factors such as RNase, pH, and UV rays, and under field conditions. The stability (shelf-life) of chitosan-based nanomaterials in different storage conditions, is relevant to its potential use as a delivery agent, as this can alter the functioning of the nanoconjugate itself (Hu *et al.*, 2008; Tsai *et al.*, 2011). Therefore, it is important to understand the relationship between storage conditions and the effects on nanoconjugate stability (Morris *et al.*, 2011). Our shelf-life analysis for the different storage conditions used (see section 4.2.5.), indicated that both after 6 and 12 months, the nanoconjugates remain in their initial condition and that the released dsRNA appears to be unaltered, although the condition (g) in which the nanoconjugates, after their synthesis, were resuspended in ddH_2O, sonicated, and stored at +25°C, gave a more intense dsRNA band. This could be due to sonication, which allows better resuspension of nanoconjugates in

the aqueous solution. These results are not surprising, given that in literature it is described that storage conditions at 4°C and 25°C are the most efficient (Morris *et al.*, 2011), even using different procedures. Finally, to test the efficacy of the synthesized Chi/Hum-dsRNA nanoconjugate in the delivery of dsRNA, we used *S. littoralis* as a model insect and *Sl102* as a target gene. A bioassay was performed comparing the efficacy of the dsRNA-nanoconjugate with the naked dsRNA by feeding. Larvae fed with Chi/Hum-*dsSl102* showed high levels of gene silencing, both 24 and 48 hours after treatment, comparable to those obtained with the naked dsRNA, suggesting that the nanoconjugate did not inhibit the RNAi response to the dsRNA, which was released and active. In conclusion, we have synthesized a new type of nanoconjugate based on chitosan and humic substances for the delivery and protection of dsRNA molecules (Chi/Hum-*dsSl102*), with the aim of improving the efficiency of their field application for insect pest control. We demonstrated that the synthesis protocol used lead to a high percentage of dsRNA entrapment, although size and shape of nanoconjugates can be improved by modifying some parameters, such as the concentration of chitosan polymer and/or humic substances used for the synthesis. Furthermore, our results confirm the potential use of the Chi/Hum-dsRNA nanoconjugate for the delivery of bioactive molecules. Moreover, the proposed delivery strategy could be profitably used also for other bioactive molecules, such as peptides and proteins, trying also to enhance the efficiency of their entrance in plant and insect tissue where they exert their biological activity.

References

Caccia, S., Di Lelio, I., La Storia, A., Marinelli, A., Varricchio, P., Franzetti, E., ... & Pennacchio, F. (2016). Midgut microbiota and host immunocompetence underlie *Bacillus thuringiensis* killing mechanism. *Proceedings of the National Academy of Sciences*, *113*(34), 9486-9491.

Caccia, S., Astarita, F., Barra, E., Di Lelio, I., Varricchio, P., & Pennacchio, F. (2020). Enhancement of *Bacillus thuringiensis* toxicity by feeding *Spodoptera littoralis* larvae with bacteria expressing immune suppressive dsRNA. *Journal of Pest Science*, *93*(1), 303-314.

Christiaens, O., Whyard, S., Vélez, A. M., & Smagghe, G. (2020). Double-stranded RNA technology to control insect pests:

Current status and challenges. *Frontiers in plant science*, *11*, 451.

da Costa Cunha, G., Romão, L. P. C., & Macedo, Z. S. (2014). Production of alpha-alumina nanoparticles using aquatic humic substances. *Powder technology*, *254*, 344-351.

Dass, C. R., & Choong, P. F. (2008). The use of chitosan formulations in cancer therapy. *Journal of microencapsulation*, *25*(4), 275-279.

De Schutter, K., Christiaens, O., Taning, C. N. T., & Smagghe, G. (2021). 11 Boosting dsRNA Delivery in Plant and Insect Cells with Peptide-and Polymer-based Carriers: Case-based Current Status and Future Perspectives. *RNAi for plant improvement and protection*, 102.

Dhandapani, R. K., Gurusamy, D., Howell, J. L., & Palli, S. R. (2019). Development of CS-TPP-dsRNA nanoparticles to enhance RNAi efficiency in the yellow fever mosquito, *Aedes aegypti*. *Scientific reports*, *9*(1), 1-11.

Di Lelio, I., Varricchio, P., Di Prisco, G., Marinelli, A., Lasco, V., Caccia, S., ... & Pennacchio, F. (2014). Functional analysis of an immune gene of *Spodoptera littoralis* by RNAi. *Journal of insect physiology*, *64*, 90-97.

Di Lelio, I., Illiano, A., Astarita, F., Gianfranceschi, L., Horner, D., Varricchio, P., ... & Caccia, S. (2019). Evolution of an insect immune barrier through horizontal gene transfer mediated by a parasitic wasp. *PLoS genetics*, *15*(3), e1007998.

Gerke, J. (2018). Concepts and misconceptions of humic substances as the stable part of soil organic matter: A review. *Agronomy*, *8*(5), 76.

Howard, K. A., Rahbek, U. L., Liu, X., Damgaard, C. K., Glud, S. Z., Andersen, M. Ø., ... & Kjems, J. (2006). RNA interference in vitro and *in vivo* using a novel chitosan/siRNA nanoparticle system. *Molecular Therapy*, *14*(4), 476-484.

Hu, B., Pan, C., Sun, Y., Hou, Z., Ye, H., Hu, B., & Zeng, X. (2008). Optimization of fabrication parameters to produce chitosan− tripolyphosphate nanoparticles for delivery of tea catechins. *Journal of agricultural and food chemistry*, *56*(16), 7451-7458.

Huvenne, H., & Smagghe, G. (2010). Mechanisms of dsRNA uptake in insects and potential of RNAi for pest control: a review. *Journal of insect physiology*, *56*(3), 227-235.

Jain, R. G., Robinson, K. E., Fletcher, S. J., & Mitter, N. (2020). RNAi-based functional genomics in Hemiptera. *Insects*, *11*(9), 557.

Kim, E., Park, Y., & Kim, Y. (2015). A transformed bacterium expressing double-stranded RNA specific to integrin β1 enhances *Bt* toxin efficacy against a polyphagous insect pest, *Spodoptera exigua*. *PloS one*, *10*(7), e0132631.

Kumar, D. R., Kumar, P. S., Gandhi, M. R., Al-Dhabi, N. A., Paulraj, M. G., & Ignacimuthu, S. (2016). Delivery of chitosan/dsRNA nanoparticles for silencing of *wing development vestigial (vg)* gene in *Aedes aegypti* mosquitoes. *International journal of biological macromolecules*, *86*, 89-95.

Lichtenberg, S. S., Laisney, J., Elhaj Baddar, Z., Tsyusko, O. V., Palli, S. R., Levard, C., ... & Unrine, J. M. (2020). Comparison of nanomaterials for delivery of double-stranded RNA in *Caenorhabditis elegans*. *Journal of Agricultural and Food Chemistry*, *68*(30), 7926-7934.

Livak, K. J., & Schmittgen, T. D. (2001). Analysis of relative gene expression data using real-time quantitative PCR and the 2−ΔΔCT method. *methods*, *25*(4), 402-408.

Martinez, Z., De Schutter, K., Van Damme, E. J., Vogel, E., Wynant, N., Broeck, J. V., ... & Smagghe, G. (2021). Accelerated delivery of dsRNA in lepidopteran midgut cells by a *Galanthus nivalis* lectin (GNA)-dsRNA-binding domain fusion protein. *Pesticide Biochemistry and Physiology*, *175*, 104853.

Menezes, P. S., Yan, Y., Yang, Y., Mitter, N., Mahony, T. J., & Mody, K. T. (2022). RNAi-Based Biocontrol of Pests to Improve the Productivity and Welfare of Livestock Production. *Applied Biosciences*, *1*(3), 229-243.

Morris, G. A., Castile, J., Smith, A., Adams, G. G., & Harding, S. E. (2011). The effect of prolonged storage at different temperatures on the particle size distribution of tripolyphosphate (TPP)–chitosan nanoparticles. *Carbohydrate polymers*, *84*(4), 1430-1434.

Mudo, L. M. D., Queiroz, A. F. S., de Melo, N. F., Barbosa, M. A. G., de Andrade, E. C., & de Britto, D. (2022). Stability Evaluation of dsRNA and DNA Encapsulated in Chitosan Nanoparticles. *BioNanoScience*, *12*(3), 774-784.

Mujtaba, M., Morsi, R. E., Kerch, G., Elsabee, M. Z., Kaya, M., Labidi, J., & Khawar, K. M. (2019). Current advancements in chitosan-based film production for food technology; A review. *International journal of biological macromolecules*, *121*, 889-904.

Nardi, S., Pizzeghello, D., Muscolo, A., & Vianello, A. (2002). Physiological effects of humic substances on higher plants. *Soil Biology and Biochemistry*, *34*(11), 1527-1536.

Nardi, S., Schiavon, M., & Francioso, O. (2021). Chemical structure and biological activity of humic substances define their role as plant growth promoters. *Molecules*, *26*(8), 2256.

Pantchev, I., Rakleova, G., & Atanassov, A. (2021). 10 The Stability of dsRNA During External Applications–an Overview. *RNAi for plant improvement and protection*, 94.

Papadimitriou, S. A., Achilias, D. S., & Bikiaris, D. N. (2012). Chitosan-g-PEG nanoparticles ionically crosslinked with poly (glutamic acid) and tripolyphosphate as protein delivery systems. *International Journal of Pharmaceutics*, *430*(1-2), 318-327.

Pfaffl, M. W. (2001). A new mathematical model for relative quantification in real-time RT–PCR. *Nucleic acids research*, *29*(9), e45-e45.

Pinton, R., Cesco, S., Iacolettig, G., Astolfi, S., & Varanini, Z. (1999). Modulation of NO 3-uptake by water-extractable humic substances: involvement of root plasma membrane H+ ATPase. *Plant and soil*, *215*(2), 155-161.

Sathiyabama, M., & Parthasarathy, R. (2016). Biological preparation of chitosan nanoparticles and its *in vitro* antifungal efficacy against some phytopathogenic fungi. *Carbohydrate Polymers*, *151*, 321-325.

Schuster, S., Miesen, P., & van Rij, R. P. (2019). Antiviral RNAi in insects and mammals: parallels and differences. *Viruses*, *11*(5), 448.

Singh, I. K., Singh, S., Mogilicherla, K., Shukla, J. N., & Palli, S. R. (2017). Comparative analysis of double-stranded RNA degradation and processing in insects. *Scientific reports*, *7*(1), 1-12.

Terenius, O., Papanicolaou, A., Garbutt, J. S., Eleftherianos, I., Huvenne, H., Kanginakudru, S., ... & Smagghe, G. (2011). RNA interference in Lepidoptera: an overview of successful and unsuccessful studies and implications for experimental design. *Journal of insect physiology*, *57*(2), 231-245.

Tsai, M. L., Chen, R. H., Bai, S. W., & Chen, W. Y. (2011). The storage stability of chitosan/tripolyphosphate nanoparticles in a phosphate buffer. *Carbohydrate Polymers*, *84*(2), 756-761.

Vandenberg, G. W., Drolet, C., Scott, S. L., & De la Noüe, J. (2001). Factors affecting protein release from alginate–chitosan

coacervate microcapsules during production and gastric/intestinal simulation. *Journal of Controlled Release*, *77*(3), 297-307.

Varanini, Z., & Pinton, R. (1995). Humic substances and plant nutrition. *Progress in botany*, 97-117.

Vogel, E., Santos, D., Mingels, L., Verdonckt, T. W., & Broeck, J. V. (2019). RNA interference in insects: protecting beneficials and controlling pests. *Frontiers in physiology*, *9*, 1912.

Wieczorek, H., Beyenbach, K. W., Huss, M., & Vitavska, O. (2009). Vacuolar-type proton pumps in insect epithelia. *Journal of Experimental Biology*, *212*(11), 1611-1619.

Yang, W., Wang, B., Lei, G., Chen, G., & Liu, D. (2022). Advances in nanocarriers to improve the stability of dsRNA in the environment. *Frontiers in Bioengineering and Biotechnology*, 1401.

Yang, Z., Liu, T., Xie, Y., Sun, Z., Liu, H., Lin, J., ... & Nie, S. (2015). Chitosan layered gold nanorods as synergistic therapeutics for photothermal ablation and gene silencing in triple-negative breast cancer. *Acta biomaterialia*, *25*, 194-204.

You, L., Zhang, F., Huang, S., Merchant, A., Zhou, X., & Li, Z. (2020). Over-expression of rna interference (rnai) core machinery improves susceptibility to rnai in silkworm larvae. *Insect Molecular Biology*, *29*(4), 353-362.

Yu, J., Wang, D., Geetha, N., Khawar, K. M., Jogaiah, S., & Mujtaba, M. (2021). Current trends and challenges in the synthesis and applications of chitosan-based nanocomposites for plants: A review. *Carbohydrate Polymers*, *261*, 117904.

Zhang, X., Zhang, J., & Zhu, K. Y. (2010). Chitosan/double-stranded RNA nanoparticle-mediated RNA interference to silence *chitin synthase* genes through larval feeding in the African malaria mosquito (*Anopheles gambiae*). *Insect molecular biology*, *19*(5), 683-693.

APPENDIX

- **Abroad research experience**

Institution:
School of Natural and Environmental Sciences, Newcastle University Ridley Building, NE1 7RU, Newcastle upon Tyne, United Kingdom
Tutor:
Prof. Angharad M. R. Gatehouse, Professor of Invertebrate Molecular Biology and Director of Expertise for BioEconomy
Period:
From 12/03/22 to 09/09/22

- **Participations in Conferences and meetings**

1. European PhD Network "Insect Science" (XI annual meeting) 30/11 to 3/12, 2020 – oral presentation. Title: *RNAi silencing of an immune gene disrupts the embryonic development of Spodoptera littoralis.*
   Authors: **G. Volpe**, I. Di Lelio, E. Barra, F. Pennacchio
2. XXVI Congresso Nazionale Italiano di Entomologia (XXVI CNIE) 7/06 to 11/06, 2021 – oral presentation. Title: *RNAi silencing of an immune gene disrupts the embryonic development of Spodoptera littoralis*
   Authors: **G. Volpe**, I. Di Lelio, E. Barra, F. Pennacchio
3. European PhD Network "Insect Science" (XII annual meeting) 17/11 to 19/11, 2021 – oral presentation. Title: *RNAi-mediated silencing of an immune gene in Spodoptera littoralis (Lepidoptera, Noctuidae) alters its embryonic development*
   Authors: **G. Volpe**, I. Di Lelio, A. Becchimanzi, S. Gigliotti, F. Pennacchio
4. XVI FISV Congress 3R: Research, Resilience, Reprise 14/09 to 16/09, 2022 – poster. Title: *RNAi-mediated silencing of an immune gene in Spodoptera littoralis (Lepidoptera, Noctuidae) alters its embryonic development*
   Authors: **G. Volpe**, I. Di Lelio, A. Becchimanzi, N. Baranzini, D. Bruno, G. Tettamanti, S. Gigliotti, F. Pennacchio 7
5. European PhD Network "Insect Science" (XIII annual meeting) 16/11 to 18/11, 2022 – oral presentation. Title: *RNAi-mediated silencing of an immune gene in Spodoptera littoralis (Lepidoptera, Noctuidae) alters its embryonic development*

Authors: **G. Volpe**, I. Di Lelio, A. Becchimanzi, N. Baranzini, D. Bruno, G. Tettamanti, S. Gigliotti, F. Pennacchio

- **Journal Articles:**

1. Primo, P., Meccariello, A., Inghilterra, M.G., Gravina, A., Del Corsano, G., **Volpe, G.**, Sollazzo, G., Aceto, S., Robinson, M.D., Salvemini, M. and Saccone, G., 2020. Targeting the autosomal *Ceratitis capitata* transformer gene using Cas9 or dCas9 to masculinize XX individuals without inducing mutations. *BMC genetics*, *21*(2), pp.1-11.

2. Di Lelio, I., Salvatore, M.M., Della Greca, M., Mahamedi, A.E., Alves, A., Berraf-Tebbal, A., **Volpe, G.**, Russo, E., Becchimanzi, A., Nicoletti, R. and Andolfi, A., 2022. Defensive mutualism of endophytic fungi: Effects of sphaeropsidin A against a model lepidopteran pest. *Chemistry Proceedings*, *10*(1), p.42.

3. Salvatore, M.M., Di Lelio, I., DellaGreca, M., Nicoletti, R., Salvatore, F., Russo, E., **Volpe, G.**, Becchimanzi, A., Mahamedi, A.E., Berraf-Tebbal, A. and Andolfi, A., 2022. Secondary Metabolites, including a New 5, 6-Dihydropyran-2-One, Produced by the Fungus *Diplodia corticola*. Aphicidal Activity of the Main Metabolite, Sphaeropsidin A. *Molecules*, *27*(7), p.2327.

Primo et al. BMC Genetics 2020, 21(Suppl 2):150
https://doi.org/10.1186/s12863-020-00941-4

BMC Genetics

RESEARCH Open Access

Targeting the autosomal *Ceratitis capitata transformer* gene using Cas9 or dCas9 to masculinize XX individuals without inducing mutations

Pasquale Primo[1†], Angela Meccariello[1†], Maria Grazia Inghilterra[1], Andrea Gravina[1], Giuseppe Del Corsano[1], Gennaro Volpe[1], Germano Sollazzo[1], Serena Aceto[1], Mark D. Robinson[2], Marco Salvemini[1] and Giuseppe Saccone[1*]

Abstract

Background: Females of the Mediterranean fruit fly *Ceratitis capitata* (Medfly) are major agricultural pests, as they lay eggs into the fruit crops of hundreds of plant species. In Medfly, female sex determination is based on the activation of *Cctransformer* (*Cctra*). A maternal contribution of *Cctra* is required to activate *Cctra* itself in the XX embryos and to start and epigenetically maintain a *Cctra* positive feedback loop, by female-specific alternative splicing, leading to female development. In XY embryos, the male determining *Maleness-on-the-Y* gene (*MoY*) blocks this activation and *Cctra* produces male-specific transcripts encoding truncated CcTRA isoforms and male differentiation occurs.

Results: With the aim of inducing frameshift mutations in the first coding exon to disrupt both female-specific and shorter male-specific CcTRA open reading frames (ORF), we injected Cas9 ribonucleoproteins (Cas9 and single guide RNA, sgRNA) in embryos. As this approach leads to mostly monoallelic mutations, masculinization was expected only in G_1 XX individuals carrying biallelic mutations, following crosses of G_0 injected individuals. Surprisingly, these injections into XX-only embryos led to G_0 adults that included not only XX females but also 50% of reverted fertile XX males. The G_0 XX males expressed male-specific *Cctra* transcripts, suggesting full masculinization. Interestingly, out of six G_0 XX males, four displayed the *Cctra* wild type sequence. This finding suggests that masculinization by Cas9-sgRNA injections was independent from its mutagenic activity. In line with this observation, embryonic targeting of *Cctra* in XX embryos by a dead Cas9 (enzymatically inactive, dCas9) also favoured a male-specific splicing of *Cctra*, in both embryos and adults.

Conclusions: Our data suggest that the establishment of *Cctra* female-specific autoregulation during the early embryogenesis has been repressed in XX embryos by the transient binding of the Cas9-sgRNA on the first exon of the *Cctra* gene. This hypothesis is supported by the observation that the shift of *Cctra* splicing from female to male mode is induced also by dCas9. Collectively, the present findings corroborate the idea that a transient embryonic inactivation of *Cctra* is sufficient for male sex determination.

Keywords: iCRISPR, Sex determination, *Ceratitis capitata*, Epigenetics, Autoregulation, *Transformer*

* Correspondence: giuseppe.saccone@unina.it
†Pasquale Primo and Angela Meccariello contributed equally to this work.
[1]Department of Biology, University of Naples Federico II, 80126 Naples, Italy
Full list of author information is available at the end of the article

Background

In the last few decades, the Mediterranean fruit fly *Ceratitis capitata* (Tephritidae, Medfly) has become a major invasive agricultural pest worldwide, following its spread from Africa and its globalization [1]. For the local suppression of this invasive species, alternatives to the use of pesticides are genetic control strategies. One of them is the Sterile Insect Technique (SIT), which has been applied successfully over the last six decades in various countries [2].

The prerequisites of SIT include a method to mass rear the target species in a cost-effective way and a method to sterilize them with a low impact on their fitness once released. As the released sterile females contribute to the fruit crop mechanical damage with the ovipositor and consequent infections, and the sterile males tend to mate with the released females rather than with the wild ones, it is highly preferable to develop a method of sexing and only release sterile males [3]. A number of strategies have been developed, including transgenic approaches for sexing, which allow the mass rearing of the two sexes, and sorting the males at the expanded last generation before the release. These strains can be based on the expression of a conditional female-lethal dominant gene [4] or on the transformation of genotypic female individuals into males by manipulating a gene involved in female sex determination [5]. Molecular genetics studies on Medfly sex determination have been useful for this aim, uncovering a cascade of regulatory genes widely conserved in the Tephritidae family (Fig. 1) [6–10]. This taxon includes many other invasive agricultural pests, such as species of the *Bactrocera* and *Anastrepha* genera [11, 12]. This fundamental knowledge is not only interesting and valuable per se [13], but also useful to develop novel sexing strategies necessary to improve the applicability of SIT. Evolutionary conservation of homologous genes and the use of transgenesis and/or CRISPR/Cas9 potentially will enable the realization of additional versatile sexing methods that can be applied in different species [8, 9, 14–16].

The sex determination of Medfly is based, as in *Drosophila melanogaster*, on sex-specific alternative splicing

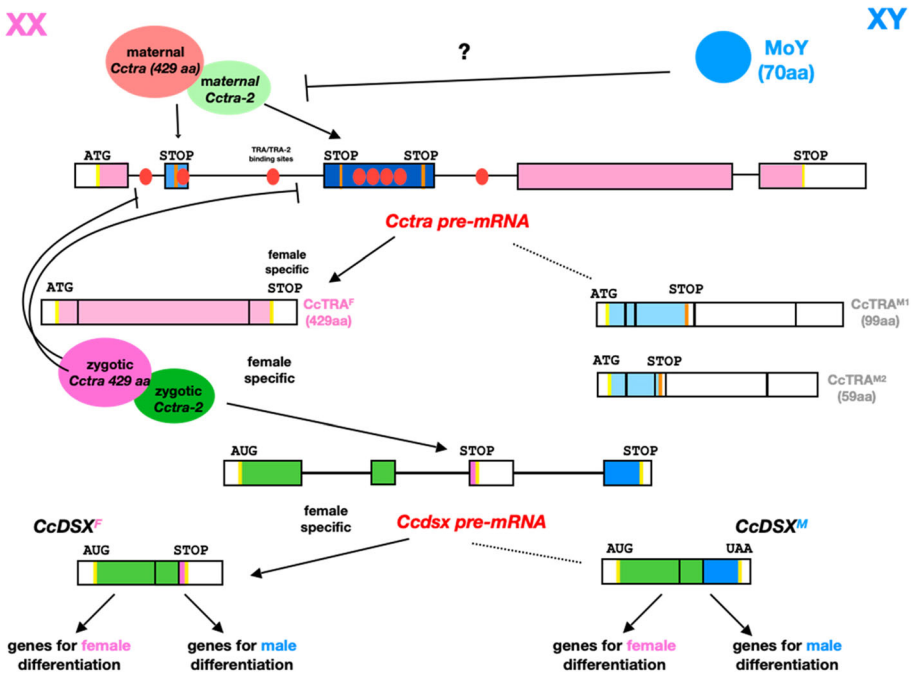

Fig. 1 Genetic pathway of sex determination in *Ceratitis capitata*. *Cctra* and *Ccdoublesex* (*Ccdsx*) pre-mRNAs exon-intron structures and sex-specific transcripts are shown. Female-specific and male-specific *Cctra* exons are indicated as pink and dark blue boxes, respectively. *Cctra* female-specific transcript on the left contains a 429 aa long ORF. *Cctra* male-specific exons introduce premature stop codons in male-specific longer transcripts (orange vertical bars). CcTRA M1 and M2 male-specific isoforms contain truncated CcTRA ORFs represented by azul regions. In XX embryos, maternal CcTRA (orange circle) and CcTRA-2 (green circle) proteins promote female-specific splicing of newly transcribed *Cctra* pre-mRNA, suppressing male-specific splicing by binding to TRA/TRA-2 *cis* regulatory elements (red spots). Female-specific *Cctra* mRNA encodes zygotic CcTRA (violet circle) that maintains (together with zygotic CcTRA-2; dark green circle) the *Cctra* autoregulation induced by the maternal contributions by a feedback loop. Both CcTRA and CcTRA-2 proteins promote also female-specific splicing of the downstream *Ccdsx* pre-mRNA, producing mRNAs that include a female-specific exon (pink) and encode CcDSXF isoform inducing female sexual differentiation [6]. In XY embryos the Y-linked *Maleness-on-the-Y* gene (*MoY*) induces male-specific *Cctra* splicing and, hence, the collapse of the positive feedback loop [7]. By default, male-specific splicing of *Ccdsx* leads to male-specific splicing and CcDSM isoform inducing male sexual differentiation [6, 8]

of key regulatory genes, including *transformer* (*tra*), *transformer-2* (*tra-2*) and *doublesex* (*dsx*) orthologues (Fig. 1) [6, 7, 17–20]. *Cctra* is a sex determining genetic switch, which is set to ON in XX embryos and to OFF in XY embryos during a narrow temporal window at 5–6 h from oviposition [8]. In contrast to *Drosophila*, in XX Medfly embryos, *Cctra* and the auxiliary *Cctransformer-2* (*Cctra-2*) maternal mRNAs are also required to establish a stable activation of *Cctra* by female-specific splicing which relies on a positive feedback loop [6, 19]. The female-specific *Cctra* mRNA encodes a full-length 429 aa protein arising from the translation of an evolutionarily conserved ORF contained in the first, fourth and fifth exons (Fig. 1). In males, two longer alternative *Cctra* RNA isoforms, containing all five exons, encode for two truncated CcTRA proteins called CcTRA M1 (59 aa) and CcTRA M2 (99 aa) (Fig. 1). Embryonic transient RNA interference targeting mRNAs of either genes led to XX males, which are fertile even in the absence of the Y chromosome [6, 19]. As in *Drosophila*, *Cctra* and *Cctra-2* are required for the female-specific splicing of *Ccdoublesex* (*Ccdsx*). The observation that some XX individuals are transformed in gynandromorphs (showing male-specific antennae and ovipositor or no antennae and male gonads) suggests that sex determination is cell-autonomous, as in *Drosophila* [6]. A TRA/TRA-2 binding element (13 nt long) is present in multiple copies in the *Ccdsx* female-specific exon, permitting a positive regulation by CcTRA/CcTRA-2, which leads to the use of this exon in *Ccdsx* transcripts of XX individuals, similarly to *Drosophila* [7, 18]. In contrast to *Drosophila*, multiple copies of this splicing regulatory element are also present in *Cctra* locus, within and in proximity to the male-specific exons. In this other novel case, these cis elements mediate, by CcTRA/CcTRA-2 binding, exon skipping in XX individuals leading to CcTRA-encoding female-specific mRNAs [6]. In XY embryos, *Maleness-on-the-Y* (*MoY*) encodes a novel short protein, MOY, of still unknown biochemical function, that leads, either directly or indirectly, to male-specific splicing of *Cctra* and exons inclusion, at 5–6 h from oviposition [8]. The presence of male-specific exons introducing stop codons in the 429 aa long *Cctra* ORF leads to two major RNAs encoding truncated polypeptides (respectively 59 and 99 aa long) and hence considered to be non-functional [6].

We planned to experimentally confirm this deduction, by Cas9-induced mutations in the *Cctra*, which would impact both the male- and female-specific ORFs. Furthermore, the availability of an efficient single RNA to induce mutations in a female-determining gene would open the future possibility to develop a gene drive strategy aimed at manipulating the sex ratio and hence the reproduction rate of this harmful species [4]. CRISPR/Cas9 has been used in the Medfly genome to target autosomal genes having two copies for each cell [16, 21, 22]. After targeting the *white eye* Medfly gene by injecting into early embryos in vitro pre-assembled and solubilized Cas9 ribonucleoprotein complexes (RNPs), containing sgRNA, adults showed partial mutant phenotypes caused by somatic mosaicism [16]. The most extreme mutant phenotype consisted of a fly mosaic with one of the two eyes fully colorless. While biallelic mutations were observed only in somatic clones of the fly, the germ line transmission rate was very high, reaching 100% in one case. On the contrary, targeting a Medfly single copy gene, as the Y-linked *MoY,* in XY individuals by Cas9 ribonucleoproteins injections, 70% of mutant G_0 individuals showed intersexual phenotype and 30% were transformed into XY mutant G_0 females [8].

We reasoned that introducing loss-of-function frameshift mutations in the first *Cctra* exon with CRISPR/Cas9 would lead to mutant alleles coding for truncated CcTRA proteins. The expected truncations would affect not only the 429 aa long female-specific ORF, but also the carboxy-terminal ends of two male-specific 59 and 99 aa ORFs. A masculinization of XX individuals by permanent loss-of-function mutations of *Cctra* altering also the male-specific CcTRA polypeptides would support the previous suggestion that these products are indeed non-functional.

Since in *Drosophila tra* and *tra-2* mutant alleles are recessive, we reasoned that also in the Medfly the presence in the same cell and in its clonal descendants of only monoallelic indel (insertion/deletion) mutations in *Cctra* (+/− heterozygous state) would be insufficient to masculinize XX cells. Thus, in the somatic mutant clones of these XX individuals, the CcTRA protein expressed from the wild-type allele would lead to female-specific splicing of *Cctra* pre-mRNAs from both wild-type and mutant alleles, leading to female sexual phenotype. Hence, only biallelic loss-of-function *Cctra* mutations (Fig. 2; $Cctra^{1-}/Cctra^{2-}$) in the same XX cell and its cellular descendants would lead to a male-specific *Cctra* and the downstream *Ccdsx* RNAs, causing a partial (mosaicism) or full (very early and high biallelic mutagenesis) masculinization of XX adults.

Results

Cas9-RNP injections targeting *Cctra* lead to fully masculinized XX flies in the G_0 progeny

With the aim of inducing indels leading to frameshift mutations in *Cctra*, we used Cas9 RNPs injections as a delivery method. In particular, a CRISPR/Cas9 *Cctra* target site was chosen within the coding region of exon 1 on the antisense strand to design a single guide RNA, named sgtraEx1 (Additional file 1: Fig. S1A). The targeted 20 bp long sequence is about 20 bp upstream of the first donor splicing site and upstream to the female-

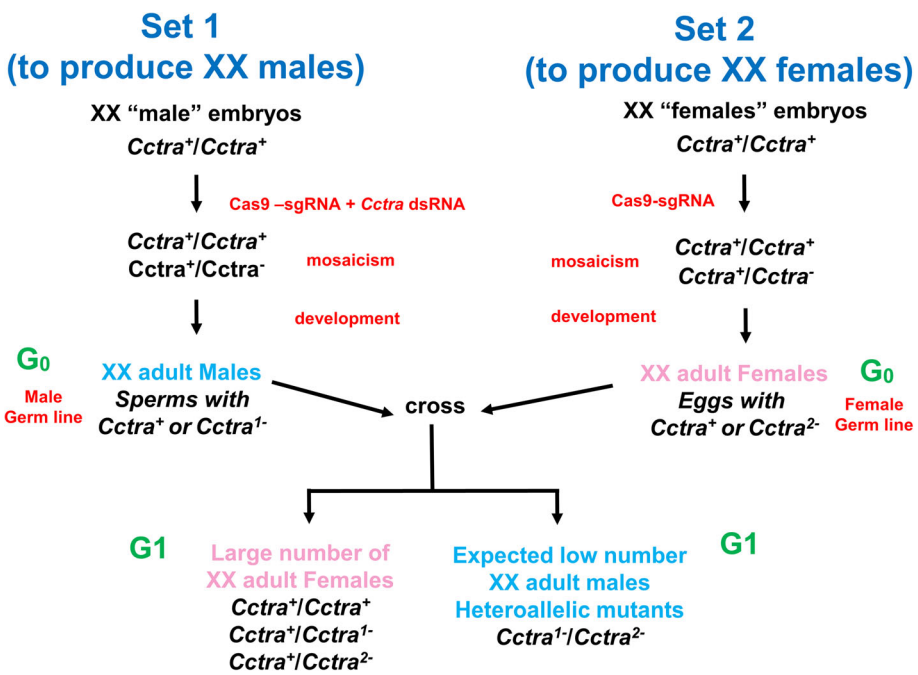

Fig. 2 Experimental design to produce G_1 XX males bearing heteroallelic mutation of *Cctra*. Two sets of parallel Cas9-RNP injections to target *Cctra* into XX embryos can lead to both G_0 XX males and XX females. The G_0 adults from the two sets can bear some *Cctra* monoallelic independent mutations (mosaicism) both in the soma and in the germ line. In set n. 1, the injection mix contains also *Cctra*-dsRNA to induce full masculinization of XX embryos (Pane et al., 2002). Hence, the G_0 XX males from set n. 1 can be crossed with G_0 XX females from set n. 2, to produce a G_1 XX progeny, expected to be composed mostly of XX females (carrying either none or monoallelic mutations) and of few G_1 XX males, carrying heteroallelic mutations of *Cctra* ($Cctra^{1-}/Cctra^{2-}$) inherited from the respective parents

specific long open reading frame encoding the CcTRA protein (Additional file 1: Fig. S1B). As described above, previous literature data showed that Cas9 RNPs applied to Medfly embryos led to a relatively low somatic biallelic mutation rate overall but a high rate in the germ line [16]. Based on this study, we speculated to observe masculinization of XX *Cctra* mutant individuals only at G_1 after crossing G_0 XY males and G_0 XX females developed from Cas9-injected. However, the discrimination of rare $Cctra^{1-}/Cctra^{2-}$ heteroallelic mutant XX males among the 50% of the G_1 progeny being XY males would have been tedious and challenging. We simplified their identification by planning to detect them among a G_1 female-only XX progeny, obtained crossing XX males and females obtained from RNP-injected embryos (Fig. 2). Among these G_1 XX females, $Cctra^{-1-}/Cctra^{2-}$ XX males would be easily detected even if very few, with the respect of the majority of XX females carrying either none or only one *Cctra* mutant allele (Fig. 2).

To produce a larger number of XX males (Fig. 2, set 1), from Cas9-injected XX embryos, a mix of Cas9-sgtraEx1 RNP and *Cctra* dsRNA, to efficiently masculinize XX, was injected into 370 XX embryos (Table 1, set n. 1). The aim was to obtain XX fertile males potentially carrying Cas9-induced *Cctra* monoallelic mutations also in the germ line. However, no pupae and adult flies emerged from this set of injections. When Cas9-sgtraEx1 RNP alone targeting *Cctra* were delivered into 400 XX embryos, few adults developed (3%; 12/400) (Table 1, set n. 2). It is likely that the co-presence of dsRNA+Cas9/sgRNA molecules could have a combined higher lethal effect for unclear reasons. Injections of dsRNA-*Cctra* alone resulted in 78 adults out of 200 XX embryos injected, with 73 XX being masculinized individuals and 5 being intersexes (Table 1, set n. 3). A similar survival rate was obtained when we injected sgtraEx1 RNA molecules but no effect (1 μg/μL), at a 5 times higher concentration being more susceptible to RNA degradation (70 females out of 160 injected embryos; Table 1, set n. 4).

Although upon Cas9-sgtraEx1 RNP injections we observed a very limited survival rate, the XX adults displayed some interesting features (Table 1, set n. 2). Indeed, the G_0 progeny was composed not only of six unaffected females, as we expected (Fig. 2 set 2), but also six XX males. These findings are suggestive of an unusually high rate of biallelic mutations. It is also worth noting that no intersexes were observed, suggesting an all-or-none effect on *Cctra* female-specific function of the Cas9 + sgtraEx1 injection.

Considering the apparently high efficiency of the ribonucleoprotein injections in set n. 2 (Table 1) in masculinizing 50% of the G_0 XX individuals, we reasoned that 1) also the XX females contained at least some somatic

Table 1 XX-only embryonic injection sets

Injection set	Cas9 delivery / []	sgRNA name / []	dsRNA name / []	XX embryos	XX Larvae	XX Females	XX Males	XX intersexes	*Cctra* male-specific in XX
1	Cas9 Protein / 1,8 μg/μL	sgtraEx1 / 200 ng/μL	dsRNA-Cctra / 0.5 μg/μL	370	48	0	0	0	–
2	Cas9 Protein / 1,8 μg/μL	sgtraEx1 / 200 ng/μL	–	400	60	6	6	0	yes in XX males
3	–	–	dsRNA-Cctra / 0.5 μg/μL	200	83	0	73	5	–
4	–	sgtraEx1 / 1 μg/μL	–	160	75	70	0	0	no
5	Plasmid-dCas9 / 1 μg/μL	sgtraEx1 / 1 μg/μL	–	290	37	7	0	3	yes
6	Cas9 Protein / 1,8 μg/μL	sgtraEx1 / 200 ng/μL	–	40	–	–	–	–	yes
7	Plasmid-Cas9 / 1 μg/μL	sgtraEx1 / 1 μg/μL	–	40	–	–	–	–	yes
8	Plasmid-dCas9 / 1 μg/μL	sgtraEx1 / 1 μg/μL	–	40	–	–	–	–	yes
9	buffer	buffer	buffer	40	–	–	–	–	no
10	–	sgtraEx1 / 1 μg/μL	–	40	–	–	–	–	no
11	Cas9 Protein / 1,8 μg/μL	–	–	40	–	–	–	–	no
12	Plasmid-Cas9 / 1 μg/μL	–	–	40	–	–	–	–	no
13	Plasmid-dCas9 / 1 μg/μL	–	–	40	–	–	–	–	no

clones bearing monoallelic *Cctra* mutations, though with no phenotypic effect, and that 2) a high mutagenic rate could also be present in the germ lines of these XX female adults as in the XX males. Assuming a 20–50% transmission rate of mutant alleles for each G_0 parent to the next progeny as previously observed in the Medfly [16], the probability to observe a double mutant individual in the G_1 progeny (Fig. 2) would be in a range of 4–25%. When we crossed among them the six XX males and six XX females from injection set n. 2 (Table 1), all 100 individuals of G_1 were females, indicating that the six XX masculinized fathers were fertile. However, the absence of XX males in the G_1 progeny indicated that, if any *Cctra* mutation was induced by Cas9 in the parental germ lines (male and female ones), the transmission rate was lower than 10% for each parent as the expected G_1 heteroallelic mutants frequency would be less than 1% of the progeny (hence not detectable among a number of 100 individuals).

Lack of indels in the targeted *Cctra* region in most cDNA clones from XX G_0 males and in all genomic DNA clones from G_0 XX females

The six females and six XX males, which composed the G_0 progeny of set n. 2, were analyzed respectively by RT-PCR and genomic PCR, to investigate *Cctra* splicing and DNA sequence of the targeted site.

The six reverted XX G_0 males showed only male-specific *Cctra* transcripts, as expected for adult flies having a full fertile male phenotype (Fig. 3). These data, together with the absence of female-specific *Cctra* mRNAs in all six males, suggested the presence of biallelic mutations in most, if not all, of the somatic cells of these XX G_0 males. Shotgun plasmid cloning of the RT-PCR reactions from the six XX G_0 males, followed by PCR colony screening of 30 clones (five colonies A-E, for each of the six XX males) led us to arbitrarily select 13 clones for sequencing (two or three cDNA clones for each male) (Additional file 1: Figure S2 and Figure S3)(Additional file 2). The splicing isoforms detected in the six XX males corresponded mostly to the know M1 and M2 *Cctra* male-specific isoforms. Out of 13 cDNA clones from the six XX males, seven correspond to male-specific *Cctra* isoform M1 (59 aa), two correspond to the male-specific isoform M2 (99 aa), one to a new splicing male-specific isoform (Male 1D encoding a 44 aa long protein isoform, named M3), one to the female-specific isoform (429 aa) and one to an unspliced longer isoform (male 5C) (Additional file 1: Figure S3; Additional file 2) [6]. Very surprisingly, despite the observed *Cctra* male-specific full shift, 11 cDNA clones showed

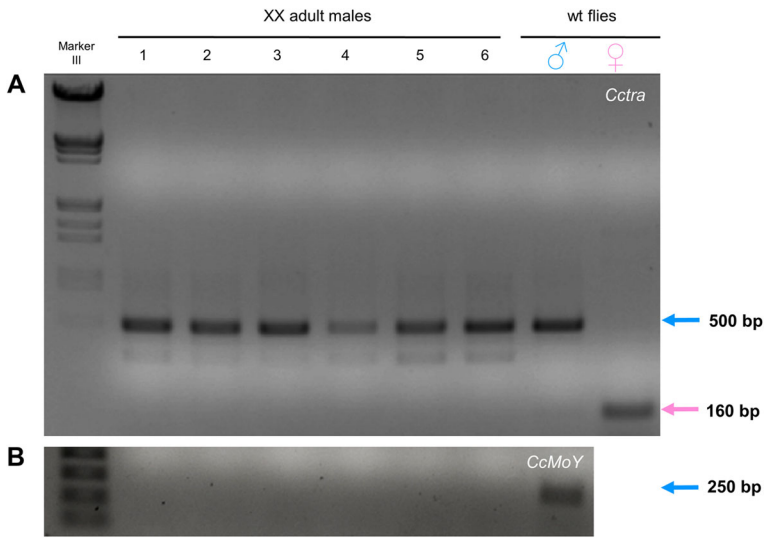

Fig. 3 RT-PCR analysis of reverted XX males. **(A)** The six XX males from injection set n. 2 (Table 1) showed only male-specific *Cctra* transcripts (500 bp) and shorter less abundant splicing variants. No traces of female-specific transcripts were visible in the gel electrophoresis (160 bp) **(B)** RT-PCR with *MoY*-specific primers indirectly confirmed the absence of the Y chromosome in these six fully reverted XX males and its presence in XY flies (positive control)

only wild-type sequences (Additional file 1: Figure S3). In one XX male, we have found a cDNA showing a 16 bp long deletion (cDNA 3E), in addition to a wild type cDNA clone (cDNA 3B) (Additional file 1: Figure S1D). The mutated cDNA encodes a 35 aa long CcTRA truncated protein. Another XX male contained two wild type (5B and 5D) cDNA clones and a mutated one lacking of 5 bp (5C) (Additional file 1: Figure S1C). This cDNA Male 5C encoded a truncated CcTRA protein of only 42 aa (Additional file 1: Figure S1C). The male 5C cDNA from unspliced *Cctra* RNA seems to correspond to a previously described RNA only present in adult females [6]. The female specificity of this unspliced product could be due to the binding of female-specific CcTRA/CcTRA-2 complex to the *Cctra* pre-mRNA required for the autoregulation. Interestingly, the *Cctra* unspliced isoform we found in one XX male contains also the Cas9-induced 5 bp deletion. We speculated that the 5 bp long deleted region of *Cctra* could be involved in enhancing the recognition of the 5′ donor site, which is only 20 bp downstream to the deletion by the spliceosome. We have found that these 5 bp are perfectly conserved in other Tephritidae *tra* orthologues, suggesting their requirement for proper *Cctra* male-specific default splicing (Additional file 1: Figure S1E). On the other hand, the cDNA 3E containing even a larger deletion (16 bp) of the same *Cctra* region performed a male-specific splicing, indicating that this sequence (14 bp out of 20 bp targeted sequence conserved in 5 distantly related Tephritidae species; Additional file 1: Figure S1E) is not strictly required to perform this alternative splicing but could be involved in performing the female-specific one. Collectively, these data showed intriguingly that the six XX males had a full switch from female-specific to male-specific splicing of *Cctra*, even in the presence of a very low (hence, mostly monoallelic) or even zero number of mutant *Cctra* alleles.

As the six XX females showed a normal female phenotype, female-specific *Cctra* splicing was expected to be found, even if they were carrying monoallelic *Cctra* mutations (Fig. 2). Hence, *Cctra* genomic DNA (rather than RNA or cDNA) was analyzed and eight plasmid clones showed only *Cctra* wild-type sequences (Additional file 1: Figure S4; Additional file 3). The lack of *Cctra* mutations in the DNA clones from all six G_0 females and in most of the cDNA from the six XX males is consistent with the absence of XX mutant heteroallelic $Cctra^{-1}/Cctra^{-2}$ males we observed in their G_1 progeny.

Embryos co-injections of dCas9 and sgtraEx1 lead to partially masculinized XX embryos and adult flies, indicating a long-lasting effect in the absence of mutations

We speculated that this Cas9 ribonucleoprotein complex was able to bind but not efficiently cut the *Cctra* DNA target site. The dead Cas9 (dCas9) is a mutant Cas9 which lacks of only the endonuclease activity and it can be used to perform transient transcriptional repression, named CRISPR interference, or iCRISPR [23–25]. We co-injected the sgRNA sgtraEx1 (1 μg/μl) with a plasmid bearing a dCas9 transgene under a *Drosophila* actin promoter, expecting that dCas9 would be produced after

transcription and translation and would bind the available sgRNA [24] (Table 1, set n. 5). A higher concentration of sgRNA (1 μg/μl; see mat. & meth.) was used in the injected mix because we expected that these RNA molecules being not pre-assembled with Cas9 before injections, could have been more exposed to degradation. This high concentration of sgRNA alone had no effect on *Cctra* female-specific splicing in injected XX embryos and in developed XX adults (Table 1, set n. 10; Fig. 4, B). Three out of ten XX adult females showed malformations of the gonadal apparatus, which suggested a mild masculinization effect (Additional file 1: Figure S5A). RT-PCR analysis of *Cctra* on RNA from these three XX adult flies confirmed the presence of also male-specific RNAs, indicating that the ovipositor malformations are likely the result of a partial masculinization during development (Additional file 1: Figure S5B). These data indicated that the dCas9 can induce a partial masculinization of XX embryos and a stable shift toward male-specific splicing of *Cctra* likely in some somatic clones.

We investigated the sex-specific splicing pattern of *Cctra* in XX-only embryos, injected at 1 h after egg laying, and developed for additional 14 h (set n. 6–13). Injections of Cas9 recombinant protein+sgtraEx1 RNP (set n. 6), or co-injections of sgtraEx1 with plasmids encoding either Cas9 (driven by E1 early promoter [23]) or dCas9 (set n. 7 and set n. 8) led to the appearance of additional male-specific *Cctra* transcripts (Table 1, Fig. 4A). Injections of only buffer, sgtraEx1, Cas9 protein, Cas9-encoding and dCas9-encoding plasmids had no effect (Fig. 4B). These data suggest that, as Cas9, also dCas9 can induce male-specific splicing of *Cctra* during the first hours of development. Hence, no *Cctra* mutations are required for this splicing change.

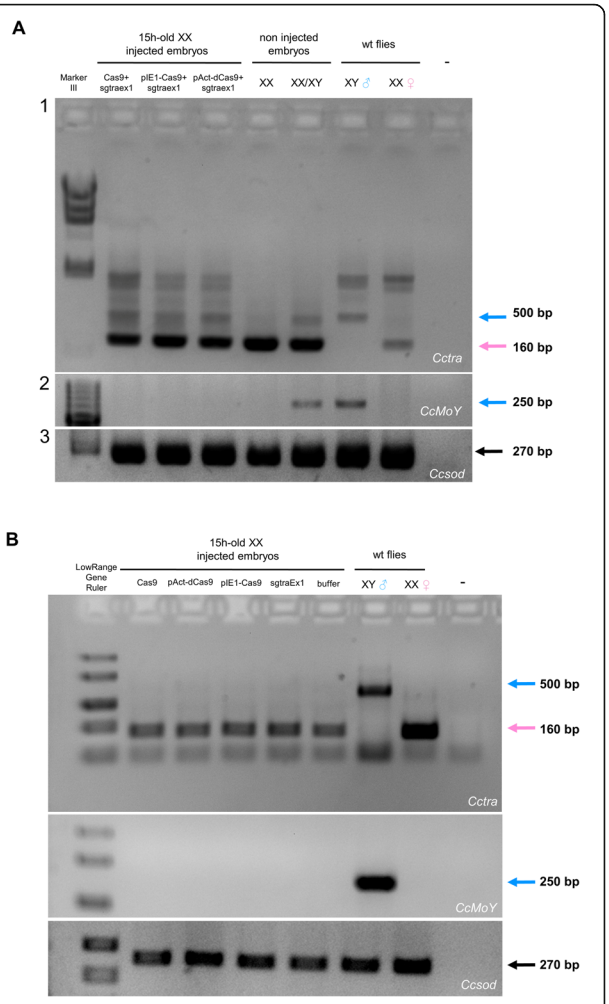

Fig. 4 Molecular partial masculinization of XX embryos by dCas9 targeting *Cctra*. **(A)** RT-PCR analysis of *Cctra* sex-specific transcripts in 15 h old XX embryos, following injections of various samples (Table 1, set n. 6–8) at 1 h after egg laying (Panel 1). The XX embryos were injected respectively with Cas9 protein+sgtraEx1 (first lane), with sgtraEx1 + Cas9-encoding plasmid (pIE1-Cas9; second lane) and with dCas9-encoding plasmid (pAct-dCas9) (third lane). Male-specific *Cctra* transcripts were detected (500 bp cDNA fragment) in all three samples of injected XX embryos, in addition to the female-specific transcripts (160 bp cDNA fragment). RT-PCR analysis of the Y-linked *MoY* gene indirectly confirmed the absence of Y chromosome in all 3 samples and in XX females, and its presence in a mixed XX/XY embryos sample and in adult XY flies (Panel 2). *CcSOD* positive control is shown in panel 3. **(B)** Negative controls. RT-PCR of *Cctra* sex-specific transcripts in 15 h old XX embryos, following injections at 1 h after egg laying (Table 1, set n. 9–13). The XX embryos were injected respectively with Cas9 protein, Cas9-encoding plasmid, dCas9-encoding plasmid, with sgtraEx1 and with buffer alone. Only female-specific *Cctra* transcripts were detected (160 bp) in all samples of injected XX embryos (Panel 1). In Panel 2 and 3, the control of the karyotype and positive controls, conducted as in A, are shown

Discussion

The Cas9-sgtraEx1 RNPs injected into XX Medfly embryos led to a masculinization of 50% of XX individuals. All six XX males showed by RT-PCR and cDNA sequencing analyses mostly male-specific *Cctra* isoforms, concordant with the observed male phenotype. Unexpectedly, no indel mutations were detected in cDNA fragments from the Cas9 targeted site in four out of six males. Two XX males showed a mix of wild type and mutated cDNA fragments, suggesting the presence of monoallelic mutations in some cellular regions. XX males and XX females from injected embryos produced a G_1 consisting of only XX females, which indicated absence of homozygous individuals for mutant *Cctra* alleles. We concluded that very low mutation rate, if any, was reached not only in the soma but also in the germ line of injected G_0 individuals. In contrast, Meccariello et al. [16], observed that mutant mosaic G_0 flies

mutagenized by Cas9 in the *white-eye* gene transmitted germ line mutations to the progeny at a very high rate (up to 100%). Hence, the Cas9-sgtraEx1 is likely very inefficient in mediating Cas9 gene disruption but surprisingly very efficient in masculinizing XX individuals. These data suggested that the Cas9 ribonucleoprotein promoted masculinization by inducing male-specific *Cctra* splicing in 50% of XX embryos which developed into adults by a mechanism different than gene disruption.

We reasoned that the sgRNA designed for the CRISPR experiment and/or the *Cctra* targeted region structural features posed limitations in the second step of the Cas9 action, namely the endonuclease activity, but not in the first step, the binding to the *Cctra* genetic locus. Indeed, a two-state model for Cas9 binding and cleavage was recently proposed: a seed match triggers binding but only extensive pairing with target DNA leads to cleavage [26]. Target sequence mismatches can induce the Cas9-RNP complex to bind also off-target sites without DNA cleavage, because the transition to the active conformation is prevented [26, 27]. Co-injections of sgtraEx1 and a plasmid encoding dCas9 into XX embryos induced a partial shift of *Cctra* splicing toward male-specific pattern after few hours of development and the development of XX females (three out of ten) with malformed ovipositor. These females were found to be molecular intersexes, as they showed both female-specific and male-specific *Cctra* isoforms. Also, these malformed females showed a mix of male and female-specific *Cctra* transcripts and, hence, correspond to partially masculinized individuals (intersexes) [6]. Similar malformed ovipositors were observed by Pane et al. [6] following embryonic RNA against *Cctra*. The lack of fully masculinized XX individuals in the progeny of ten individuals suggests a reduced efficiency of dCas9 in masculinizing XX individuals. However, this could be due to the different delivery methods of Cas9 and dCas9. In the first case, purified recombinant Cas9 ready to act was injected, while in the second case a dCas9 encoding transgene was transcribed from a *Drosophila* actin promoter, after embryos injections of a plasmid. Lower efficiency is to be expected in the second delivery method, due to the transcription and translation steps required to express dCas9. The transient binding of Cas9 RNPs to the 5′ *Cctra* DNA region could have reduced the *Cctra* zygotic transcription during the first hours of embryogenesis and, hence, the accumulation of female specifically spliced *Cctra* mRNA, promoted by the maternal *Cctra* contribution in XX embryos. This transient reduction of newly transcribed *Cctra* female-specific mRNA and of the encoded CcTRA protein in the XX embryos could have blocked the establishment of *Cctra* female-specific autoregulation leading to a negative epigenetic effect on *Cctra*. Similarly, a transient depletion of *Cctra* mRNA by embryonic RNAi led to a collapse of its positive autoregulation and to obtain XX fertile males expressing male-specific *Cctra* RNAs [6].

Conclusions

The question if CcTRA male-specific ORFs are required for male-specific *Cctra* splicing remains still open, as biallelic *Cctra* mutant XX males were not obtained. The second question if the chosen sgtraEx1 guide RNA is suitable for future gene drive strategy aimed to efficient mutagenesis by Cas9 had a conclusive and negative reply, as very low mutagenesis rate was observed. However, these data support the hypothesis that the transient binding of the Cas9-sgtraEx1 ribonucleoprotein complex on the first *Cctra* exon during the first hours of embryogenesis led to a repression of the establishment of the *Cctra* female-specific autoregulation in XX embryos even in the absence of induced mutations. Our study raises new general issues concerning the use of CRISPR/Cas9 method. We serendipitously uncovered a novel problem of unplanned stable changes in the expression of genes able to autoregulate, which calls for further investigation. If a Cas9 + sgRNA binds to off target sequences of autoregulating bistable genes, this event can provoke long lasting epigenetic effects even in the absence of DNA mutations.

Methods

Rearing of *Ceratitis capitata*

Wild type (WT) and transgenic Medfly lines were maintained under standard rearing conditions. The WT *Benakeion* strain, which has been reared in laboratories for more than 20 years, was obtained from P. A. Mourikis 30 years ago (Benakeion Institute of Phytopathology, Athens, Greece). The strains were reared in standard laboratory conditions at 25 °C, 70% relative humidity and 12:12 h light–dark regimen. Adult flies were fed yeast/sucrose powder (1:2).

RNP complex assembly and injections

Cas9 was expressed as his-tagged protein and purified from bacteria [16, 19]. sgRNA was designed using the CHOPCHOP online software [28]. The lack of SNPs within this 20 nt long sequence in three different *Ceratitis* lines (Benakeion, used in this study, ISPRA [22] and FAM18 *Ceratitis* [8]) suggested that no Cas9-resistant *Cctra* alleles would be already present in individuals of these lab strains. Template for sgRNA in vitro transcription were generated by annealing two complementary oligonucleotides (PAGE-purified, Life Technologies) as previously described [16, 21], using the primers F-sgtraEx1 and Reverse-Crispr from Life Technologies (Additional file 4). sgRNA was synthesized according to

instructions of the Megascript® T7 kit (Ambion) with 1 μg of DNA template and a 5′ flanking T7 promoter. After RNA synthesis, the template was removed by incubating with TurboDNase® (Ambion) for 15 min at 37°. Prior to the injection, the RNP complex was prepared by mixing 1.8 μg/μL of purified Cas9 protein with approximately 200 ng/μL of sgtraEx1, containing 300 mM KCl [16]. The mix was incubated for 10 min at 37 °C. A glass needle was filled with the pre-loaded sgtraEx1-Cas9 mix and the injection was performed into the posterior end of embryos collected 45 min after egg laying as described for RNA interference in *Ceratitis capitata* [6]. When injecting sgRNA alone, a 5 times higher concentration (1 μg/μL) was used in the injected mix, because we expected that these RNA molecules, being not pre-assembled with Cas9 before injections, could have been more exposed to degradation.

RNAi and XX-only progeny production

A *Cctra c*DNA 800 bp long fragment was PCR amplified using RNA from female adults of *C. capitata* and longer 164+/900- primers, introducing a T7 promoter sequence at each extremity. In vitro transcription of *Cctra* dsRNA was performed using the Ambion MEGAscript® RNAi kit T7 RNA polymerase, following manufacturer instructions. Embryonic RNAi (0.5 μg/μL dsRNA solution) was used to repress *Cctra* in XX/XY embryos and to produce male only progeny. Single males from this progeny were crossed with three females in small cages and the crosses having XX males were identify by Y-specific PCR (Y-specific primers) [8] on a small sample of laid embryos.

dCas9 encoding plasmid and injections

Plasmid expressing dCas9 under the control of the *Drosophila melanogaster* actin promoter was kindly provided to GS by Lenny Rabinow (Perrimon's lab, Harvard, USA) [23]. A mix containing 1 μg/μL of pAct-dCas9 plasmid and 1 μg/μL of sgtraEx1 transcribed in vitro into the posterior end of embryos. We used 5 times higher concentration of sgRNA because we expected that these small RNA molecules being not pre-assembled with Cas9 before injections, could have been more exposed to degradation.

RNA extraction and RT-PCR

Total RNA was extracted from pools of embryos, intersexes, male and female adults using TRIzol® Reagent (Invitrogen®) following manufacturer instructions. Oligo-dT-primed cDNA was prepared from DNAse-treated total RNA using EuroScript® m-MLV reverse transcriptase (Euroclone®). RT-PCR expression analysis was performed with the following primers: *Cctra* 164+/320-, *CcSOD+/CcSOD-* and *CcMoY A+/CcMoY A-* (Additional file 4). For XX malformed females obtained from XX only embryos with dCas9 and sgtraEx1 *Cctra* RT-PCR was performed using *Cctra* 164+/900- primers pair, annealing on the same exon as *Cctra* 320- primer (Additional file 4). Gel electrophoresis diagnostic amplicon run was performed using Marker III (Lambda genomic DNA digested with EcoRI/HindIII) or 100 bp ladder from Thermo Scientific®.

DNA extraction and molecular analysis

DNA extraction was performed, with minor modifications, according to the protocol of Holmes and Bonner et al. [29]. Adult XX female flies G_0 were placed in a 1.5 ml tube and manually crushed with a pestle in 200 ml Holmes Bonner buffer (Urea 7 M, 281 Tris-HCl 100 mM pH 8.0, EDTA 10 mM pH 8.0, NaCl 350 mM, SDS 2%). Subsequently, DNA was purified by phenol/chloroform extraction, followed by chloroform extraction and ethanol precipitation. The pellet was resuspended in 30 μl water containing RNase A.

cDNA and gDNA cloning and sequencing

PCR cDNA fragments from XX adult males were cloned into pGEM-T Easy Promega® vector according manufacturer instruction. PCR colony screening was carried out using 164+ and 320- primers. Positive colonies were used to extract plasmid DNA which was sequenced using Applied Biosystem® Big Dye v 3.1. Genomic DNA from the six G_0 XX females was used as template to amplify the region encompassing the target sites, using the primers *Cctra* 164+ and *Cctra* 164-Rev (Additional file 4). DreamTaq (Life Technologies) polymerase was used for PCR amplifications according to the manufacturer's instructions. The PCR products were purified with StrataPrep PCR Purification Kit (Agilent Technologies) and subcloned using StrataClone PCR cloning Kit (Agilent Technologies). Positive clones were sequenced by Sanger method and ABI 310 Automated Sequencer (Applied Biosystems) using the primer *Cctra* 164+ (Additional file 4).

RNA extraction from injected embryos after 15 h of development

The pools of 40 embryos injected with various mixes (Table 1) were let develop for 15 h at 25 °C, 70% relative humidity. The embryos were then detached from the cover slip using heptane, which dissolves the glue, and collected in a 1.5 mL tube. They were then washed three times with 1X PBS to remove heptane before RNA extraction was performed using TRIzol® Reagent (Invitrogen®) following manufacturer instructions. The RNA samples were analyzed for *Cctra* splicing pattern by RT-PCR using the primers *Cctra* 164+ and *Cctra* 900- (Additional file 4).). The cDNA and genomic sequences

were deposited at the GenBank database with the following accession numbers: MW200161 to MW200180.

Supplementary Information

The online version contains supplementary material available at https://doi.org/10.1186/s12863-020-00941-4.

Additional file 1.
Additional file 2.
Additional file 3.
Additional file 4.
Additional file 5.

Abbreviations

SIT: Sterile Insect Technique; *ORF*: Open Reading Frame; *CRISPR*: Clustered Regulated InterSpaced Palindromic Repeats; *RNP*: Ribo-Nucleo-Proteic Complex; *dsRNA*: double strand RNA; *sgRNA*: single guide RNA; *iCRISPR*: interference CRISPR; *dCas9*: dead Cas9; *SNP*: Single Nucleotide Polymorphism; *RNAi*: RNA interference; *WT*: Wild-Type

Acknowledgements

We would like to thank Lenny Rabinow (Harvard University, USA) for providing dCas9 plasmid vector and Donald L. Jarvis (University of Wyoming, USA) for providing E1-P-Cas9. GSA and AM initiated the project. We wish to thank Luigi Vitagliano (IBB-CNR, Italy) for in depth discussion, insights and manuscript reviewing. This study was benefited from discussions at International Atomic Energy Agency funded meetings for the Coordinated Research Project "Comparing Rearing Efficiency and Competitiveness of Sterile Male Strains Produced by Genetic, Transgenic or Symbiont-based Technologies". We thank the anonymous reviewers and the guest editor for their helpful and generous suggestions to improve the description of this study.

About this supplement

This article has been published as part of *BMC Genetics Volume 21 Supplement 2, 2020: Comparing rearing efficiency and competitiveness of sterile male strains produced by genetic, transgenic or symbiont-based technologies.* The full contents of the supplement are available online at https://bmcgenet.biomedcentral.com/articles/supplements/volume-21-supplement-2.

Authors' contributions

AM, AG, MGI, GDC, performed set n. 1–4 embryonic injections (Table 1) and the embryonic injections of *Cctra* dsRNA+Cas9 + sgtraEx1, which led to 100% lethality. PP performed PCR, cloning and sequencing analyses of the 6 XX males and 6 XX females from of injection set n. 2 (Table 1). PP and GSO performed injection set n. 5 and RT-PCR of the 3 XX malformed females. PP and GV performed injection set n. 6–9 and GV performed RT-PCR analyses on the 15 h-old injected embryos. PP performed the cross of G_0 males and females from set n. 2 and visually screened the G_1 progeny. AM, PP, AG, MGI, GDC, GSO and GV maintained the Medfly strains, preparing larval and adult food, performing crosses and collecting embryos. GSA wrote the paper, with the inputs of MDR, SA, MS, and AM. GS prepared the figures, with contributions of AM, MS and PP. All authors contributed with minor corrections/editing of the manuscript, especially AG. All the authors have read and approved the final version of the manuscript.

Funding

The PhD Biology program at University of Naples Federico II supported this study with fellowships to AM and PP. The Department of Biology supported this study with small-budget grants (Ricerca Dipartimentale) to GSA, SA and MS, for data collection and their interpretation. MDR acknowledges support from the UZH University Research Priority Program Evolution in Action. Publication costs are funded by the Joint FAO/IAEA Division of Nuclear Techniques in Food and Agriculture, IAEA (CRP No.: D4.20.16) Vienna, Austria. The funding bodies provided the financial means to allow the authors to carry out the study and the funding bodies played no role in the design of the study and collection, analysis, and interpretation of data and in writing the manuscript.

Availability of data and materials

The cDNA and genomic sequences were deposited at the GenBank database with the following accession numbers: MW200161 to MW200180.

Ethics approval and consent to participate

Not applicable.

Consent for publication

Not applicable.

Competing interests

The authors declare absence of competing interests.

Author details

[1]Department of Biology, University of Naples Federico II, 80126 Naples, Italy. [2]Department of Molecular Life Sciences and SIB Swiss Institute of Bioinformatics, University of Zurich, Winterthurerstrasse 190, CH-8057 Zurich, Switzerland.

Published: 18 December 2020

References

1. De Meyer M, Robertson MP, Peterson AT, Mansell MW. Ecological niches and potential geographical distributions of Mediterranean fruit Fly (*Ceratitis capitata*) and Natal fruit Fly (Ceratitis rosa). J Biogeogr. 2008;35(2):270–81.
2. Franz G. Genetic Sexing Strains in Mediterranean Fruit Fly, an Example for Other Species Amenable to Large-Scale Rearing for the Sterile Insect Technique. In: Dyck VA, Hendrichs J, Robinson A, editors. Sterile Insect Technique. Dordrecht: Springer; 2005. https://doi.org/10.1007/1-4020-4051-2_16.
3. Rendon P, McInnis D, Lance D, Stewart J. Medfly (Diptera: Tephritidae) genetic sexing: large-scale field comparison of males-only and bisexual sterile fly releases in Guatemala. J Econ Entomol. 2004;97:1547–53.
4. Lutrat C, Giesbrecht D, Marois E, Whyard S, Baldet T, Bouyer J. Sex Sorting for Pest Control: It's raining men! Trends Parasitol. 2019;35(8):649–62. https://doi.org/10.1016/j.pt.2019.06.001 Epub 2019 Jun 26.
5. Saccone G, Pane A, De Simone M, Salvemini M, Milano A, Annunziata L, Mauro U, Polito LC. New Sexing Strains for Mediterranean Fruit Fly *Ceratitis capitata*: Transforming Females into Males. In: MJB V, Robinson AS, Hendrichs J, editors. Area-Wide Control of Insect Pests. Dordrecht: Springer; 2007.
6. Pane A, Salvemini M, Delli Bovi P, Polito C, Saccone G. The *transformer* gene in *Ceratitis capitata* provides a genetic basis for selecting and remembering the sexual fate. Development. 2002;129:3715–25. Development (Cambridge, England). 129. 3715–25. https://doi.org/10.3410/f.1001642.116658.
7. Tian M. Maniatis TA splicing enhancer exhibits both constitutive and regulated activities. Genes Dev. 1994;8(14):1703–12.
8. Meccariello A, Salvemini M, Primo P, Hall B, Koskinioti P, Dalíková M, Gravina A, Gucciardino MA, Forlenza F, Gregoriou ME, Ippolito D, Monti SM, Petrella V, Perrotta MM, Schmeing S, Ruggiero A, Scolari F, Giordano E, Tsoumani KT, Marec F, Windbichler N, Nagaraju J, Arunkumar K, Bourtzis K, Mathiopoulos KD, Ragoussis J, Vitagliano L, Tu Z, Papathanos PA, Robinson MD, Saccone G. Maleness-on-the-Y (MoY) orchestrates male sex determination in major agricultural fruit fly pests. Science. 2019;365(6460):1457–60. https://doi.org/10.1126/science.aax1318.
9. Saccone G, Salvemini M, Polito LC. The *transformer* gene of *Ceratitis capitata*: a paradigm for a conserved epigenetic master regulator of sex determination in insects. Genetica. 2011;139:99–111.
10. Bopp D, Saccone G, Beye M. Sex determination in insects: variations on a common theme. Sex Dev. 2014;8(1–3):20–8.
11. Vargas Rl, Piñero JC, Leblanc L. An overview of pest species of Bactrocera fruit flies (diptera: Tephritidae) and the integration of biopesticides with other biological approaches for their management with a focus on the Pacific region. Insects. 2015;6(2):297–318. https://doi.org/10.3390/insects6020297 Review.
12. Ekesi S, De Meyer M, Mohamed SA, Virgilio M, Borgemeister C. Taxonomy, ecology, and Management of Native and Exotic Fruit fly Species in Africa. Annu Rev Entomol. 2016;61:219–38.
13. Nagaraju J, Saccone G. How sex is determined in insects? Preface. J Genet. 2010;89(3):269–70.
14. Handler AM. Prospects for using genetic transformation for improved SIT and new biocontrol methods. Genetica. 2002;116(1):137–49 Review.

15. Louis C, Savakis C, Kafatos FC. Possibilities For Genetic Engineering In Insects Of Economic Interest, Elsevier 1986, Il. In: Tern Symp Fruit Flies/Crete Sept; 1986.
16. Meccariello A, Monti SM, Romanelli A, Colonna R, Primo P, Inghilterra MG, Del Corsano G, Ramaglia A, Iazzetti G, Chiarhours A, Patti F, Heinze SD, Salvemini M, Lindsay H, Chiavacci E, Burger A, Robinson MD, Mosimann C, Bopp D, Saccone G. Highly efficient DNA-free gene disruption in the agricultural pest Ceratitis capitata by CRISPR-Cas9 ribonucleoprotein complexes. Sci Rep. 2017;7(1):10061.
17. Saccone G, Peluso I, Artiaco D, Giordano E, Bopp D, Polito LC. The *Ceratitis capitata* homologue of the Drosophila sex-determining gene *Sex-lethal is* structurally conserved, but not sex-specifically regulated. Development. 1998;125(8):1495.
18. Saccone G, Salvemini M, Pane A, Polito LC. Masculinization of XX Drosophila transgenic flies expressing *Ceratitis capitata* DSXM isoform. Inter Journal of Dev Biol. 2008;52(8):1051–7.
19. Salvemini M, Robertson M, Aronson B, Atkinson P, Polito C, Saccone G. *Ceratitis capitata transformer-2 g*ene is required to establish and maintain the autoregulation of Cctra, the master gene for female sex determination. Int J Dev Biol. 2009;53:109–20. https://doi.org/10.1387/ijdb.082681ms.
20. Nagoshi RN, McKeown M, Burtis KC, Belote JM, Baker BS. The control of alternative splicing at genes regulating sexual differentiation in *D. melanogaster*. Cell. 1988 Apr 22;53(2):229–36.
21. Lee JS, Kwak SJ, Kim J, Kim AK, Noh HM, Kim JS, Yu K. RNA-Guided Genome Editing in Drosophila with the Purified Cas9 Protein. G3-Genes Genom Genet. 2014;4:1291–5.
22. Papanicolaou A, Schetelig MF, Arensburger P, Atkinson PW, Benoit JB, Bourtzis K, Castañera P, Cavanaugh JP, Chao H, Childers C, Curril I, Dinh H, Doddapaneni H, Dolan A, Dugan S, Friedrich M, Gasperi G, Geib S, Georgakilas G, Gibbs RA, Giers SD, Gomulski LM, González-Guzmán M, Guillem-Amat A, Han Y, Hatzigeorgiou AG, Hernández-Crespo P, Hughes DST, Jones JW, Karagkouni D, Koskinioti P, Lee SL, Malacrida AR, Manni M, Mathiopoulos K, Meccariello A, Murali SC, Murphy TD, Muzny DM, Oberhofer G, Ortego F, Paraskevopoulou MD, Poelchau M, Qu J, Reczko M, Robertson HM, Rosendale AJ, Rosselot AE, Saccone G, Salvemini M, Savini G, Schreiner P, Scolari F, Siciliano P, Sim SB, Tsiamis G, Ureña E, Vlachos IS, Werren JH, Wimmer EA, Worley KC, Zacharopoulou A, Richards S, Handler AM. The whole genome sequence of the Mediterranean fruit fly, *Ceratitis capitata* (Wiedemann), reveals insights into the biology and adaptive evolution of a highly invasive pest species. Genome Biol. 2016;17:192.
23. Lin S, Ewen-Campen B, Ni X, Housden BE, Perrimon N. In vivo transcriptional activation using CRISPR/Cas9 in Drosophila. Genetics. 2015;201(2):433–42.
24. Mabashi-Asazuma H, Jarvis DL. CRISPR-Cas9 vectors for genome editing and host engineering in the baculovirus–insect cell system. Proc Natl Acad Sci. 2017;114(34):9068–73.
25. Qi LS, Larson MH, Gilbert LA, Doudna JA, Weissman JS, Arkin AP, Lim WA. Repurposing CRISPR as an RNA-guided platform for sequence-specific control of gene expression. Cell. 2013;152:1173–83.
26. Dagdas YS, Chen JS, Sternberg SH, Doudna JA, Yildiz A. A conformational checkpoint between DNA binding and cleavage by CRISPR-Cas9. Sci Adv. 2017;3(8):eaao0027.
27. Zhang L, Rube HT, Bussemaker HJ, Pufall MA. The effect of sequence mismatches on binding affinity and endonuclease activity are decoupled throughout the Cas9 binding site. bioRxiv. 2017:176255. https://doi.org/10.1101/176255.
28. Montague TG, Cruz JM, Gagnon JA, Church GM, Valen E. CHOPCHOP: a CRISPR/Cas9 and TALEN web tool forgenome editing. Nucleic Acids Res. 2014; 42:401–7.
29. Holmes DS, Bonner J. Preparation, molecular weight, base composition, and secondary structure of giant nuclear ribonucleic acid. Biochemistry. 1973; 12(12):2330–8.

Publisher's Note

molecules

MDPI

Article

Secondary Metabolites, including a New 5,6-Dihydropyran-2-One, Produced by the Fungus *Diplodia corticola*. Aphicidal Activity of the Main Metabolite, Sphaeropsidin A

Maria Michela Salvatore [1,2,†], Ilaria Di Lelio [3,†], Marina DellaGreca [1], Rosario Nicoletti [3,4], Francesco Salvatore [1], Elia Russo [3], Gennaro Volpe [3], Andrea Becchimanzi [3], Alla Eddine Mahamedi [5], Akila Berraf-Tebbal [6] and Anna Andolfi [1,7,*]

1 Department of Chemical Sciences, University of Naples Federico II, 80126 Naples, Italy; mariamichela.salvatore@unina.it (M.M.S.); dellagre@unina.it (M.D.); frsalvat@unina.it (F.S.)
2 Institute for Sustainable Plant Protection, National Research Council, 80055 Portici, Italy
3 Department of Agriculture, University of Naples Federico II, 80055 Portici, Italy; ilaria.dilelio@unina.it (I.D.L.); rosario.nicoletti@crea.gov.it (R.N.); elia.russo@unina.it (E.R.); gennaro.volpe2@unina.it (G.V.); andrea.becchimanzi@unina.it (A.B.)
4 Research Center for Olive, Fruit, and Citrus Crops, Council for Agricultural Research and Economics, 81100 Caserta, Italy
5 Department of Biology, Faculty of Natural Sciences, Life and Earth Sciences, University of Ghardaia, Ghardaia 47000, Algeria; aladin1342@yahoo.com
6 Mendeleum-Institute of Genetics, Faculty of Horticulture, Mendel University in Brno, 69144 Lednice, Czech Republic; berraf.a@hotmail.fr
7 BAT Center-Interuniversity Center for Studies on Bioinspired Agro-Environmental Technology, University of Naples Federico II, 80055 Portici, Italy
* Correspondence: andolfi@unina.it
† These authors contributed equally to this work.

Abstract: An undescribed 5,6-dihydropyran-2-one, namely diplopyrone C, was isolated and characterized from the cultures of an isolate of the fungus *Diplodia corticola* recovered from *Quercus suber* in Algeria. The structure and relative stereostructure of (5*S*,6*S*,7*Z*,9*S*,10*S*)-5-hydroxy-6-(2-(3-methyloxiran-2-yl)vinyl)-5,6-dihydro-2H-pyran-2-one were assigned essentially based on NMR and MS data. Furthermore, ten known compounds were isolated and identified in the same cultures. The most abundant product, the tetracyclic pimarane diterpene sphaeropsidin A, was tested for insecticidal effects against the model sucking aphid, *Acyrthosiphon pisum*. Results showed a toxic dose-dependent oral activity of sphaeropsidin A, with an LC_{50} of 9.64 mM.

Keywords: fungal metabolites; botryosphaeriaceae; metabolomics; natural products; sphaeropsidins

check for updates

Citation: Salvatore, M.M.; Di Lelio, I.; DellaGreca, M.; Nicoletti, R.; Salvatore, F.; Russo, E.; Volpe, G.; Becchimanzi, A.; Mahamedi, A.E.; Berraf-Tebbal, A.; et al. Secondary Metabolites, including a New 5,6-Dihydropyran-2-One, Produced by the Fungus *Diplodia corticola*. Aphicidal Activity of the Main Metabolite, Sphaeropsidin A. *Molecules* **2022**, *27*, 2327. https://doi.org/10.3390/molecules27072327

Academic Editor: RuAngelie Edrada-Ebel

Received: 28 February 2022
Accepted: 31 March 2022
Published: 4 April 2022

1. Introduction

Diplodia (Dothideomycetes, Botryosphaeriaceae) is a widely diffused genus of fungi with more than 1000 described species [1]. Over the years, these species have been reported as pathogens or endophytes of many woody plants [1,2]. Moreover, they represent a prolific source of bioactive products with huge structural variability and bioactivities [3–6]. In this respect, the capacity of *Diplodia* spp. to have distinct habitus and interactions with plants may be related to the release of bioactive compounds during the spread in host tissues.

Among the *Diplodia* species, *Diplodia corticola* A.J.L. Phillips, A. Alves, and J. Luque is particularly regarded for the production of secondary metabolites [7–10]. It is frequently associated with dieback and canker diseases of oaks in many Mediterranean countries [11–13]. Among the metabolites frequently isolated from in vitro cultures of *D. corticola*, sphaeropsidin A is particularly promising for practical applications in agriculture and medicine due

to its exciting biological properties, including antimicrobial, insecticidal, herbicidal, and anticancer activities [14]. Besides potential applications, the documented antimicrobial and insecticidal effects of sphaeropsidin A [15–18] are relevant for further consideration of the ecological role of the fungus.

In this work, a strain of *D. corticola* isolated from *Quercus suber* in Algeria was investigated in order to increase the available data on the secondary metabolism of this fungus, leading to the isolation of a new 5,6-dihydropyran-2-one, namely diplopyrone C, and ten known compounds which include sphaeropsidin A. Following documented evidence of insecticidal properties [15,18], sphaeropsidin A was tested for aphicidal activity on the pea aphid *Acyrthosiphon pisum* (Harris) (Hemiptera, Aphididae), which is a cosmopolitan polyphagous insect and one of the primary species used as laboratory models for testing the susceptibility of sucking insects to oral administration of insecticidal products by using a feeding bioassay on an artificial diet.

2. Results

2.1. Secondary Metabolites from Cultures of Diplodia corticola B305

Crude extract obtained from the culture of *D. corticola* (strain B305), through a chromatographic purification process (see Section 4.3), gave a new metabolite, herein named diplopyrone C (**1**, Figure 1). Its structure was determined by spectroscopic methods, essentially 1D and 2D NMR, IR, and UV combined with mass spectrometry, as reported below (Figures S1–S8). Moreover, ten known metabolites were identified by comparison of their proton spectra (Figures S9–S18), and eventually optical rotation, with those reported in the literature for: sphaeropsidins A and B (**2** and **3**, [19]), sphaeropsidin C (**4**) [20], (*R*)-mellein, (3*R*,4*R*)- and (3*R*,4*S*)-4-hydroxymelleins (**5**–**7**) [21], sapinofuranone B (**8**) [22], pinofuranoxin A (**9**) [23], diplobifuranylone B (**10**) [24], and tyrosol (**11**) [25] (Figure 1).

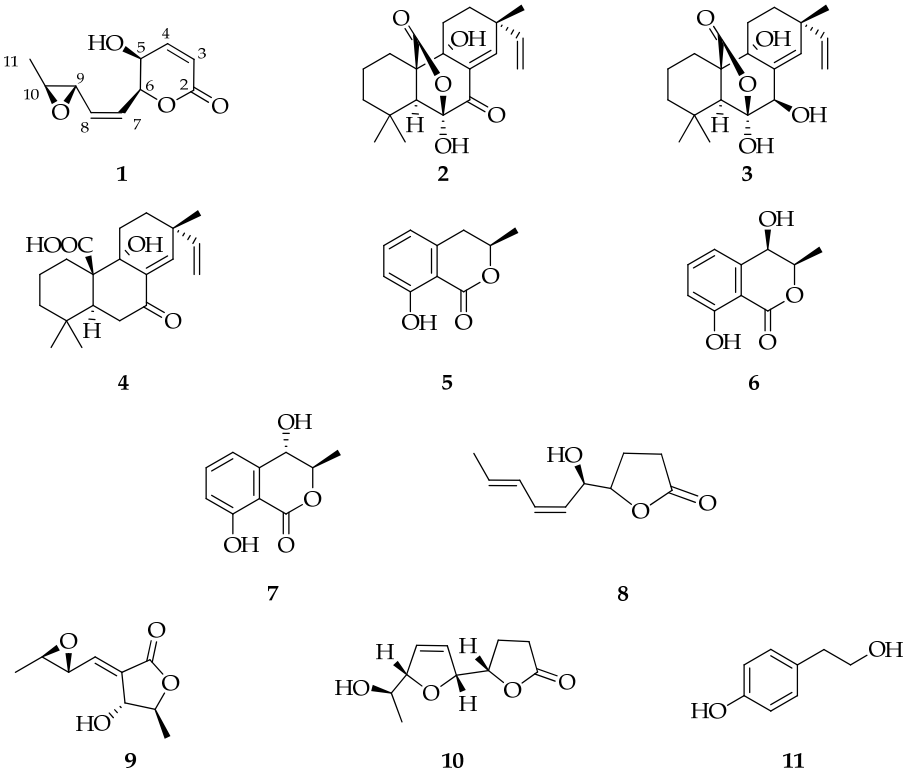

Figure 1. Structures of diplopyrone C (**1**), sphaeropsidins A (**2**), B (**3**), and C (**4**), (3*R*)-mellein (**5**), (3*R*,4*R*)-(**6**), and, (3*R*,4*S*)-4-hydroxymelleins (**7**), sapinofuranone B (**8**), pinofuranoxin A (**9**), diplobifuranylone B (**10**), and tyrosol (**11**).

The HRESI-MS of compound **1** showed picks at m/z = 235.0395 $[M + K]^+$, and 219.1860 $[M + Na]^+$ suggesting the molecular formula $C_{10}H_{12}O_4$ and five degrees of unsaturation. Moreover, fragment ion at m/z = 179.0721 $[M\text{-}OH]^+$ was evident (Figure S8).

^1H and ^{13}C NMR analysis showed signals typical of 5,6-disubstitute-5,6-dihydropyran-2-one (Figures S1 and S2) [26] in agreement with IR and UV spectra. In fact, the ^1H NMR spectrum showed signals at δ (*J* in Hz): 7.03 (dd, 9.8, 5.4), 6.17 (d, 9.8) 5.40 (dd, 7.9, 3.3), and 4.28 (dd, 5.4, 3.3) assigned to H-4, H-3, H-6 and H-5 of 5,6-dihydropyran-2-one ring (Table 1). The COSY spectrum (Figure S3) confirmed this hypothesis, and chemical shifts H-3 to H-6 protons were assigned. In the ^{13}C NMR spectrum (Figure S2), signals at δ 162.8, 122.9, 144.3, and 76.9 confirmed the presence of an α,β-unsaturated lactone. Moreover, the signal at δ 4.28 (H-5) correlated to the carbon at δ 63.2 in the HSQC spectrum (Figure S4), indicating the presence of the hydroxyl group at C-5. The remaining signals observed in the 1H NMR spectrum at δ (*J* in Hz): 5.93 (ddd, 11.7, 7.9, 1.1), 5.63 (ddd, 11.7, 6.7, 1.1), 3.34 (dd, 5.2, 2.1 H), 3.00 (dq, 5.2, 2.1 Hz), and 1.40 (d, 5.2) were correlated, in the HSQC spectrum, to δ 127.2, 132.4, 55.5, 56.7, and 17.5, respectively. Analysis of the HMBC spectrum (Figure S5) showed correlations between H-6 and C-7 and C-8, and H-8 with C-9 and C-10 indicated a 3,4-oxirane-1-pentenyl side chain at C-6 (Figure 2).

Table 1. NMR data of diplopyrone C (**1**) in $CDCl_3$ [1,2].

No.	δC	δH (*J* in Hz)	HMBC
1	-	-	
2	162.8	-	
3	122.9	6.17 (1H) br d (9.8)	C-2, C-5
4	144.3	7.03 (1H) dd (9.8, 5.4)	C-2, C-5, C-6
5	63.2	4.28 (1H) dd (5.4, 3.3)	C-3, C-4, C-6
6	76.9	5.40 (1H) dd (7.9, 3.3)	C-7, C-8
7	127.2	5.93 (1H) ddd (11.7, 7.9, 1.1)	C-9
8	132.4	5.63 (1H) ddd (11.7, 6.7, 1.1)	C-6, C-9, C-10
9	55.5	3.34 (1H) dd (6.7, 2.1)	C-8, C-7, C-10
10	56.7	3.00 (1H) dq (5.2, 2.1)	C-11
11	17.5	1.40 (3H) d (5.2)	C-9, C-8

[1] The chemical shifts are in δ values (ppm). [2] 2D ^1H, ^1H (COSY) ^{13}C, and ^1H (HSQC) NMR experiments delineated the correlations of all the protons and the corresponding carbons. Numbering is according to that in Figure 1.

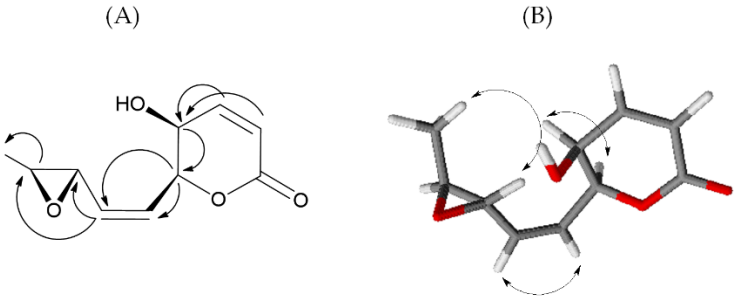

Figure 2. Significant HMBC (**A**) and NOESY (**B**) correlations of **1**.

The *Z* configuration of the double bond at C-7-C-8 was assigned on the basis of the typical coupling constant (11.7 Hz) [27]. The relative configuration of compound **1** was assigned on the basis of the NOE effects observed in the NOESY spectrum (Figure S6). The NOE effect of H-7 with H-8 confirmed the *Z* configuration of the chain double bond. The NOE effect of H-5 with H-6 and the coupling constant of 3.3 Hz indicated a *cis* configuration of the hydroxyl group and the side chain of the dihydropyrone ring. The absence of

the NOE effect between the H-9 and the H-10 and the NOE effect of the H-11 methyl with the H-9 indicated a *trans* configuration of the oxirane ring (Figure 2). All spectral data allowed to the determine the structure and relative stereostructure of compound **1** as (5*S*,6S,7*Z*,9*S*,10*S*)-5-hydroxy-6-(2-(3-methyloxiran-2-yl)vinyl)-5,6-dihydro-2H-pyran-2-one, named diplopyrone C.

2.2. Oral Toxicity of Sphaeropsidin A on Acyrthosiphon pisum

Sphaeropsidin A showed an oral lethal activity on aphids at all the doses tested, and the resulting survival rate was significantly lower compared to the control (log-rank test: $\chi^2 = 561.1$, $p < 0.0001$, dF = 4). The highest doses induced mortality starting from day 2. The mortality increased over time in a dose-dependent manner, and no aphids survived after 7 days of administration (Figure 3).

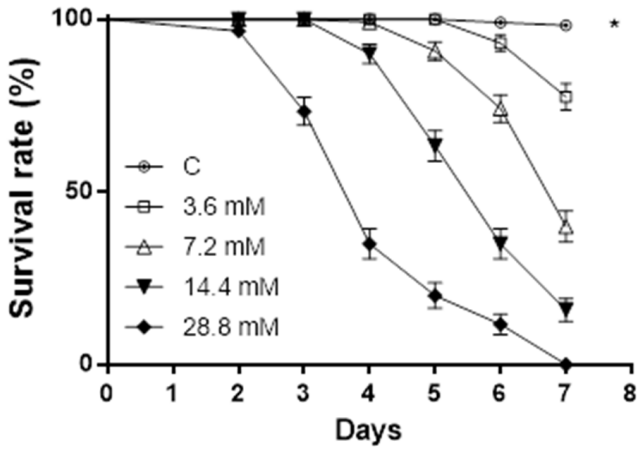

Figure 3. Sphaeropsidin A oral toxicity on *A. pisum*. Aphids' survival rate was negatively affected by sphaeropsidin A oral administration. Asterisk indicates a statistical difference to log-rank (Mantel–Cox) test ($p < 0.0001$).

The lethal concentrations of sphaeropsidin A, resulting in 10%, 50%, and 90% mortality of the pea aphids (LC_{10}, LC_{50}, and LC_{90}, respectively) and 95% confidence intervals, were determined on day 6 and showed that LC_{10} (95% CI) is 4.5 mM (4.12–4.93), LC_{50} (95% CI) is 9.64 mM (9.23–10.06), and LC_{90} is 20.43 mM (18.81–21.57). The lethal activity of sphaeropsidin A on day 6 is shown in Figure 4.

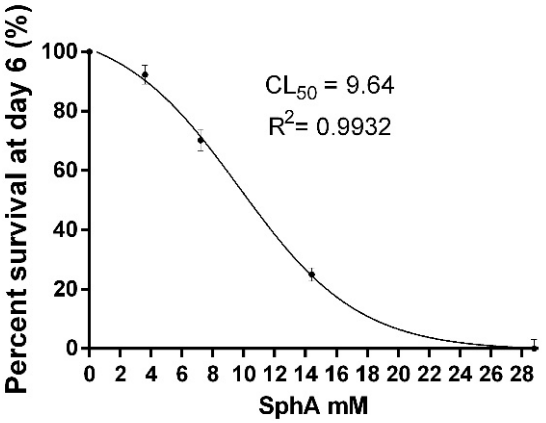

Figure 4. The dose-dependent survival rate of aphids exposed to sphaeropsidin A. Values are reported as mean ± standard deviation (SD) of three replicates in four separate experiments and expressed as a percentage of the control aphids.

3. Discussion

Secondary metabolites are often used by microbes to enable unique trophic lifestyles, overcome competition with other microbes, or cope with environmental biotic and abiotic stress [28–31]. Hence, in this study, the production of secondary metabolites from a strain of *D. corticola* was examined with reference to its possible ecological role.

The new 5,6-dihydropyran-2-one, namely diplopyrone C, and several known metabolites were isolated and identified from the fungal strain under examination. This metabolite is closely related to diplopyrone B, which was recently isolated from the same fungal species associated with *Q. suber* in Sardinia (Italy) and characterized as the 5-hydroxy-6-(penta-1,3-dienyl)-5,6-dihydro-pyran-2-one [7]. The 6-substituted derivatives of 5,6-dihydropyran-2-ones (or 5,6-dihydro-α-pyrones) are polyketides produced by several microorganisms and plants. Many of these products are biologically active, exhibiting phytotoxicity, cytotoxicity against tumor cells, and antimicrobial activity [32,33].

Moreover, accurate screening of the existing literature showed that a number of metabolites identified in this study were previously reported as products of *Diplodia* species. In particular, sphaeropsidins A–C (**2**–**4**), (3*R*,4*R*)- and (3*S*,4*R*)-hydroxymelleins (**6**,**7**), sapinofuranone B (**8**), and diplobifuranylone B (**10**) were already identified from cultures of *D. coriticola* (Table 2).

Table 2. Secondary metabolites identified in this work and previously reported as products of *Diplodia* spp.

Code	Name	Source	Ref.
2	Sphaeropsidin A	*D. corticola*, *D. sapinea*, *D. africana*, *D. quercivora*	[3,10,34–37]
3	Sphaeropsidin B	*D. corticola*, *D. sapinea*	[10,34,37]
4	Sphaeropsidin C	*D. corticola*, *D. sapinea*, *D. quercivora*	[10,34,36,37]
5	(*R*)-mellein	*D. africana*, *D. fraxini*, *D. mutila*, *D. seriata*, *D. sapinea*	[3,4,21,38]
6	(3*R*,4*R*)-4-hydroxymellein	*D. corticola*, *D. africana*, *D. sapinea*	[3,10,21]
7	(3*S*,4*R*)-4-hydroxymellein	*D. corticola*, *D. africana*, *D. sapinea*	[3,10,21]
8	Sapinofuranone B	*D. corticola*	[10]
9	Pinofuranoxin A	*D. sapinea*	[23]
10	Diplobifuranylone B	*D. corticola*	[10]
11	Tyrosol	*D. fraxini*, *D. mutila*	[4,38]

(*R*)-Mellein, (3*R*,4*R*)- and (3*S*,4*R*)-hydroxymelleins (**5**–**7**) belong to the group of 3,4-dihydroisocoumarins, also known as melleins, which are lactonic natural products [39] commonly produced in vitro by botryosphaeraceous fungi, such as *Lasiodiplodia* spp., *Macrophomina* spp., and *Neofusicoccum* spp. [40–42]. Furthermore, (*R*)-mellein is considered a vivotoxin since it was also isolated from plants inoculated with the mycelium of *Neofusicoccum parvum* [43].

The high production rate of sphaeropsidin A suggests its possible involvement in the dynamic interaction with the host plant; in this regard, the anti-insectan properties deserve particular attention in regard to the hypothesis that this compound is also released in vivo. In fact, a widespread anti-insectan effect is corroborated by results of previous studies showing fagodeterrent and larvicidal activity against the mosquito *Aedes aegypti* (Diptera, Culicidae) [15] and oral toxic activity against larvae of the chewing model insect *Spodoptera littoralis* (Lepidoptera, Noctuidae) [18].

Here we have demonstrated the possible effects of sphaeropsidin A on sucking insects based on a dose-dependent toxic oral activity against the model phloem sucking insect,

A. pisum. Hence, if confirmed in planta, production of this secondary metabolite may reduce the impact of herbivorous insects, representing an indication of defensive mutualism established during the development of this fungus as an endophyte or latent pathogen.

Moreover, the oral toxic activity shown by sphaeropsidin A on pea aphids stimulates further investigation of its mode of action from the perspective of its possible application as a new pesticide that meets the growing demand for alternative products with low environmental impact.

4. Materials and Methods

4.1. General Experimental Procedures

The optical rotations of pure metabolites were measured in $CHCl_3$ or MeOH on a Jasco P-1010 digital polarimeter (Tokyo, Japan). FT–IR spectra were recorded in modality ATR (attenuated total reflectance) with model Nicolet 5700 by Thermo Electric Corporation (Waltham, MA, USA). The measuring cell consisted of a mono crystal of zinc selenide. The blank was recorded using air as reference. UV spectra were recorded in CH_3CN by Cary model 5000 Spectrophotometer by Varian C. (Palo Alto, CA, USA). ^1H and ^{13}C NMR spectra were recorded on a Bruker AMX instrument at 400 and 100 MHz, respectively, in $CDCl_3$. The same solvents were used as internal standards. COSY-45, HSQC, HMBC, and NOESY were performed using standard Bruker microprograms. TLC was performed on silica gel (Kieselgel 60, F_{254}, 0.25 mm, Merck, Darmstadt, Germany) or reverse-phase plates (Whatman, KC18 F_{254}, 0.20 mm). The spots were visualized by exposure to UV radiation (253 nm) or by spraying first with 10% H_2SO_4 in methanol followed by heating at 110 °C for 10 min. Chromatography was performed on silica gel column (Merck, Kieselgel 60, 0.063–0.200 mm). HRESI-TOF mass spectra were measured on an Agilent Technologies ESI-TOF 6230DA instrument in the positive ion mode (Milan, Italy).

4.2. Fungal Strain and Cultures Production

Diplodia corticola strain (B305) employed in this study was previously isolated from *Q. suber* trees showing canker and dieback symptoms in Algeria. The strain was identified and characterized as a pathogen in a previous work [11] based on the integration of morphological features and phylogenetic analysis of the combined ITS and *tef1-α* sequence data. The nucleotide sequences of *D. corticola* are available in GenBank database under accession numbers MT015626 and MT066136.

Liquid cultures of the strain were prepared in Czapek-Dox broth (Oxoid, Thermo Scientific, Waltham, MA, USA) amended with 2% cornmeal in 500 mL Erlenmeyer flasks containing 250 mL of the substrate [44] and grown in a stationary phase in the dark at 25 °C for 30 days.

4.3. Extraction and Purification Processes of Metabolites 1–11

The culture broth and mycelia were homogenized in a mixer with 350 mL of MeOH (1% NaCl). Then, the suspension was centrifuged for 40 min at 7000 rpm and 10 °C. The pellet was resuspended in 150 mL of a mixture of H_2O:MeOH (45:55 *v*/*v*, 1% NaCl) and submitted to a second homogenization followed by centrifugation. Supernatants were collected, and MeOH was evaporated under reduced pressure to obtain an aqueous solution for the subsequent extraction (3 times) with ethyl acetate at native pH (=6.0). The organic phases were combined, dried with anhydrous Na_2SO_4, and evaporated under reduced pressure, yielding crude extract as brown oil (156.7 mg). The organic extract was purified by column chromatography (CC) on silica gel (40 cm × 1.5 cm i.d.) eluted with $CHCl_3$/*i*-PrOH (95:5, *v*/*v*), originating 8 homogeneous fractions (A 3.7 mg, B 6.7 mg, C 43.3 mg, D 15.2 mg, E 9.1 mg, F 15.9 mg, G 2.3 mg, H 32.4 mg), the last of which was collected by eluting with methanol. Fraction C was purified by TLC on silica gel eluted with *n*-hexane/EtOAc (6:4, *v*/*v*) to give **2** (35.4 mg, white crystalline solid, R_f 0.59), **4** (2.0 mg white solid R_f 0.50), and **5** (1.2 mg yellowing oil, R_f 0.79). Fraction D was purified by TLC on silica gel eluted with *n*-hexane/EtOAc (1:1, *v*/*v*) to give **3** (5.2 mg, white crystalline solid, R_f 0.76), and a mixture

of **6** and **7**, which was separated by reversed-phase TLC using H_2O-EtOH (1:1, *v/v*) (2.5 and 3.1 mg, white amorphous solids, R_f 0.54 and 0.58, respectively), **9** (2.1 mg, homogeneous oil, R_f 0.48), and **8** (1.3 mg, yellowing oil, R_f 0.45). Fraction F was purified by TLC on silica gel eluted with $CHCl_3$/*i*-PrOH (95:5, *v/v*), giving **10** (7.8 mg as colorless oil, R_f 0.42), **11** (1.5 mg as white amorphous solid, R_f 0.39), and **1** (5.4 mg, yellowing amorphous solid, R_f 0.37).

Diplopyrone C (**1**): yellowing amorphous solid; $[\alpha]^{25}_D$ +36 (c 0.24); IR ν_{max}: 3433, 1720, 1629, 1373, 1254, 1221 cm^{-1}; UV λ_{max} nm (log ε) 203 (2.87); ^1H and ^{13}C NMR spectra: see Table 1; HR-ESIMS (+) *m/z*: 235.0395 [calcd. for $C_{10}H_{12}KO_4$ 235.0373, M + K]$^+$, 219.1860 [calcd. for $C_{10}H_{12}NaO_4$ 219.1896, M + Na]$^+$, 179.0721 [calcd. for $C_{10}H_{11}O_3$ 179.0708 M-OH]$^+$.

4.4. Insects Rearing and Oral Toxicity Bioassay

Acyrthosiphon pisum was reared on potted broad bean plants (*Vicia faba*) at 20 ± 1 °C, 75 ± 5% RH, and under a 16:8 h light:dark photoperiod, starting with insects originally collected from alfalfa plants in Eboli, southern Italy. In order to synchronize the aphid population, parthenogenetic adult females were placed on plants for 6 h, resulting in neonate nymphs with an age of 0–6 h that were used throughout the experiments.

The oral toxicity of sphaeropsidin A (**2**) on *A. pisum* was investigated using a standard basal diet previously developed for assays of test compounds [45]. The feeding system for the pea aphid was realized as described in [45] with minor modifications. Each experimental unit was a feeding system with 10 aphids; four replications per treatment were realized, each replicate consisting of three experimental units per treatment. A total of 120 aphids per treatment were used. In each feeding system, 300 µL of artificial diet containing **1** 3.6 mM, 7.2 mM, 14.4 mM, and 28.8 mM was dispensed; negative control was realized using the artificial diet only. The experiment was carried out under the rearing conditions described above. Briefly, on day 0, neonate nymphs were transferred to a freshly prepared diet sachet feeding apparatus. Mortality was recorded daily for one week, and dead nymphs were removed. The artificial diet was replaced every two days. The lethal concentrations of **1** resulting in 10%, 50%, and 90% aphid mortality (defined as LC_{10}, LC_{50}, and LC_{90}) and the corresponding 95% confidence intervals were determined.

4.5. Statistical Analysis

Aphid survival curves were compared using Kaplan–Meier and log-rank analysis. The results obtained were analyzed using non-linear sigmoid curve fitting, and the activity of each treatment was evaluated on day 6 on the basis of dose–response concentrations; the goodness of fit to the curve model was evaluated on the basis of R^2 values. Data were analyzed using Prism 6 (GraphPad Software Inc. version 6.0b, San Diego, CA, USA).

Supplementary Materials: The following supporting information can be downloaded at: https://www.mdpi.com/article/10.3390/molecules27072327/s1, Figure S1: ^1H NMR spectrum of diplopyrone C (**1**) recorded in $CDCl_3$ at 400 MHz; Figure S2: ^{13}C NMR spectrum of diplopyrone (**1**) recorded in $CDCl_3$ at 100 MHz; Figure S3: ^1H,^1H COSY spectrum of diplopyrone C (**1**) recorded in $CDCl_3$ at 400 MHz; Figure S4: HSQC spectrum of diplopyrone C (**1**) recorded in $CDCl_3$ at 400 MHz; Figure S5: HMBC spectrum of diplopyrone C (**1**) recorded in $CDCl_3$ at 400 MHz; Figure S6: NOESY spectrum of diplopyrone C (1) recorded in $CDCl_3$ at 400 MHz; Figure S7: IR spectrum of diplopyrone C (**1**); Figure S8: HRESI MS spectrum of diplopyrone C (**1**) recorded in positive mode; Figure S9: ^1H NMR spectrum of sphaeropsidin A (**2**) recorded in $CDCl_3$ at 400 MHz; Figure S10: ^1H NMR spectrum of sphaeropsidin B (**3**) recorded in $CDCl_3$ at 400 MHz; Figure S11: ^1H NMR spectrum of sphaeropsidin C (**4**) recorded in $CDCl_3$ at 400 MHz; Figure S12: ^1H NMR spectrum of (3*R*)-mellein (**5**) recorded at 400 MHz in CDCl3; Figure S13: ^1H NMR spectrum of (3*R*,4*R*)-4-hydroxymellein (**6**) recorded at 400 MHz in $CDCl_3$; Figure S14: ^1H NMR spectrum of (3*R*,4*S*)-4-hydroxymellein (**7**) recorded at 400 MHz in $CDCl_3$; Figure S15: ^1H NMR spectrum sapinofuranone B (**8**) recorded at 400 MHz in $CDCl_3$; Figure S16: ^1H NMR spectrum of pinofuranoxin A (**9**) recorded at 400 MHz in $CDCl_3$; Figure S17: ^1H NMR spectrum of diplobifuranylone B (**10**) recorded at 400 MHz in $CDCl_3$; Figure S18: ^1H NMR spectrum tyrosol (**11**) recorded at 400 MHz in $CDCl_3$.

Author Contributions: Conceptualization, I.D.L., A.A. and R.N.; investigation, G.V., E.R., I.D.L., M.D., M.M.S., A.B.-T. and A.E.M.; data curation, I.D.L., M.M.S., F.S., A.A. and M.D.; supervision, I.D.L., A.B. and A.A.; writing—review and editing, R.N., M.M.S., I.D.L. and A.A. All authors have read and agreed to the published version of the manuscript.

Funding: This research received no external funding.

Data Availability Statement: The data that support the findings of this study are available from the corresponding author upon reasonable request.

Conflicts of Interest: The authors declare no conflict of interest.

References

1. Phillips, A.J.L.; Lopes, J.; Abdollahzadeh, J.; Bobev, S.; Alves, A. Resolving the *Diplodia* complex on apple and other *Rosaceae* hosts. *Pers. Mol. Phylogeny Evol. Fungi* **2012**, *29*, 29–38. [CrossRef] [PubMed]
2. Slippers, B.; Wingfield, M.J. Botryosphaeriaceae as endophytes and latent pathogens of woody plants: Diversity, ecology and impact. *Fungal Biol. Rev.* **2007**, *21*, 90–106. [CrossRef]
3. Evidente, A.; Masi, M.; Linaldeddu, B.T.; Franceschini, A.; Scanu, B.; Cimmino, A.; Andolfi, A.; Motta, A.; Maddau, L. Afritoxinones A and B, dihydrofuropyran-2-ones produced by *Diplodia africana* the causal agent of branch dieback on *Juniperus phoenicea*. *Phytochemistry* **2012**, *77*, 245–250. [CrossRef] [PubMed]
4. Reveglia, P.; Savocchia, S.; Billones-Baaijens, R.; Masi, M.; Cimmino, A.; Evidente, A. Phytotoxic metabolites by nine species of Botryosphaeriaceae involved in grapevine dieback in Australia and identification of those produced by *Diplodia mutila*, *Diplodia seriata*, *Neofusicoccum australe* and *Neofusicoccum luteum*. *Nat. Prod. Res.* **2019**, *33*, 2223–2229. [CrossRef]
5. Liu, X.Y.; Wang, X.L.; Shen, T.; Ren, D.M.; Lou, H.X.; Wang, X.N. Two new triterpenoids from the fungus *Diplodia cupressi*. *Nat. Prod. Res.* **2020**, *34*, 2179–2185. [CrossRef]
6. Tuzi, A.; Andolfi, A.; Maddau, L.; Masi, M.; Evidente, A. Structure and stereochemical assignment of spheropsidone, a phytotoxin from *Diplodia cupressi*. *J. Struct. Chem.* **2012**, *53*, 786–792. [CrossRef]
7. Masi, M.; Maddau, L.; Linaldeddu, B.T.; Cimmino, A.; D'Amico, W.; Scanu, B.; Evidente, M.; Tuzi, A.; Evidente, A. Bioactive secondary metabolites produced by the oak pathogen *Diplodia corticola*. *J. Agric. Food Chem.* **2016**, *64*, 217–225. [CrossRef]
8. Di Lecce, R.; Masi, M.; Linaldeddu, B.T.; Pescitelli, G.; Maddau, L.; Evidente, A. Bioactive secondary metabolites produced by the emerging pathogen *Diplodia olivarum*. *Phytopathol. Mediterr.* **2021**, *60*, 129–138. [CrossRef]
9. Cimmino, A.; Maddau, L.; Masi, M.; Evidente, M.; Linaldeddu, B.T.; Evidente, A. Further secondary metabolites produced by *Diplodia corticola*, a fungal pathogen involved in cork oak decline. *Tetrahedron* **2016**, *72*, 6788–6793. [CrossRef]
10. Evidente, A.; Andolfi, A.; Fiore, M.; Spanu, E.; Franceschini, A.; Maddau, L. Diplobifuranylones A and B, 5′-monosubstituted tetrahydro-2H-bifuranyl-5-ones produced by *Diplodia corticola*, a fungus pathogen of cork oak. *J. Nat. Prod.* **2006**, *69*, 671–674. [CrossRef]
11. Mahamedi, A.E.; Phillips, A.J.L.; Lopes, A.; Djellid, Y.; Arkam, M.; Eichmeier, A.; Zitouni, A.; Alves, A.; Berraf-Tebbal, A. Diversity, distribution and host association of Botryosphaeriaceae species causing oak decline across different forest ecosystems in Algeria. *Eur. J. Plant Pathol.* **2020**, *158*, 745–765. [CrossRef]
12. Félix, C.; Pinto, G.; Amaral, J.; Fernandes, I.; Alves, A.; Esteves, A.C. Strain-related pathogenicity in *Diplodia corticola*. *For. Pathol.* **2017**, *47*, e12366. [CrossRef]
13. Linaldeddu, B.T.; Maddau, L.; Franceschini, A. First report of *Diplodia corticola* causing canker and dieback of *Quercus ilex*, *Q. petraea*, and *Q. suber* in Corsica (France). *Plant Dis.* **2017**, *101*, 256. [CrossRef]
14. Masi, M.; Evidente, A. Sphaeropsidin A: A pimarane diterpene with interesting biological activities and promising practical applications. *ChemBioChem* **2021**, *22*, 3263–3269. [CrossRef] [PubMed]
15. Cimmino, A.; Andolfi, A.; Avolio, F.; Ali, A.; Tabanca, N.; Khan, I.A.; Evidente, A. Cyclopaldic acid, seiridin, and sphaeropsidin A as fungal phytotoxins, and larvicidal and biting deterrents against *Aedes aegypti* (Diptera: Culicidae): Structure-activity relationships. *Chem. Biodivers.* **2013**, *10*, 1239. [CrossRef]
16. Evidente, A.; Venturi, V.; Masi, M.; Degrassi, G.; Cimmino, A.; Maddau, L.; Andolfi, A. In vitro antibacterial activity of sphaeropsidins and chemical derivatives toward *Xanthomonas oryzae* pv. *oryzae*, the causal agent of rice bacterial blight. *J. Nat. Prod.* **2011**, *74*, 2520–2525. [CrossRef]
17. Padhi, S.; Masi, M.; Cimmino, A.; Tuzi, A.; Jena, S.; Tayung, K.; Evidente, A. Funiculosone, a substituted dihydroxanthene-1,9-dione with two of its analogues produced by an endolichenic fungus *Talaromyces funiculosus* and their antimicrobial activity. *Phytochemistry* **2019**, *157*, 175–183. [CrossRef]
18. Di Lelio, I.; Salvatore, M.M.; DellaGreca, M.; Mahamedi, A.E.; Alves, A.; Berraf-Tebbal, A.; Volpe, G.; Russo, E.; Becchimanzi, A.; Nicoletti, R. Defensive mutualism of endophytic fungi: Effects of sphaeropsidin A against a model lepidopteran pest. *Proceeding Pap.* **2022**. [CrossRef]
19. Ellestad, G.A.; Kunstmann, M.P.; Mirando, P.; Morton, G.O. Structures of fungal diterpene antibiotics LL-S491/3 and -y. *J. Am. Chem. Soc.* **1972**, *236*, 6206–6208. [CrossRef]

20. Evidente, A.; Sparapano, L.; Fierro, O.; Bruno, G.; Giordano, F.; Motta, A. Sphaeropsidins B and C, phytotoxic pimarane diterpenes from *Sphaeropsis sapinea* f. Sp. *Cupressi Diplodia Mutila*. *Phytochemistry* **1997**, *45*, 705–713. [CrossRef]
21. Cabras, A.; Mannoni, M.A.; Serra, S.; Andolfi, A.; Fiore, M.; Evidente, A. Occurrence, isolation and biological activity of phytotoxic metabolites produced in vitro by *Sphaeropsis sapinea*, pathogenic fungus of *Pinus radiata*. *Eur. J. Plant Pathol.* **2006**, *115*, 187–193. [CrossRef]
22. Evidente, A.; Sparapano, L.; Fierro, O.; Bruno, G.; Motta, A. Sapinofuranones A and B, two new 2(3H)-dihydrofuranones produced by *Sphaeropsis sapinea*, a common pathogen of conifers. *J. Nat. Prod.* **1999**, *62*, 253–256. [CrossRef] [PubMed]
23. Masi, M.; Di Lecce, R.; Marsico, G.; Linaldeddu, B.T.; Maddau, L.; Superchi, S.; Evidente, A. Pinofuranoxins A and B, bioactive trisubstituted furanones produced by the invasive pathogen *Diplodia sapinea*. *J. Nat. Prod.* **2021**, *84*, 2600–2605. [CrossRef] [PubMed]
24. Cheng, X.; Quintanilla, C.D.; Zhang, L. Total synthesis and structure revision of diplobifuranylone B. *J. Org. Chem.* **2019**, *84*, 11054–11060. [CrossRef] [PubMed]
25. Félix, C.; Salvatore, M.M.; DellaGreca, M.; Ferreira, V.; Duarte, A.S.; Salvatore, F.; Naviglio, D.; Gallo, M.; Alves, A.; Esteves, A.C.; et al. Secondary metabolites produced by grapevine strains of *Lasiodiplodia theobromae* grown at two different temperatures. *Mycologia* **2019**, *111*, 466–476. [CrossRef]
26. D'Annibale, A.; Ciaralli, L.; Bassetti, M.; Pasquini, C. Synthesis of alkyl-substituted six-membered lactones through ring-closing metathesis of homoallyl acrylates. An easy route to pyran-2-ones, constituents of tobacco flavor. *J. Org. Chem.* **2007**, *72*, 6067–6074. [CrossRef]
27. Badertscher, M.; Bühlmann, P.; Pretsch, E. *Structure Determination of Organic Compounds*; Springer: Berlin/Heidelberg, Germany, 2009; ISBN 978-3-540-93809-5.
28. Salvatore, M.M.; Andolfi, A.; Nicoletti, R. The thin line between pathogenicity and endophytism: The case of *Lasiodiplodia theobromae*. *Agriculture* **2020**, *10*, 488. [CrossRef]
29. Félix, C.; Salvatore, M.M.; Dellagreca, M.; Meneses, R.; Duarte, A.S.; Salvatore, F.; Naviglio, D.; Gallo, M.; Jorrín-Novo, J.V.; Alves, A.; et al. Production of toxic metabolites by two strains of *Lasiodiplodia theobromae*, isolated from a coconut tree and a human patient. *Mycologia* **2018**, *110*, 642–653. [CrossRef]
30. Shabuer, G.; Ishida, K.; Pidot, S.J.; Roth, M.; Dahse, H.M.; Hertweck, C. Plant pathogenic anaerobic bacteria use aromatic polyketides to access aerobic territory. *Science* **2015**, *350*, 670–674. [CrossRef]
31. Salvatore, M.M.; Andolfi, A. Phytopathogenic fungi and toxicity. *Toxins* **2021**, *13*, 689. [CrossRef]
32. Davies-Coleman, M.T.; Rivett, D.E.A. Naturally occurring 6-substituted 5, 6-dihydro-α-pyrones. In *Fortschritte der Chemie Organischer Naturstoffe/Progress in the Chemistry of Organic Natural Products*; Springer: Vienna, Austria, 1998; pp. 181–209, ISBN 978-3-7091-9004-3.
33. Dickinson, J.M. Microbial pyran-2-ones and dihydropyran-2-ones. *Nat. Prod. Rep.* **1991**, *10*, 71–98. [CrossRef] [PubMed]
34. Sparapano, L.; Bruno, G.; Fierro, O.; Evidente, A. Studies on structure-activity relationship of sphaeropsidins A-F, phytotoxins produced by *Sphaeropsis sapinea* f. sp. *cupressi*. *Phytochemistry* **2004**, *65*, 189–198. [CrossRef] [PubMed]
35. Evidente, A.; Sparapano, L.; Motta, A.; Giordano, F.; Fierro, O.; Frisullo, S. A phytotoxic pimarane diterpene of *Sphaeropsis sapinea* f. sp. *cupressi*, the pathogen of a canker disease of cypress. *Phytochemistry* **1996**, *42*, 1541–1546. [CrossRef]
36. Andolfi, A.; Maddau, L.; Basso, S.; Linaldeddu, B.T.; Cimmino, A.; Scanu, B.; Deidda, A.; Tuzi, A.; Evidente, A. Diplopimarane, a 20-nor-ent-pimarane produced by the oak pathogen *Diplodia quercivora*. *J. Nat. Prod.* **2014**, *77*, 2352–2360. [CrossRef]
37. Evidente, A.; Sparapano, L.; Andolfi, A.; Bruno, G.; Giordano, F.; Motta, A. Chlorosphaeropsidone and epichlorosphaeropsidone, two new chlorinated dimedone methyl ethers isolated from liquid cultures of *Sphaeropsis sapinea* f. sp. *cupressi*. *Phytopathol. Mediterr.* **2000**, *39*, 299–330.
38. Cimmino, A.; Maddau, L.; Masi, M.; Linaldeddu, B.T.; Pescitelli, G.; Evidente, A. Fraxitoxin, a new isochromanone isolated from *Diplodia fraxini*. *Chem. Biodivers.* **2017**, *14*, e1700325. [CrossRef]
39. Saeed, A. Isocoumarins, miraculous natural products blessed with diverse pharmacological activities. *Eur. J. Med. Chem.* **2016**, *116*, 290–317. [CrossRef]
40. Salvatore, M.M.; Alves, A.; Andolfi, A. Secondary metabolites produced by *Neofusicoccum* species associated with plants: A review. *Agriculture* **2021**, *11*, 149. [CrossRef]
41. Salvatore, M.M.; Alves, A.; Andolfi, A. Secondary metabolites of *Lasiodiplodia theobromae*: Distribution, chemical diversity, bioactivity, and implications of their occurrence. *Toxins* **2020**, *12*, 457. [CrossRef]
42. Salvatore, M.M.; Félix, C.; Lima, F.; Ferreira, V.; Naviglio, D.; Salvatore, F.; Duarte, A.S.; Alves, A.; Andolfi, A.; Esteves, A.C. Secondary metabolites produced by *Macrophomina phaseolina* isolated from *Eucalyptus globulus*. *Agriculture* **2020**, *10*, 72. [CrossRef]
43. Abou-Mansour, E.; Débieux, J.L.; Ramírez-Suero, M.; Bénard-Gellon, M.; Magnin-Robert, M.; Spagnolo, A.; Chong, J.; Farine, S.; Bertsch, C.; L'Haridon, F.; et al. Phytotoxic metabolites from *Neofusicoccum parvum*, a pathogen of Botryosphaeria dieback of grapevine. *Phytochemistry* **2015**, *115*, 207–215. [CrossRef] [PubMed]
44. Salvatore, M.M.; DellaGreca, M.; Nicoletti, R.; Salvatore, F.; Tuzi, A.; De Tommaso, G.; Alves, A.; Mahamedi, A.E.; Berraf-Tebbal, A.; Andolfi, A. Mitidjospirone, a new spirodioxynaphthalene and GC-MS screening of secondary metabolites produced by strains of *Lasiodiplodia mitidjana* associated to *Citrus sinensis* dieback. *Nat. Prod. Res.* **2021**, 1–10. [CrossRef] [PubMed]
45. Sadeghi, A.; Van Damme, E.J.M.; Smagghe, G. Evaluation of the susceptibility of the pea aphid, *Acyrthosiphon pisum*, to a selection of novel biorational insecticides using an artificial diet. *J. Insect Sci.* **2009**, *9*, 65. [CrossRef] [PubMed]

chemistry proceedings

MDPI

Proceeding Paper

Defensive Mutualism of Endophytic Fungi: Effects of Sphaeropsidin A against a Model Lepidopteran Pest †

Ilaria Di Lelio [1,*], Maria Michela Salvatore [2,3], Marina Della Greca [2], Alla Eddine Mahamedi [4], Artur Alves [5], Akila Berraf-Tebbal [6], Gennaro Volpe [1], Elia Russo [1], Andrea Becchimanzi [1], Rosario Nicoletti [1,7,*] and Anna Andolfi [2,8,*]

1 Department of Agricultural Sciences, University of Naples Federico II, 80055 Portici, Italy; gennaro.volpe2@unina.it (G.V.); elia.russo@unina.it (E.R.); andrea.becchimanzi@unina.it (A.B.)
2 Department of Chemical Sciences, University of Naples Federico II, 80126 Naples, Italy; mariamichela.salvatore@unina.it (M.M.S.); dellagre@unina.it (M.D.G.)
3 Institute for Sustainable Plant Protection, National Research Council, 80055 Portici, Italy
4 Département de Biologie, Faculté des Sciences de la Nature et de la Vie et Sciences de la Terre, Université de Ghardaia, Ghardaïa 47000, Algeria; aladin1342@yahoo.com
5 CESAM Centre for Environmental and Marine Studies, Department of Biology, University of Aveiro, 3810-193 Aveiro, Portugal; artur.alves@ua.pt
6 Mendeleum-Institute of Genetics, Faculty of Horticulture, Mendel University in Brno, 69144 Lednice, Czech Republic; berraf.a@hotmail.fr
7 Council for Agricultural Research and Economics, Research Center for Olive, Fruit and Citrus Crops, 81100 Caserta, Italy
8 BAT Center-Interuniversity Center for Studies on Bioinspired Agro-Environmental Technology, University of Naples Federico II, 80055 Portici, Italy
* Correspondence: ilaria.dilelio@unina.it (I.D.L.); rosario.nicoletti@crea.gov.it (R.N.); andolfi@unina.it (A.A.)
† Presented at the 1st International Online Conference on Agriculture—Advances in Agricultural Science and Technology (IOCAG2022), 10–25 February 2022; Available online: https://iocag2022.sciforum.net/.

Citation: Di Lelio, I.; Salvatore, M.M.; Della Greca, M.; Mahamedi, A.E.; Alves, A.; Berraf-Tebbal, A.; Volpe, G.; Russo, E.; Becchimanzi, A.; Nicoletti, R.; et al. Defensive Mutualism of Endophytic Fungi: Effects of Sphaeropsidin A against a Model Lepidopteran Pest. *Chem. Proc.* **2022**, *10*, 42. https://doi.org/10.3390/IOCAG2022-12216

Academic Editor: Bin Gao

Published: 10 February 2022

Abstract: Sphaeropsidin A (SphA) is a pimarane diterpene produced by several fungi associated with plants. Following previous evidence of insecticidal properties of SphA, we investigated its contact and oral toxicity against the model chewing lepidopteran *Spodoptera littoralis*. The compound showed no lethal effect when directly sprayed on larvae, while it produced an evident oral toxic effect, associated with sublethal effects. These results demonstrated that SphA might play a defensive role against lepidopteran insects in plants harboring the producing fungus, depending on the extent at which the endophytic strains are able to perform biosynthesis of this and eventually other bioactive metabolites in vivo.

Keywords: endophytic fungi; secondary metabolites; oral toxicity; lepidopteran pests

1. Introduction

Microbiome associated to plants is more and more regarded as a basic factor regulating their fitness, with reference to the effects of the mutual interactions among and between the holobiont constituents [1–3]. In most instances, symbiotic relationships between fungi and plants are considered with reference to the opposite categories of 'antagonists' and 'mutualists'; nevertheless, in the absence of indications enabling their circumstantial ascription to one or the other, endophytic fungi are often considered as neutral [4]. Studies on host genotype versus symbiotic lifestyle expression revealed that individual isolates of some fungal species could span the symbiotic continuum by expressing either mutualistic or pathogenic lifestyles in different host plants [5,6]. In recent years, the increasing evidence that many fungal pathogens are able to spread endophytically in unrelated plant species has introduced the perspective that they can actually shift between these categories depending on a series of ecological factors [7]. Indeed, recent papers have reported how fungi

colonizing plants can either directly or indirectly interfere with arthropod development [8], particularly, in the case of fungi producing bioactive secondary metabolites, this adaptation could be related to the toxic or phagodeterrent effects on pests possibly induced by these products [9,10].

The secondary metabolites are not essential for the primary metabolic processes but modulate the microorganism interactions with the surrounding environment [11], underline survival functions by modulating competition, parasitism or symbiosis [12]. These natural compounds also exhibit several biological activities, which may offer potential applications in medicine [13,14] and in agriculture as natural biopesticides [15,16].

Mainly described as a secondary metabolite of *Diplodia* species (Dothideomycetes, Botryosphaeriaceae) [17,18], sphaeropsidin A (SphA, Figure 1) is a pimarane diterpene which was previously reported with the number LL-S491β as a product of a strain of *Aspergillus chevalieri* [19]. However, it is produced also by other fungi which are associated as endophytes with plants [20–26]. This compound has displayed larvicidal and phagodeterrent effects against the yellow fever mosquito (*Aedes aegypti*) (Diptera: Culicidae) [27]. Here we have further explored the spectrum of activity of this compound focusing on a herbivore insect, the lepidopteran *Spodoptera littoralis.*

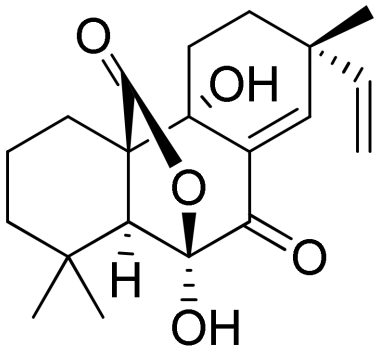

Figure 1. Structure of sphaeropsidin A (SphA).

2. Materials and Methods

2.1. Fungal Strain and Culturing

Diplodia corticola strain (B305) used in this study was previously isolated from *Quercus suber* trees showing canker and dieback symptoms in Algeria. The strain has been identified and characterized, using morphological characters and phylogenetic analysis of molecular data [28]. The nucleotide sequences of B305 are available in GenBank database, under accession numbers MT015626 and MT066136. Liquid cultures of the strain were prepared in Czapek-Dox broth (Oxoid) amended with 2% corn meal in 500 mL Erlenmayer flasks containing 250 mL of the substrate [29] and grown on stationary phase in the dark at 25 °C for 30 days.

2.2. Isolation of SphA from Crude Extract

The culture broth and mycelia were homogenised in a mixer with 350 mL of MeOH (1% NaCl). Subsequently, the suspension was centrifuged for 40 min at 7000 rpm and 10 °C. The pellet was resuspended in 150 mL of a mixture H_2O:MeOH (9:11 *v*/*v*, 1% NaCl) and submitted to a second homogenization followed by centrifugation. Supernatants were collected and MeOH was evaporated under reduced pressure obtaining an aqueous solution for the subsequent extraction (3 times) with ethyl acetate at native pH (=6.0). The organic phases were combined, dried with anhydrous Na_2SO_4 and evaporated under reduced pressure yielding crude extract as brown oil (156.7 mg). The organic extract was purified by column chromatography (CC) on silica gel (40 cm × 1.5 cm i.d.) eluted with $CHCl_3$/*i*-PrOH (19:1, *v*/*v*), originating 8 homogeneous fractions (A: 3.7 mg, B: 6.7 mg, C: 40.3 mg, D: 15.2 mg, E: 9.1 mg, F: 15.9 mg, G: 2.3 mg, H: 32.4 mg), the last of which was

collected by eluting with methanol. Fraction C was purified by TLC on silica gel eluted with *n*-hexane/EtOAc (6:4, *v*/*v*) to obtain SphA (35.4 mg, white crystalline solid, R_f 0.70, in the same chromatographic conditions).

2.3. General Experimental Procedures

Optical rotation of SphA measured in MeOH on a Jasco polarimeter (Tokyo, Japan). ^{1}H NMR spectrum was recorded at 400 MHz in deuterated chloroform ($CDCl_3$) on Bruker (Karlsruhe, Germany) spectrometer and the same solvent was used as internal standards. Thin Layer Chromatography were performed on silica gel plates (Kieselgel 60, F254, 0.25 Merck, Darmstadt, Germany). The spots were visualized by exposure to UV radiation (253 nm), or by spraying first with 10% H_2SO_4 in methanol followed by heating at 110 °C for 10 min. Chromatography was performed on silica gel column (Merck, Kieselgel 60, 0.063–0.200 mm).

2.4. Bioassays on Spodoptera littoralis

Larvae of *S. littoralis* (Lepidoptera, Noctuidae) were reared on artificial diet at 25 ± 1 °C and 70 ± 5% RH, with 16:8 h light-dark period as previously described [30] and used in two different bioassays hereafter described.

2.4.1. Topical Application

Newborn larvae were allowed to grow on the artificial diet until they molted in 2nd and in 5th instar. The 2nd instar larvae were collected and tested in 4 replicates of 25 larvae each (n = 100), while 5th instar larvae (n = 16) were singly treated as described below. The larvae were kept on sterile filter paper in Petri dishes and were directly sprayed with a water/ethanol 50% (*v*/*v*) solution containing SphA at the concentration of 0.4 μg/cm^2, using a fine perfume atomizer. Control larvae were identically treated with a water/ethanol 50% (*v*/*v*) solution (C_{EtOH}) and with water alone (C_{water}). After treatment, the experimental larvae were kept, with a piece of diet (1 cm^2), in 4-well plastic rearing trays (RT32W, Frontier Agricultural Sciences, Pitman, NJ, USA) closed by perforated plastic lids (RTCV4, Frontier Agricultural Sciences). Larval mortality was daily recorded for six days for 2nd instar larvae and until pupation for 5th instar larvae. All bioassays were carried out in duplicate, under the same rearing conditions reported above.

2.4.2. Oral Administration

Newly molted 5th instar larvae, obtained as described above, were anesthetized on ice and 2 μL of a water/ethanol 50% (*v*/*v*) solution, containing SphA at the concentration of 0.02 μg/μL, were poured into the foregut lumen of the larvae by means of a Hamilton Microliter syringe (1701RNR 10 ll, gauge 26 s, length 55 mm, needle 3). Control larvae were treated as described above. The treatment was repeated for 3 consecutive days, for a total amount of 0.12 μg/larvae of SphA. After treatment, larvae were singly isolated in the bioassay tray as described above. Larval development and larval mortality were recorded until pupation: larval weight, pupal weight and the adults' fertility were also recorded. The bioassays were carried out in duplicate, under the same rearing conditions reported above.

2.5. Statistical Analysis

Differences in larval weights were analyzed by One-Way ANOVA followed by the Tukey-Kramer Honestly Significant Difference (HSD) multiple range test ($p < 0.05$). Differences in survival rate were compared by using Kaplan-Meier and long-rank analysis. Data were analyzed using GraphPad Prism version 6.01 (GraphPad software; San Diego, CA, USA).

3. Results and Discussion

SphA (Figure 1) used in this study was obtained as white crystals (35.4 mg) from culture of *D. corticola* B305. In particular, the organic extract was subjected to a chromato-

graphic purification process as described in detail in Section 2.2. This compound was identified on the basis of spectroscopic (^{1}H NMR) and optical rotation data previously determined [13].

Topical application of SphA did not affect the survival rate of both 2nd (Log-Rank test: $p = 0.9437$) (Figure 2A) and 5th instar larvae (100% survival) (Figure 2B). These latter achieved the same weight before pupation (One Way ANOVA. $p = 0.7536$) (Figure 2C) and when they attained the pupal stage (One Way ANOVA: $p = 0.6772$) (Figure 2D).

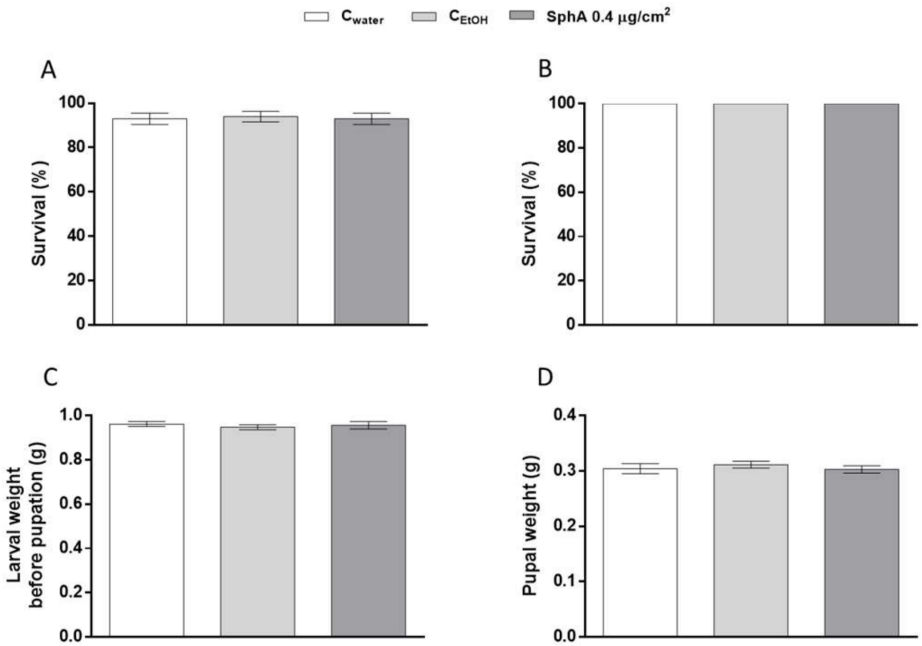

Figure 2. Effect of SphA topical application on *S. littoralis* larvae. SphA sprayed at the concentration of 0.4 µg/cm^2 on *S. littoralis* larvae did not affect the survival rate of 2nd instar (**A**) (Log-Rank test: $\chi^2 = 0.1159$, $p = 0.9437$, dF = 2) and 5th instar larvae (**B**), as well as the larval weight before pupation (**C**) (One Way ANOVA: $F_{(2, 93)} = 0.2838$, $p = 0.7536$) and the pupal weight (**D**) (One Way ANOVA: $F_{(2, 93)} = 0.3914$, $p = 0.6772$). Values are reported as means ± SE.

Experimental larvae orally treated with SphA showed a very strong reduction of the survival rate, which was significantly lower compared to controls (Log-Rank test: $p < 0.0001$) (Figure 3A). The larval mortality started from the last administration of SphA (day 3) and increased over the time until pupation (Figure 3A) with a recorded pupal survival rate of about 67% (for the controls 100%). A significant difference was recorded also for the larval weight before pupation (One Way ANOVA: $p < 0.0001$) (Figure 3B). SphA-treated larvae also showed a modified bodily appearance, and they were smaller than controls (Figure 4). Moreover, despite no alteration of the development time was observed, the pupal weight of the SphA-treated larvae resulted lower than controls (One Way ANOVA: $p < 0.0001$) (Figure 3C). All the adults obtained survived, without differences in their longevity, and no differences in their fecundity was observed (One Way ANOVA: $p = 0.8695$) (Figure 3D).

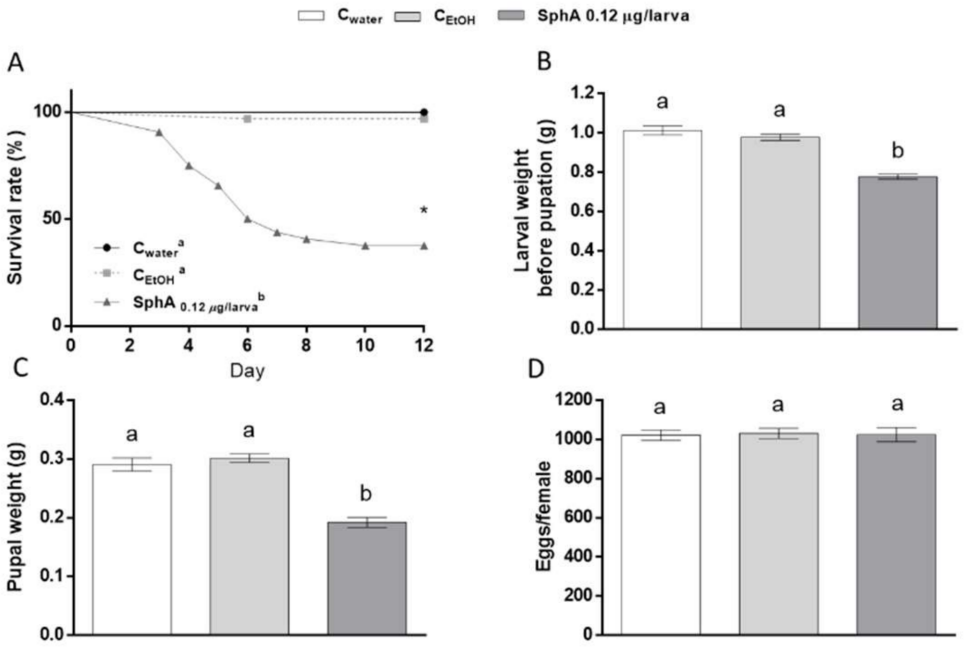

Figure 3. Effect of SphA oral administration 5th instar *S. littoralis* larvae. Orally treated larvae showed a strong reduction of the survival rate compared to controls, decreasing from day three to pupation. (**A**) (Log-Rank test: $\chi^2 = 53.66$, $p < 0.0001$, dF = 2). A significant reduction of the larval weight before pupation (**B**) (One Way ANOVA: $F_{(2, 71)} = 22.14$, $p < 0.0001$) and of the pupal weight (**C**) (One Way ANOVA: $F_{(2, 71)} = 21.41$, $p < 0.0001$) was also observed. No differences were observed in the fecundity of adults obtained from SphA-treated larvae compared with controls (**D**) (One Way ANOVA: $F_{(2, 21)} = 0.1408$, $p = 0.8695$ Asterisk indicate significant differences in the survival curves (Log-Rank test, $p < 0.0001$)). The values in the histograms are means ± SE. Different letters indicate a statistical difference (One Way ANOVA, $p < 0.0001$).

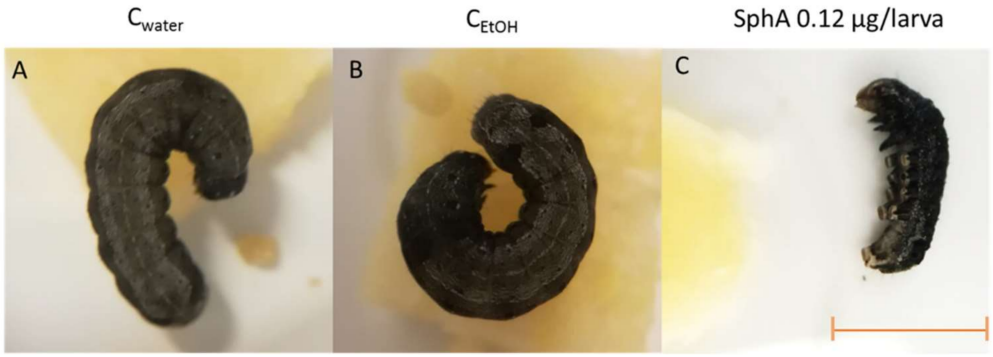

Figure 4. Alteration of *S. littoralis* larval development following oral administration of SphA. Larvae treated with SphA for three days showed a clear reduction of vitality and body size (**C**) No difference in the larval head capsule size indicates that all the larvae are in the same instar. compared to control larvae treated with water (**A**) or EtOH 50% (**B**). Scale bar, 0.5 cm.

Taken together our results indicate that although SphA has no lethal contact activity against *S. littoralis* larvae it showed clear lethal and sublethal effects after ingestion in 5th instar larvae, unequivocally indicating the oral direct toxicity of SphA. Further investigations are needed to better define the insecticidal role of SphA against chewing insects. In case its production by endophytic fungi is demonstrated in planta, SphA might be considered to play a role in the modulation of insect-plant interactions, which is worth of further research efforts aiming to elucidate its mechanism of action and functional role under in vivo conditions.

Author Contributions: A.A. (Anna Andolfi), R.N. and I.D.L. contributed to the study design; G.V., E.R., I.D.L., M.D.G., M.M.S., A.B.-T., A.A. (Artur Alves) and A.E.M., performed the experiments, I.D.L., M.M.S. and A.A. (Anna Andolfi) analyzed the results; I.D.L., A.B. and A.A. (Anna Andolfi) supervised the experiments; R.N., A.A. (Anna Andolfi) and I.D.L. wrote the manuscript. All authors contributed to revise the manuscript. All authors have read and agreed to the published version of the manuscript.

Funding: This research received no external funding.

Institutional Review Board Statement: Not applicable.

Informed Consent Statement: Not applicable.

Data Availability Statement: The data that support the findings of this study are available from the corresponding author upon reasonable request.

Conflicts of Interest: The authors declare no conflict of interest.

References

1. Lu, H.; Wei, T.; Lou, H.; Shu, X.; Chen, Q. A Critical Review on Communication Mechanism within Plant-Endophytic Fungi Interactions to Cope with Biotic and Abiotic Stresses. *J. Fungi* **2021**, *7*, 719. [CrossRef] [PubMed]
2. Zhang, H.W.; Song, Y.C.; Tan, R.X. Biology and chemistry of endophytes. *Nat. Prod. Rep.* **2006**, *23*, 753–771. [CrossRef] [PubMed]
3. Rodriguez, R.J.; White, J.F.; Arnold, A.E.; Redman, R.S. Fungal endophytes: Diversity and functional roles. *N. Phytol.* **2009**, *182*, 314–330. [CrossRef] [PubMed]
4. Sieber, T.N. Endophytic fungi in forest trees: Are they mutualists? *Fung. Biol. Rev.* **2007**, *21*, 75–89. [CrossRef]
5. Redman, R.S.; Dunigan, D.D.; Rodriguez, R.J. Fungal symbiosis: From mutualism to parasitism, who controls the outcome, host or invader? *N. Phytol.* **2001**, *151*, 705–716. [CrossRef]
6. Rodriguez, R.; Redman, R. More than 400 million years of evolution and some plants still can't make it on their own: Plant stress tolerance via fungal symbiosis. *J. Exp. Bot.* **2008**, *59*, 1109–1114. [CrossRef]
7. Salvatore, M.M.; Andolfi, A.; Nicoletti, R. The thin line between pathogenicity and endophytism: The case of *Lasiodiplodia theobromae*. *Agriculture* **2020**, *10*, 488. [CrossRef]
8. Berestetskiy, A.; Hu, Q. The Chemical Ecology Approach to Reveal Fungal Metabolites for Arthropod Pest Management. *Microorganisms* **2021**, *9*, 1379. [CrossRef]
9. Nicoletti, R.; Fiorentino, A. Plant bioactive metabolites and drugs produced by endophytic fungi of Spermatophyta. *Agriculture* **2015**, *5*, 918–970. [CrossRef]
10. Popay, A.J.; Rowan, D.D. Endophytic fungi as mediators of plant-insect interactions. In *Insect-Plant Interactions*, 5th ed.; Bernays, E.A., Ed.; CRC Press: Boca Raton, FL, USA, 2017; pp. 83–104. [CrossRef]
11. Collemare, J.; Navarro-Munoz, J.C.; Mosunova, O. The Biosynthesis of Fungal Secondary Metabolites: From Fundamentals to Biotechnological Applications. In *Encyclopedia of Mycology*, 1st ed.; Zaragoza, O., Casadevall, A., Eds.; Elsevier: Amsterdam, The Netherlands, 2021; pp. 458–476.
12. Demain, A.L.; Fang, A. The Natural Functions of Secondary Metabolites. In *History of Modern Biotechnology I*, 1st ed.; Fiechter, A., Ed.; Springer: Berlin/Heidelberg, Germany, 2000; pp. 1–39.
13. Newman, D.J.; Cragg, G.M. Natural products as sources of new drugs over the nearly four decades from 01/1981 to 09/2019. *J. Nat. Prod.* **2020**, *83*, 770–803. [CrossRef]
14. Masi, M.; Maddau, L.; Linaldeddu, B.T.; Scanu, B.; Evidente, A.; Cimmino, A. Bioactive metabolites from pathogenic and endophytic fungi of forest trees. *Curr. Med. Chem.* **2018**, *25*, 208–252. [CrossRef]
15. Cimmino, A.; Masi, M.; Evidente, M.; Superchi, S.; Evidente, A. Fungal phytotoxins with potential herbicidal activity: Chemical and biological characterization. *Nat. Prod. Rep.* **2015**, *32*, 1629–1653. [CrossRef]
16. Marrone, P.G. Pesticidal natural products-status and future potential. *Pest Manag. Sci.* **2019**, *75*, 2325–2340. [CrossRef]
17. Andolfi, A.; Maddau, L.; Basso, S.; Linaldeddu, B.T.; Cimmino, A.; Scanu, B.; Deidda, A.; Tuzi, A.; Evidente, A.A. Diplopimarane, a 20-nor-ent-pimarane produced by the oak pathogen *Diplodia quercivora*. *J. Nat. Prod.* **2014**, *77*, 2352–2360. [CrossRef]
18. Sparapano, L.; Bruno, G.; Fierro, O.; Evidente, A. Studies on structure–activity relationship of sphaeropsidins A–F, phytotoxins produced by *Sphaeropsis sapinea f.* sp. cupressi. *Phytochemistry* **2004**, *65*, 189–198. [CrossRef]
19. Ellestad, G.A.; Kunstmann, M.P.; Mirando, P.; Morton, G.O. Structures of fungal diterpene antibiotics LL-S491. beta. and-. gamma. *J. Am. Chem. Soc.* **1972**, *94*, 6206–6208. [CrossRef]
20. Morooka, N.; Tatsuno, T.; Tsunoda, H.; Kobayashi, K.; Sakurai, T. Chemical and Toxicological Studies of the Phytotoxin, 6α,7β,9α-Trihydroxy-8,15-isopimaradiene-20,6-γ-lactone, Produced by a Parasitic Fungus, *Phomopsis* sp., in Wilting Pine Trees. *Agric. Biol. Chem.* **1986**, *50*, 2003–2007.
21. Weber, R.W.; Kappe, R.; Paululat, T.; Mösker, E.; Anke, H. Anti-Candida metabolites from endophytic fungi. *Phytochemistry* **2007**, *68*, 886–892. [CrossRef]

22. Wang, X.N.; Bashyal, B.P.; Wijeratne, E.K.; U'Ren, J.M.; Liu, M.X.; Gunatilaka, M.K.; Arnold, A.E.; Gunatilaka, A.L. Smardaesidins A–G, Isopimarane and 20-nor-Isopimarane Diterpenoids from *Smardaea* sp., a Fungal Endophyte of the Moss Ceratodon purpureus. *J. Nat. Prod.* **2011**, *74*, 2052–2061. [CrossRef]
23. Yan, T.; Guo, Z.K.; Jiang, R.; Wei, W.; Wang, T.; Guo, Y.; Song, Y.C.; Jiao, R.H.; Tan, R.X.; Ge, H.M. New flavonol and diterpenoids from the endophytic fungus *Aspergillus* sp. YXf3. *Planta Med.* **2013**, *79*, 348–352. [CrossRef]
24. Li, Y.; Scott, R.; Hooper, A.R.; Bartholomeusz, G.A.; Kornienko, A.; Bills, G.F. *Aspergillus candidus* is a newly recognized source of sphaeropsidin A: Isolation, semi-synthetic derivatization and anticancer evaluation. *Bioorg. Med. Chem. Lett.* **2017**, *27*, 5436–5440. [CrossRef] [PubMed]
25. Neuhaus, G.F.; Adpressa, D.A.; Bruhn, T.; Loesgen, S. Polyketides from marine-derived *Aspergillus porosus*: Challenges and opportunities for determining absolute configuration. *J. Nat. Prod.* **2019**, *82*, 2780–2789. [CrossRef] [PubMed]
26. Yang, H.; Liu, X.Y.; Zhang, P.L.; Gao, H.M.; Zhang, L.T.; Shen, T.; Ren, D.M.; Lou, H.X.; Wang, X.N. New terpenoids and triketides from culture of the fungus *Botrysphaeria laricina*. *Fitoterapia* **2020**, *147*, 104758. [CrossRef] [PubMed]
27. Cimmino, A.; Andolfi, A.; Avolio, F.; Ali, A.; Tabanca, N.; Khan, I.A.; Evidente, A. Cyclopaldic Acid, Seiridin, and Sphaeropsidin A as Fungal Phytotoxins, and Larvicidal and Biting Deterrents against *Aedes aegypti* (Diptera: Culicidae): Structure-Activity Relationships. *Chem. Biodivers.* **2013**, *10*, 1239–1251. [CrossRef]
28. Mahamedi, A.E.; Phillips, A.J.; Lopes, A.; Djellid, Y.; Arkam, M.; Eichmeier, A.; Zitouni, A.; Alves, A.; Berraf-Tebbal, A. Diversity, distribution and host association of Botryosphaeriaceae species causing oak decline across different forest ecosystems in Algeria. *Eur. J. Plant Pathol.* **2020**, *158*, 745–765. [CrossRef]
29. Salvatore, M.M.; DellaGreca, M.; Nicoletti, R.; Salvatore, F.; Tuzi, A.; De Tommaso, G.; Alves, A.; Mahamedi, A.E.; Berraf-Tebbal, A.; Andolfi, A. Mitidjospirone, a new spirodioxynaphthalene and GC-MS screening of secondary metabolites produced by strains of Lasiodiplodia mitidjana associated to Citrus sinensis dieback. *Nat. Prod. Res.* **2021**, 1–10. [CrossRef]
30. Di Lelio, I.; Varricchio, P.; Di Prisco, G.; Marinelli, A.; Lasco, V.; Caccia, S.; Casartelli, M.; Giordana, B.; Rao, R.; Gigliotti, S.; et al. Functional analysis of an immune gene of *Spodoptera littoralis* by RNAi. *J. Insect Physiol.* **2014**, *64*, 90–97. [CrossRef]